5-2010

A systems genetics approach to the characterization of differential low dose radiation responses in BXD recombinant inbred mice

Rachel Marie Lynch
rlynch@utk.edu

To the Graduate Council:

I am submitting herewith a dissertation written by Rachel Marie Lynch entitled "A systems genetics approach to the characterization of differential low dose radiation responses in BXD recombinant inbred mice." I have examined the final electronic copy of this dissertation for form and content and recommend that it be accepted in partial fulfillment of the requirements for the degree of Doctor of Philosophy, with a major in Life Sciences.

Brynn H. Voy, Major Professor

We have read this dissertation and recommend its acceptance:

Mitchel J. Doktycz, Stephen J. Kennel, Hayes W. McDonald

Accepted for the Council:
Dixie L. Thompson

Vice Provost and Dean of the Graduate School

(Original signatures are on file with official student records.)

To the Graduate Council:

I am submitting herewith a dissertation written by Rachel M. Lynch entitled “A systems genetics approach to the characterization of differential low dose radiation responses in BXD recombinant inbred mice.” I have examined the final electronic copy of this dissertation for form and content and recommend that it be accepted in partial fulfillment of the requirements for the degree of Doctor of Philosophy, with a major in Life Sciences.

Brynn H. Voy, Major Professor

We have read this dissertation
and recommend its acceptance:

Mitchel J. Doktycz

Stephen J. Kennel

Hayes W. McDonald

Accepted for the Council:

Carolyn R. Hodges
Vice Provost and Dean of the Graduate School

(Original signatures are on file with official student records.)

A systems genetics approach to the characterization of differential low dose radiation responses in BXD recombinant inbred mice

A Dissertation
Presented for the
Doctor of Philosophy
Degree

The University of Tennessee, Knoxville

Rachel M. Lynch
May 2010

DEDICATION

This dissertation is dedicated to three individuals:

my late father, James Kyle Goldston,

who always encouraged me to think scientifically,

work hard, live fully, and become a better person.

my loving husband and best friend, Ben Lynch,

who stays right by my side through life's most joyous and difficult times

and encourages me reach my potential.

my son, James Thomas Lynch,

who continually blesses my life with his smile

and reminds me what is truly important.

ACKNOWLEDGEMENTS

I would like to thank my family, especially my mother, Sandra Goldston, my mother-in-law, Vickie Lynch, and my sisters, Adria and Amanda Goldston, who have been very supportive and helpful while my husband and I have been working on our graduate degrees.

I thank the Genome Science and Technology Program for giving me the opportunity to pursue my graduate studies and for scientific training. I also thank Suchita Das for laboratory expertise and training throughout my graduate school journey. She personally performed many of the sample preparations and assays which were used in the research presented here.

I would like to express special thanks to my advisor, Dr. Brynn Voy, who is a patient, excellent teacher and scientist as well as a great role model. She provided me with many opportunities to attend national and international scientific conferences, which were not only helpful for my research but also allowed me to network with other graduate students and researchers. I really appreciate her personal attention in my scientific and professional development.

The project was supported by the Low Dose Radiation Research Program of the Office of Biological and Environmental Research, Office of Science, Department of Energy ERKP650 and ERKP804.

ABSTRACT

High doses of radiation (HDR) are clearly detrimental to human health, but relatively little is known about the health consequences following exposure to low doses of radiation (LDR, <10cGy). Understanding the risks associated with LDR is of great importance to the general public due to the recent dramatic increase in diagnostic radiological imaging. While HDR clearly suppress immune function, there is evidence that LDR can be immunostimulatory. Within the organism, defining the consequences of LDR is further complicated by the impact of genetic background, particularly in systems such as the immune system for which both radiosensitivity and genetic effects are profound.

We addressed the issue of genetic susceptibility to LDR using the immune system as a target system and treated the LDR response as a complex trait analyzed using a systems genetics framework. Using the BXD recombinant inbred strain mouse panel as a genetic reference population allowed us to address the radiation response within the context of natural genetic variation. Our overarching hypothesis is that, within a population, the immunological effects of LDR exposure depend in part on the individual's baseline immunoprofile and gene expression which are ultimately dependent upon genetic background. We began by establishing the immunophenotypic variation (i.e., T:B cell ratio, CD4:CD8 ratio) within the BXD panel and used baseline spleen transcriptome profiling to identify putative candidate genes controlling these traits, specifically *Acp1* and *Ptprk* for CD4:CD8 ratio. The same set of BXD strains was exposed to LDR (10cGy gamma radiation) to determine effects on immune function and oxidative stress. LDR significantly enhanced neutrophil phagocytosis in a manner that was independent of genetic background. In contrast, genetic background significantly impacted LDR-induced changes in spleen superoxide dismutase activity.

By integrating these results with our previous analyses of BXD RI strains, we have demonstrated that baseline expression of *Sod2* correlates with LDR-induced SOD activity, and baseline CD4:CD8 ratio is inversely correlated with LDR-induced neutrophil phagocytosis. In addition, spleen transcriptomic data from the BXD parental strains further highlighted the impact of genetic background on LDR responses. These data provide the groundwork for predicting LDR responses using baseline expression, immunophenotypes, and/or genotype.

TABLE OF CONTENTS

LIST OF FIGURES

LIST OF TABLES

SELECTED LIST OF SYMBOLS & ABBREVIATIONS

DSB	Double-stranded break
eQTL	Expression quantitative trait locus
ERR	Excess relative risk
GO	Gene ontology
GSH	Glutathione
GSSG	Oxidized glutathione
HDR	High dose radiation
IP	Immunophenotype
IR	Ionizing radiation
LDR	Low dose radiation
LET	Linear energy transfer
LNT	Linear no threshold
LOD	Logarithm of odds
MCF	Median channel fluorescence
MHCII	Major histocompatibility complex-II
QTL	Quantitative trait locus
RI	Recombinant inbred
ROS	Reactive oxygen species
SNP	Single-nucleotide polymorphism
SOD	Superoxide dismutatse

CHAPTER I

GENERAL EXPERIMENTAL DESIGN

Our goal is to identify networks of genes which underlie basic immune phenotypes, determine the effect of low dose radiation (LDR, 10cGy) on immune function, and characterize how genetic background impacts immune function and causes differential susceptibility to LDR. The ultimate purpose is to identify genomic regions that mediate response to LDR and eventually be able to predict an individual's susceptibility to LDR based on their genotype at those loci.

The LDR response is viewed as a complex trait which is analyzed using a systems genetics framework. Systems genetics is both an analytical framework through which to assemble gene-phenotype networks and a means to uncover genetic polymorphisms that cause variation in these networks and lead to variable disease susceptibility. The use of a genetic reference population, the BXD recombinant inbred (RI) strain panel, allows us to address the radiation response within the context of natural genetic variation. This RI panel provides a population-based, genetically characterized model system in which the parental strains (C57BL/6J and DBA/2J) exhibit known differential responses to low dose exposure as well as divergent sensitivity to radiation carcinogenesis.

This research involves the first two steps in a larger research program designed to create a comprehensive understanding of the molecular pathways and expression networks which underlie radiation-response phenotypes and how genetic variation alters these networks to result in altered sensitivity to LDR.

We began by assessing the baseline immunophenotypic variation and spleen expression networks in the BXD panel and identified genetic loci responsible for the variation

(Part 1). Immunophenotyping was performed on the peripheral blood of mice from 41 BXD strains. The lymphocyte subpopulations analyzed included total T cells ($CD3^+$), B cells ($CD79^+$), $CD4^+$ T cells, and $CD8^+$ T cells. MHCII expression on lymphocytes was also analyzed. Baseline spleen expression analysis was performed on 38 BXD strains (Fig. 1-1) and identified expression networks and candidate genes underling the immunophenotypes.

In the second phase (Part 2), we exposed BXD mice to LDR and assessed neutrophil function (e.g., phagocytosis and oxidative burst) and spleen anti-oxidant status (e.g., superoxide dismutase activity and glutathione levels) 48 hours after radiation exposure (Fig. 1-2). Radiation-induced spleen expression changes were measured in the parental strains (C57BL/6J and DBA/2J) 24 hours after exposure to high dose (1Gy) or low dose (10cGy) radiation in order to assess differential sensitivity to low dose radiation at the molecular level. The data from Parts 1 & 2 were then integrated together using graph algorithms and statistical testing to identify correlations between baseline immunophenotype and expression and LDR responses within the population (Fig. 1-2).

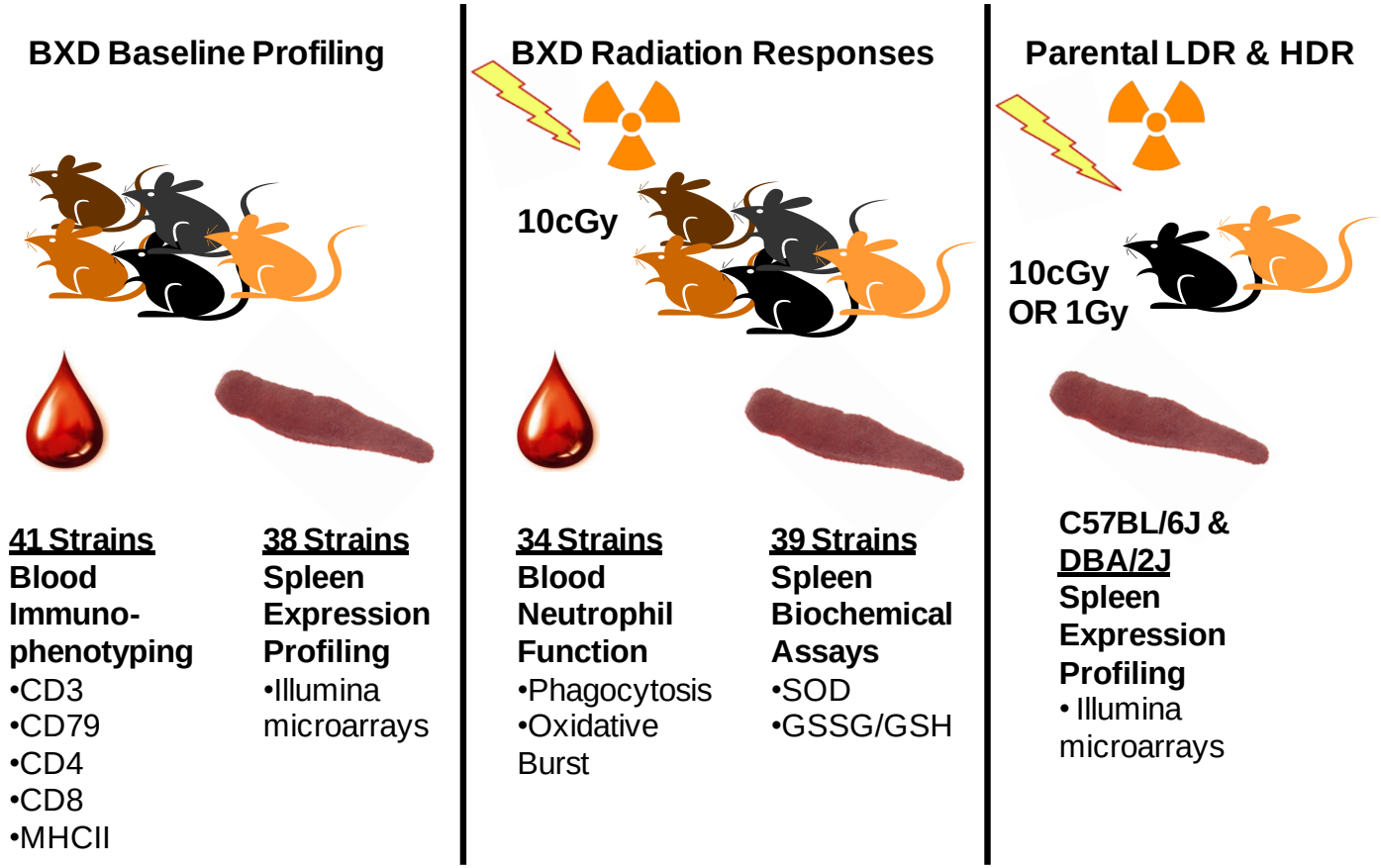

Figure 1-1. Experimental design: data collection. Part 1 included baseline immunophenotyping in the peripheral blood of 41 BXD strains and baseline spleen expression profiling in 38 strains. Part 2 involved analysis of BXD responses to LDR (10cGy γ-radiation) 48 hours after irradiation, including neutrophil function (34 strains) and spleen biochemical assays (39 strains). Spleen expression profiling was performed on the BXD parental strains (C57BL6J and DBA/2J) 24 hours after LDR.

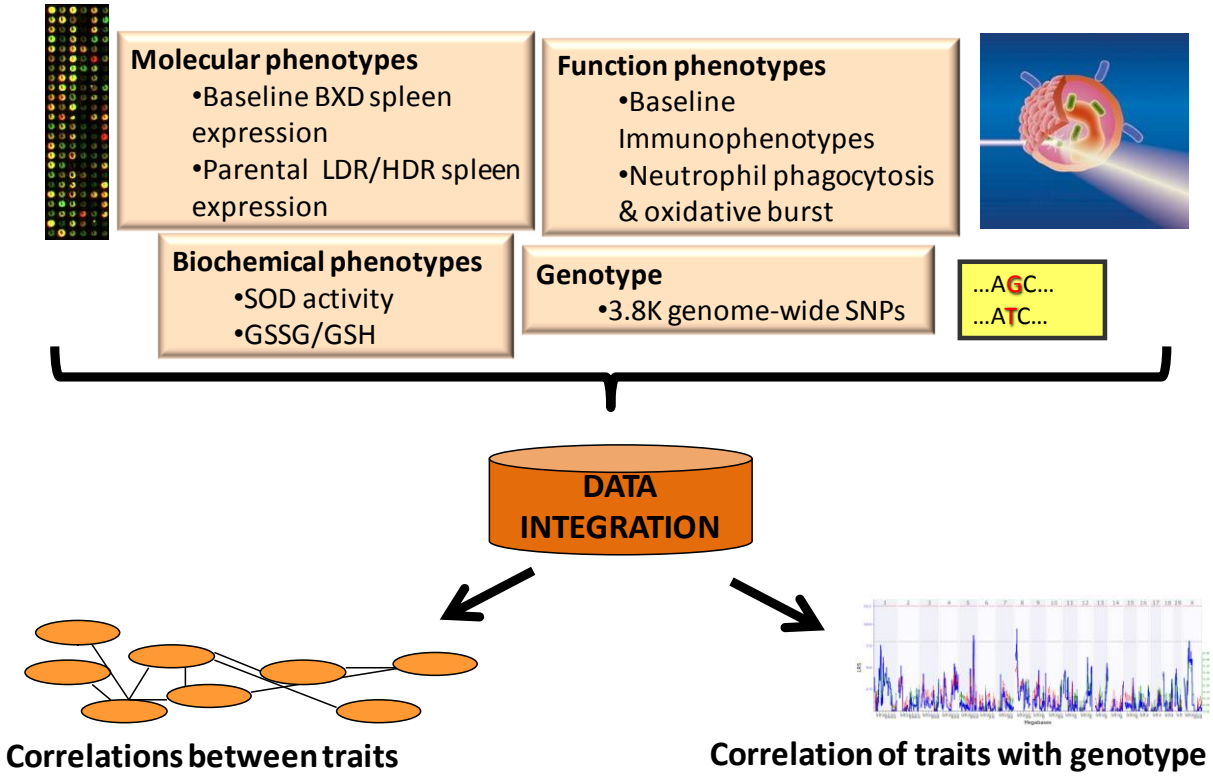

Figure 1-2. Experimental design: data integration. The data collected from Parts 1 & 2 were integrated together along with genotype information to perform quantitative trait loci mapping (QTL) of the baseline immunophenotype and LDR responses as well as to identify inter-correlated traits.

CHAPTER II

LITERATURE REVIEW

General radiation biology

Radiation biology overview

Almost twenty years after the initial discovery of x-rays by Wilhelm Conrad Röntgen in 1895, the Drosophila geneticist Herman Müller demonstrated that ionizing radiation causes mutations in living organisms (185). In the 80 years since that discovery, the biological and genetic consequences of exposure to ionizing radiation (IR) have been investigated.

In order to understand the biological effects of radiation exposure, a basic understanding of radiation is needed. Ionizing radiation, which consists of subatomic particles (i.e., alpha particles, beta particles, neutrons) or electromagnetic waves (e.g., x-rays, γ-radiation, ultraviolet radiation), contain enough energy to displace electrons and break chemical bonds. Here, we primarily focus on the biological effects from x-ray and γ-radiation, both of which are characterized as low linear energy transfer (low-LET) radiation. In contrast to high-LET radiations, low-LET radiations produce ionizations only sparsely along their tract, resulting in a more homogenous ionization within the cell. Because high-LET radiation deposits a larger amount of energy per distance traveled, it induces more cellular and molecular damage per dose than low-LET radiation.

The International Commission on Radiation Units and Measurements (107) defines radiation exposure units. The unit of absorbed radiation dose is the gray (Gy), defined as the energy absorbed per unit of mass. One Gy of ionizing radiation delivers 1 joule of energy per kilogram of matter (J/kg). Radiation dose is also commonly expressed as an “effective dose”, which is used to reflect the biological effects of radiation, e.g., high-LET radiation induces more

biological damage per Gy than low-LET radiation. Effective dose (measured in sieverts, Sv) equals the absorbed dose (in Gy) times the radiation weighting factor (Q) of the radiation type. For low-LET radiation, including x-rays and γ-radiation, Q = 1 so the absorbed dose equals the effective dose, or 1Gy = 1Sv.

The study of the health consequences of IR increased dramatically following the devastating effects of the atomic bombs which were detonated on Hiroshima and Nagasaki, Japan in 1945. The first studies focused on the immediate health detriments following acute exposure (23, 61). Additional data for the health consequences of high doses of radiation came from documenting the health of firefighters that first responded to the Chernobyl Nuclear Power Plant event in 1986 (168).

Simply stated, the detrimental health effects of exposure to IR are due to the free electrons produced when the electromagnetic wave interacts with the atoms of the cell, causing damage to the biomolecules and inducing oxidative stress. If the radiation dose is high enough, severe damage to the structure of the cell leads to cell death immediately (195). At lower levels, DNA damage (either by directly interacting with the DNA macromolecule or indirectly through the production of reactive oxygen species) can result in delayed cell death, repair of the DNA and restoration of cellular function, or incorrect repair and the possible increase in cancer risk. Various non-targeted effects also occur. These effects are discussed in length in following sections.

When exposure to radiation is relatively high (>1Gy acute exposure in humans), the symptoms of Acute Radiation Syndrome (ARS) become evident. The three classical syndromes of ARS include bone marrow syndrome (or hematopoietic syndrome), gastrointestinal (GI) syndrome, and cardiovascular (CV)/ central nervous system (CNS) syndrome (44). Hematopoietic syndrome begins with doses between 0.7 – 10Gy and is characterized by the destruction of bone marrow which results in infection and hemorrhage. GI syndrome occurs

following exposure >6Gy and results in extreme damage to the GI tract leading to dehydration and death within weeks. CV/CNS syndrome follows 20 – 50Gy doses, resulting in collapse of the circulatory system and increased cranial pressure; death occurs within days. The doses required to cause these syndromes reflect the radiosensitivity of the various tissues. The $LD_{50/60}$, or the dose which is lethal to 50% of the population within 60 days, is approximately 4Gy, while the LD_{100} (lethal dose to 100% of the population) is around 10Gy (44).

Human exposures to radiation

Humans are exposed to radiation from a variety of natural and manmade sources. Natural background radiation sources include radioactive elements within the earth's crust, radon gas released from the earth, and cosmic rays. Small traces of naturally occurring radioactive materials, including ^{3}H, ^{14}C, ^{20}K, can become incorporated into the biomolecules of the human body and become a source of internally emitted radiation. According to the United Nations Scientific Committee on the Effects of Atomic Radiation (UNSCEAR), the global average radiation dose from natural background radiation is approximately 2.4mSv (167, 268). The dose from natural background radiation can vary depending upon location. For example, inhabitants of Ramsar, Iran are exposed to 5 times more radiation from natural sources than the global average (268).

Radiation exposure in the U.S. population is monitored by National Council on Radiation Protection and Measurements (NCRP). The NCRP recently re-assessed the exposure from all radiation sources in the U.S., updating their last report published in 1987 which used data from 1980 to 1982 (189). In the last 30 years, the estimated annual per-capita dose to the U.S. population has almost doubled, from approximately 3.0mSv to 5.6mSv (189). While the average dose from natural sources has remained constant, there has been a dramatic increase in the average radiation dose from medical radiation procedures. This is mainly due to the increased

use of computed tomography (CT) scans, and it is estimated that >62 million CT scans are performed in the U.S. per year (189). CT scans account for approximately half of collective dose from all medical procedures.

The doses associated with conventional x-ray procedures is relatively low, approximately 0.1mGy for a typical chest x-ray (Table 2-1) (33). In comparison, a typical abdominal CT scan can deliver 50 times more radiation. Spiral CT scanning, which is used for the detection of potential disease in asymptomatic individuals, is becoming more common. A full-body spiral CT scan can deliver up to 100mGy (184), although newer techniques are being developed which reduces the radiation dose (52). There is intense debate concerning the cancer risk from CT scans, an issue which is discussed in detail below.

Epidemiological data for radiation exposure

Atomic bomb survivors

One of the largest cohorts for evaluating radiation risk is the Life Span Study (LSS) cohort which consists of approximately 86,000 survivors of the Hiroshima and Nagasaki atomic bombs of 1945. A couple of years after the bombings, the U.S. Atomic Bomb Casualty Commission was formed and followed the health of survivors, being particularly interested in the hematological consequences of the radiation exposure. In 1952, the first paper observing the excess of leukemia among the survivors was published (82).The LSS was created shortly afterwards to study mortality and cancer incidence among survivors. The Radiation Effects Research Foundation (RERF), a non-profit Japanese foundation supported by the U.S. and Japanese governments, oversees the LSS. The advantages of the LSS cohort is its large size, the long follow-up period after exposure, the inclusion of both sexes and all age groups, the range of radiation dosage, and the accuracy and completeness of mortality data. This data has been used to estimate radiation-induced risks for various cancers (and non-cancerous

Table 2-1. Approximate mean doses for societally-relevant radiation exposures.

Source	Dose
Radiotherapy to tumor (multiple fractions)	40-70Sv
Exposure on international space station	170mSv / year
Upper limit for full-body spiral CT scan	100mSv
Cranial CT scan	50mSv
Limit for radiation worker exposure	20mSv / year
Mammogram	3mSv
U.S. dose from medical sources	3.0mSv / year
U.S. dose from natural sources	2.4mSv / year
Chest x-ray	0.1mSv
Round-trip flight, New York to London	0.1mSv

Data obtained from Brenner, et al., 2003 (32), Mullenders, et al., 2009 (184), and Mettler et al., 2009 (167).

diseases) across a range of doses. The estimated average for the cohort is estimated to be approximately 20cGy (214), although individual exposure varied widely and estimates are poor guesses at best.

The data for the cohort increases over time due to the latent development of cancer and due to mortality (and therefore cause of death information) of the bomb survivors. Therefore, the LSS continues to be a source for updated epidemiological studies. The radiation-induced cancer risk is being continually re-assessed using updated dosing estimates and new modeling statistics.

The most recent report from the RERF on solid cancer and non-cancer disease mortality was published in 2003 (214). In the 47-year follow-up, there were 9,335 deaths from solid cancer and 31,881 deaths from non-cancer diseases. It was estimated that 5% of the solid cancer deaths were associated with radiation exposure, noting that relative risks decline with increasing attained age and are highest in those who were exposed as children. This could translate into a 47% increased risk for the development of solid cancer by age 70 for those exposed to the radiation at 30 years of age (214).

Pierce & Preston specifically analyzed cancer risk of low radiation doses in the LSS (211). Their study included 7,000 cancer cases among 50,000 survivors, most of whom received a dose less than 0.5Sv. They reported a significant increase in solid-cancer-related mortality in individuals who received 5-125mSv (P = 0.025). The authors stress that their data, which involved direct assessment of cancer incidence in the low dose cohort, did not involve any linear extrapolation. They suggest that other estimates of cancer in the LSS using linear risk estimates from a wider exposure range do not overestimate low-dose risks, an issue of intense debate in the low dose radiation field.

A recent study analyzed 310 deaths due to leukemia during period from 1950 – 2000 among 86,611 in the LSS (216). Using survivors with an estimated exposed dose >0.5cGy as a

reference (i.e., “control”), Poisson regression methods were used to evaluate the associations between estimated bone marrow radiation dose and leukemia mortality. Overall, the authors estimate that 103 of the 310 observed leukemia deaths were due to radiation exposure. They also suggest that radiation-induced leukemia death is still persistent in the cohort some 50 years after the bombings, a conclusion based on the most recent leukemia deaths.

The incidence of leukemia and solid cancers among the cohort was recently analyzed by Dropkin, where he specifically looked at cancer mortality in survivors exposed to <20mSv (72, 73). This is within the range of the International Commission on Radiological Protection’s (ICRP) current recommendation for annual occupational radiation dose (maximum average of 20mSv per year averaged over 5 years with no single year exceeding 50mSv) (106). He concluded that liver and urinary cancer mortality risk follows a linear dose response at the low doses, while the risk for 5 other cancers (stomach, liver, lung, pancreas, and leukemia) follows a non-linear model with a higher risk at low doses than what would be predicted with a linear model. Dropkin suggests that the increased cancer risk following exposure <20mSv casts doubts on the ICRP’s current annual occupational limit.

Radiation workers

In addition to the atomic bomb survivors, radiological workers provide a separate, unique population to study the cancer risks of LDR. Compared to the LSS, studying radiation workers allows for a more direct assessment of the risks of LDR. Many countries have strict regulations concerning the maximum radiation dose for radiation workers and require carful dosimetry to monitor exposure. Therefore, radiation workers provide a unique irradiated population whose exposure dosages are relatively well estimated. In addition, the exposures of radiation workers are generally of smaller dose compared to the atomic bomb survivors and are protracted over extended periods of time at a low dose rate. Many studies have shown an increase in leukemias in workers exposed to LDR (42, 243, 304). While dosimetry is more accurate in radiation worker

studies compared to the estimates in the LSS (in which dosages are primarily based on distance from the blast), dosimetry, mixed radiation types, and missing data for individuals still complicate analysis. For example, men who worked at Oak Ridge National Laboratory (ORNL) between 1943 and 1972 were found to have increased leukemia mortality (286), but adjustment procedures used to compensate for missing dose data suggested that effect of missing dose data resulted in an upward bias in dose-response coefficients (84). Indeed, one study including workers from the Hanford Site, ORNL, and Rocky Flats Weapons Plant concluded that the combined excess relative risk for leukemia was actually negative (-1.0 per Sv or ERR/Sv) (91). Of the 24 solid and non-solid cancer types tested, Gilbert, et. al. reported that half showed positive correlations and half showed negative correlations, as would be expected by chance fluctuations (91).The International Agency for Research on Cancer has coordinated studies in which radiation worker data from multiple countries are integrated together to form larger cohorts which increase power in detecting risk. One of the first such analysis included >95,000 workers from combined data of three registries from the United States (including Hanford, ORNL, and the Rocky Flats Plant), the United Kingdom (including the Atomic Energy Authority, Atomic Weapons Establishment, and Sellafield Plant), and Canada (Atomic Energy of Canada Limited) (42). Of all the cancers monitored, a significant association was observed only for multiple myeloma (one-sided $P = 0.037$, 44 deaths). More recently, a 15-country collaborative cohort was analyzed and included nearly 400,000 nuclear industry workers (278). A significant increase was found in cancer mortality (ERR/Sv = 0.90, 5,233 deaths), with a significant association for lung cancer (ERR/Sv = 1.86) and an almost significant association for multiple myeloma (ERR/Sv 6.15, 83 deaths, $P = 0.06$). However, the authors concede that other confounding factors (i.e., tobacco use) will need to be addressed in future studies (43).

In general, radiation workers can be an informative population for epidemiological studies regarding LDR risk, but there are important limitations which must be considered when

interpreting the findings. The first involves the potential for bias due to confounding when analyzing small risks (90), such as the ERR for multiple myeloma included only 83 deaths in the 400,000 workers. Another limitation involves what is considered a strength of radiation worker analyses: dosimetry. Personal dosimeters worn by workers can induce various biases. Gilbert et al. noted that the dosimeters were designed for radiation protection and likely overestimates dose to bone marrow (important for leukemia risk estimation) and most other organs (92). In addition, workers exposed to low doses (<10mSv) represent only a small percentage of the workers within the cohort, complicating the risk following LD exposure (90).

Radiotherapy patients

Additional epidemiological radiation-exposure data come from cancer patients who have undergone radiation cancer treatment. The Surveillance, Epidemiology and End Results (SEER) Program collects and publishes cancer incidence and survival data from population-based cancer registries and includes approximately 26% of the U.S. population, making it a unique resource for evaluating the potential risk of subsequent cancers following radiation treatment (http://seer.cancer.gov/about/). According to the National Cancer Institute's 2006 report using data from the SEER Program, it is estimated that cancer patients who undergo successful treatment for cancer are at a 14% higher risk for developing a new malignancy compared to the rest of the population (62). Some of the increased risk is attributable to the radiation therapy employed to fight the cancer, but there are many other risks and variables which need to be considered before developing an accurate estimate of what proportion of these new cancers are caused by the radiotherapy itself. One of the largest factors involves the individual's genetic susceptibility to cancer. If an individual has a germline mutation in a tumor suppressor gene, for example, that individual has a much higher risk of developing additional cancers even if the original malignancy is cured. One striking example is seen in pediatric patients with retinoblastoma. For those patients with germline mutations in the tumor suppressor *RB1*

(retinoblastoma-1) gene (heritable retinoblastoma), the cumulative incidence for developing a new malignancy within 50 years is 36%, compared to only 5.7% in retinoblastoma patients with non-heritable retinoblastoma (120). Other factors include sex, race, type of primary cancer, and use of chemotherapy (62). Despite all of these compounding factors, it is still evident that the radiation treatment itself increases risk. Returning to the retinoblastoma example, it was estimated that the increased risk do to radiation treatment in non-hereditary retinoblastoma patients was 3.1 fold higher, representing a significantly increased risk for sarcomas, melanoma, various brain cancers, and cancer of the nasal cavities (120). Similar results were observed with increased risk of breast cancer in female patients who underwent radiation treatment for childhood Hodgkin's disease (21). The increased risk from radiation exposure is most clearly seen in the treatment of childhood cancers, due to the long latency seen for radiogenic cancers (62). These factors must be taken into account when determining follow-up procedures to monitor the development of new malignancies. It is important to note that there is a clear benefit for radiotherapy, which exceeds that of the risk of developing new neoplasms.

Epidemiological studies, while providing the best estimates of radiation-induced cancer risks in the human population, reach their limit of detection of risk at doses at and below 100mSv (184). More research on the biological effects of lower doses of radiation is needed in order to accurately assess risk at these levels of exposure, and it is clear that controlled experiments in humans are not possible, especially with the cohorts that are available.

Radiation-induced cell damage and repair

The biological effects of IR exposure are mediated through direct damage to biomolecules (e.g., energy directly deposited on the molecule) or indirectly through the formation of reactive oxygen species (ROS).

Molecular scavenging involves the mechanisms which prevent further radiation-induced damage from free radicals. ROS are formed by the radiolysis of intracellular water, which in turn, can cause oxidative damage to DNA, proteins, and lipids (196). However, the cell is always exposed to ROS as a byproduct of normal oxygen metabolism, and various defense mechanisms are in place for protection from ROS-induced damages. These include anti-oxidant molecules (e.g., glutathione, Vitamins C and E, NADPH) and enzymatic scavengers (e.g., catalase, superoxide dismutase). During times of oxidative stress (e.g., following radiation exposure), pro-oxidant production exceeds the cellular antioxidant capacity to maintain normal redox potential (239). The cell can respond by increasing the metabolic antioxidant capacity through the elevation of antioxidant levels. Increased levels of glutathione and superoxide dismutase (Sod) have been reported in mouse tissues following exposure to low dose radiation (197, 204, 251, 292). It has been suggested that radiation-induced oxidative stress not only contributes to cellular radiation damage, but that it is the trigger for IR-induced signaling and adaptive responses (246). Sustained oxidative stress can result in the continued, amplified oxidative damage long after the initial radiation exposure, which can lead genomic instability (246), discussed below.

Radiation-induced DNA damage and its repair is perhaps the most studied effect of radiation exposure because excessive damage or inadequate repair can lead to cell death, genomic instability, or carcinogenesis. Ionizing radiation can either directly damage DNA (e.g., energy directly deposited on the DNA molecule causing single- or double-stranded breaks) or indirectly through ROS (resulting in DNA breaks or DNA adducts such as 8-oxo-7,8-dihydroguanine) (213). There are two main schools of thought regarding the mechanisms which alter signal transduction and result in the activation of DNA repair mechanisms (270). As mentioned above, radiation-induced ROS and the subsequent alterations in intracellular redox reactions could be the trigger for the induction of signal transduction pathways. While the exact

mechanisms responsible are unknown, it has been hypothesized that NADPH oxidases could play a key role (246). The other school of thought involves the sensing of DNA damage by proteins such as Atm and DNA-PK, which in turn promote activation of receptors and signaling pathways and cell cycle checkpoints (270). It is likely that both mechanisms are involved in radiation response.

While the exact mechanisms may not be fully understood, the cell must recognize the damage and respond appropriately, either by arresting the cell cycle, repairing the damage, and/or inducing apoptosis (Fig. 2-1). DNA double-stranded breaks (DSBs), the most deleterious form of radiation-induced DNA damage, are induced by radiation several fold above endogenous levels in a linear dose-dependent manner, even at very low doses (1mGy in vitro and 100mGy in vivo) (219). Once DSBs are formed, numerous DSB repair proteins are recruited to the break which creates a stabilizing complex that is vital for DSB repair and checkpoint activation (271). Decreased efficiency of DSB-repair is linked with radiosensitivity and has been proposed as a means of identifying patients who are more susceptible to radiation toxicities prior to cancer radiotherapy treatments (221).

Ataxia telangiectasia mutated (Atm) kinase is a critical DNA-damage signaling enzyme. Following DNA damage, Atm undergoes rapid autophosphorylation and phosphorylates H2AX at the site of the break (15). This phosphoylated histone (γH2AX) provides a platform on which DSB response proteins bind and initiate repair (271). The essential role of H2AX in DSB repair is seen in the H2AX(-/-) mouse, whose DNA repair defects are correlated with increased radiosensitivity and genomic instability (45). *ATM* mutations are responsible for the human radiosensitivity disease ataxia telangiectasia, discussed below (224).

Atm activates pathways which halt the cell cycle and initiate repair by phosphorylating downstream targets, including the transcription factor p53 and the checkpoint kinases Chk1 and Chk2 (220) (Fig. 2-1). DSBs can be repaired through homologous recombination involving

A

B

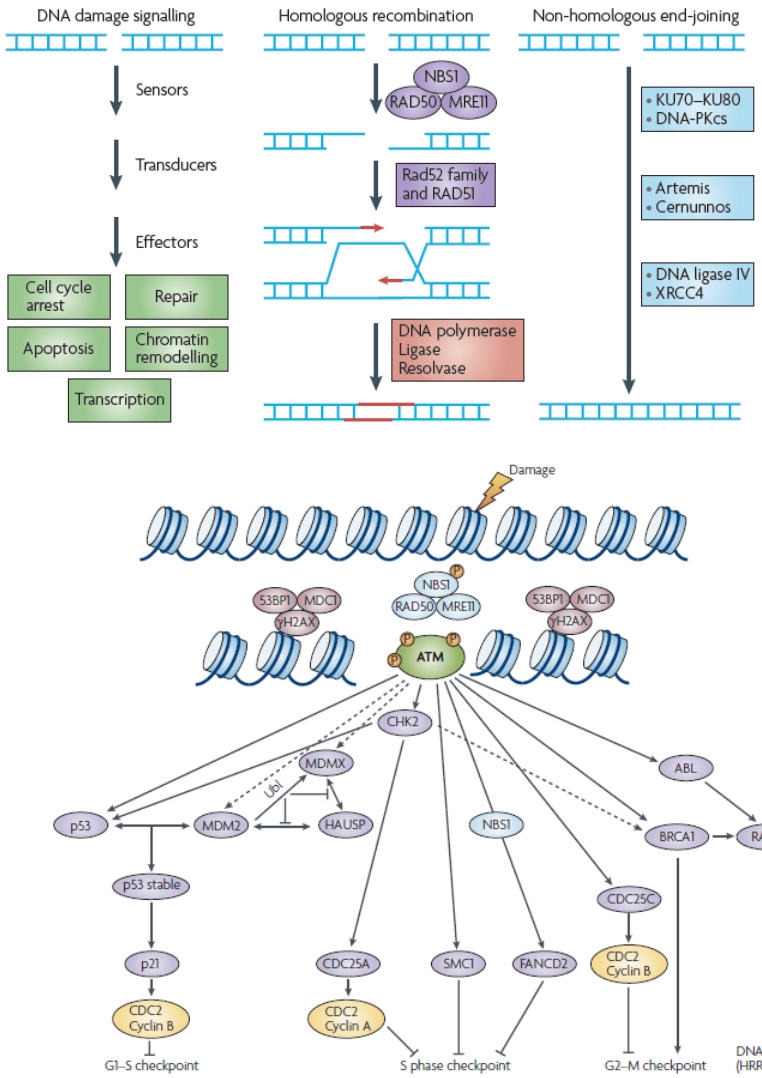

Figure 2-1. DNA damage response signaling mediated by ATM. (A) Radiation causes double-stranded DNA breaks (DSBs). The damage is recognized by “sensors” such as the MRN complex (MREII, RAD50, NBS1) and the signal is transmitted to “tranducers” such at ATM, which in turn pass the signal to “effectors” which activate various signal transduction pathways. DSBs can be repaired by homologous recombination (involving Rad51 and Rad52) or by non-homologous end joining (NHEJ). Image courtesy of Mullenders, et al., 2009 (184) (B) Activated ATM phosphorylates a series of downstream targets resulting in cell cycle arrest and DNA damage repair. Image courtesy of Lavin, 2008 (134).

Rad51, or through the more error-prone mechanism of non-homologous end-joining (NHEJ), which involves DNA-dependent protein kinase catalytic subunit (DNA-PKcs) (7, 103). Defective Atm leads to radiation hypersensitivity through inadequate DNA repair, and perhaps more importantly, through defective Atm signaling which results in compromised defense against DNA damage (134).

It is well established that the p53 pathway is central to the DNA damage response. When activated through phosphorylation by Atm and DNA-PK, p53 activates cell cycle checkpoints which allows the cell to asses DNA damage and repair the DNA prior to replication or activate apoptosis (270) (Fig. 2-2). p53 can lead to cell cycle arrest through inducing the expression of cyclin-dependent kinase inhibitor 1A (*Cdkn1a*, also known as *p21*). The p53 – p21/Rb checkpoint axis leads to G1 arrest, allowing the cell to undergo DNA-repair before resuming the cell cycle (279). Rb has the potential to either mediate apoptosis or protect against it, which appears to be dependent upon the phosphorylation status of Rb, with hyperphosphorylated Rb correlated with low apoptotic rates and non-phosphorylated Rb correlated with high apoptotic rates (279). Differences in post-radiation phosphorylation status of Rb have been linked to differing apoptotic rates in C57BL/6J mice (279).

Alternately, p53 can lead to apoptosis via the up-regulation of pro-apoptotic Bcl2-associated X protein (*Bax*) (140). Bax induces cytochrome c release and caspase activation, thereby initiating apoptosis (218). It has been demonstrated that basal p53 transcription and protein level within a tissue partially determines its sensitivity to radiation-induced apoptosis (155). This response is also affected by genomic background, with mouse strains exhibiting varied apoptotic rates and susceptibilities to radiation-induced genomic instability (212, 223, 279, 281). It should be noted that death of a damaged cell removes the possibility of the cell acquiring genomic instability and the formation of a population of daughter cells with gene and chromosomal abnormalities.

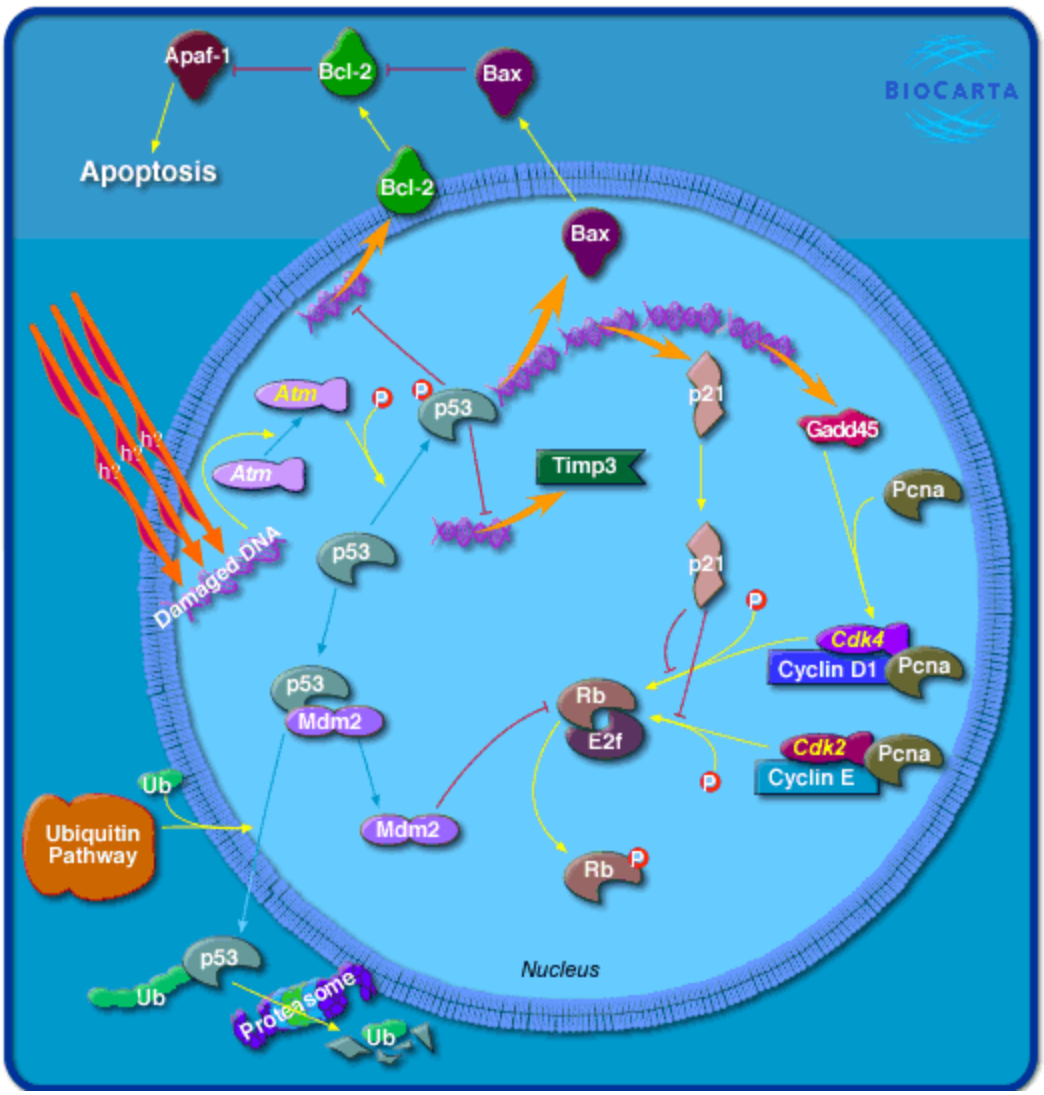

Figure 2-2. Activation of the p53 signaling pathway by radiation. p53 is a transcription factor whose activity is regulation by phosphorylation. Damage to DNA can lead to apoptosis via *Bcl2* and *Bax* transcription. Alternately, *Cdkn1a* (*p21*) transcription can halt the cell cycle until DNA is repaired http://main.biocarta.com/pathfiles/h_p53Pathway.asp).

Genetic background and radiosensitivity

Human radiosensitivity diseases

It is well-known that individuals differ in their sensitivity to radiation, and the role of genetics in radiosensitivity is most evident in humans with radiosensitivity syndromes such as ataxia telangiectasia (A-T), Nijmegen breakage syndrome, xeroderma pigmentosum, and others (86). The mutated genes responsible for many of these diseases have been identified, revealing pathways and mechanisms of radiation response.

A-T is an autosomal recessive disorder which is primarily an immunodeficiency disease (208), but radiosensitivity is also a hallmark of A-T (93). Other characteristics of the disease include cerebellar ataxia, oculocutaneous telangiectasia, bronchopulmonary disease susceptibility, lymphoid tumors, and insulin-resistant diabetes (134). The gene which is mutated in A-T (ataxia telangiectasia mutated, *ATM*) was identified in 1995 (224). As mentioned previously, ATM plays an integral role in the DNA-damage response, both in the signaling to DNA-repair machinery to repair DSBs and in signaling cascades leading to cell-cycle checkpoint activation. ATM also is involved in repairing the DSBs formed during gene rearrangement of immunoglobulin and T cell receptor genes. This V(D)J recombination mechanism is defective in A-T patients, which lead to chromosomal abnormalities in lymphocytes and development of lymphoid tumors (269).

Individuals with Nijmegen breakage syndrome and ataxia-telangiectasia-like-disorder (ATLD) share some of the same DNA repair and DNA damage signaling defects with A-T patients. Nibrin (NBN, also known as NBS1), the mutated gene in Nigmegen breakage syndrome, is involved in the sensing of DSBs and the recruitment of ATM (274). NSB1, together with RAD50 and MRE11, form the MRN complex which binds to DSBs and undergoes conformational changes which activate ATM (205). ATLD also involves disruption of the MRN

complex but via MRE11 (258). Thus, it is not surprising that A-T, ATLD, and Nijmegen breakage syndrome patients display similar clinical symptoms.

While A-T, ATLD, and Nijmegen breakage syndrome are due to defective DSB repair and signaling, xeroderma pigmentosum (XP) involves defective nucleotide excision repair (NER). XP patients have defects in one of several “XP genes”, all of which are involved in various steps in the NER pathway. Individuals with XP are particularly sensitive to DNA damage from UV radiation, resulting in a 1,000-fold increase in susceptibility to cancer (126).

Mutations in *TP53* (the gene which encodes p53) increases cancer risk. As the “guardian of the genome”, p53 is responsible for monitoring the integrity of the genome and inducing apoptosis in genetically damaged cells (132). It is estimated that more than 50% of human tumors contain a mutation or deletion of the *TP53* gene (265). Some patients with Li-Fraumeni (LF) syndrome carry inherited, heterozygous mutations of the *TP53* gene which is correlated with high cancer risk (273). Cultured fibroblasts from patients with LF sustain less IR-induced permanent G1 arrest than normal fibroblasts which leads to increased G1 chromosomal radiosensitivity (28).

While many of these diseases are associated with increased cancer risk and substantially increased radiosensitivity, more subtle mutations in these genes, and other genes in these pathways, can lead to differences in acute tissue reactions in radiotherapy-treated patients (51).Determining the polymporphisms and/or mutations underlying genetic predisposition to radiosensitivity is an area of intense research, with profound implications on radiotherapy treatment and radiation exposure guidelines.

Radiosensitivity and mouse models

Striking variation in sensitivity to radiation is also apparent in murine models. In 1963 Roderick published a seminal work on the differences in radiation sensitivity between inbred mouse strains (217). Beginning at 4 months of age, mice from 27 strains were exposed to daily

doses of 1Gy x-ray radiation until they died. The most susceptible strains, including CBA/J and BALB/cJ, succumbed to the radiation in approximately 16 days, while the most resistant strains, such as 129/J, survived more than twice as long. It has since been determined that the radiosensitivity of BALB/cJ mice is due in large part to two mutations in *Prkdc*, the gene which encodes the catalytic subunit of a DNA-break-dependent protein kinase (DNA-PK), resulting in decreased expression and enzymatic activity (298). As mentioned previously, DNA-PK is known to be involved in double-stranded break repair and signal transduction following exposure to IR (242).

According to Roderick's study, C57BL/6J and DBA/2J have an intermediate radiosensitivity phenotype, differing in survival by an average of 3 days (217). By lowering the challenge dose as low as 5cGy, Nomura, et al. revealed significant differences between C57BL/6J and DBA/2J in radiation-induced apoptotic rates within various tissues (193). Numerous studies have highlighted the innate differences in radiosensitivity of the two strains, with C57BL/6J generally considered more resistant to radiation-induced genomic instability and DBA/2J more sensitive (193, 281, 288). Wright and colleagues determined that the strains exhibit differences in apoptotic rates in the spleen following whole body exposure to 1Gy x-ray radiation (279). These differences were found to be correlated with differential induction of p53/p21 pathways (57, 140, 279). C57BL/6J mice undergo early induction of p53 and subsequent up-regulation of pro-apoptotic *Bax*, while DBA/2J mice display a later but more prolonged p53 response and increased expression of *Cdkn1a*, leading to cell cycle arrest. The increased apoptotic rate in C57BL/6J prevents the incorporation of radiation-induced mutations and chromosomal aberrations into the genome and allows the tissue to return to homeostasis (140).

While the BALB/cJ *Prkdc* mutations and human radiosensitivity diseases are examples of highly penetrant genetic variants which alter radiation response, it is assumed that radiation

sensitivity within the general population is due to the combinatorial effects of inherited genes of low penetrance, which are by nature more difficult to characterize, especially at low doses. Differing radiosensitivity between mice of different genetic backgrounds make them excellent models for understanding the underlying genetic networks responsible for radiosensitivity in the human population.

Low dose radiation biology

Importance and challenges of LDR biology

While the biological effects associated with high dose radiation (HDR) exposure are fairly well characterized, the effects and long-term cancer risks from exposure to lower doses of radiation are less understood. As defined by the Department of Energy's Low Dose Radiation Research Program, low doses of radiation (LDR) are exposures at or below 10cGy. The LDR Research Program, the source of funding for this research, is particularly interested in the study of cellular and molecular responses to IR, particularly low-LET radiation, with doses at or near current workplace exposure limits (http://lowdose.energy.gov/).

Standard epidemiological and toxicological approaches have been used for decades to attempt to characterize the health effects of LDR. However, the radiation doses of interest are just above natural background radiation levels, making measurable health risks to the human population arduous. In addition, the radiation endpoint of utmost concern, cancer, is a multi-factorial process which takes years to develop. Therefore, the current exposure standards for the protection of the public and workforce have been set by using models to predict LDR-attributable cancer risk from data obtained from much higher exposures (195).

As mentioned above, the continued increase in the use of radiological imaging has exposed a larger portion of the U.S. population to radiation doses which are significantly above natural background radiation, but are still within the "low dose range." A clear understanding of

the risks involved with LDR exposure is needed for a meaningful risk-reward analysis of such radiation exposures.

Models for estimating LDR risk

The currently accepted method for low-dose risk assessment endorsed by the U.S. National Academy of Sciences' Biological Effects of Ionizing Radiations (BEIR) VII report (195) and the International Commission on Radiological Protection (ICRP) is a linear-no-threshold (LNT) extrapolation of LD cancer risk from HD data. According to the LNT hypothesis, risk is directly proportional to radiation dose. This risk estimation model has formed the basis of human radiation protection practices since the 1960s (105). In support of this assumption, it has been shown that there is a linear relationship between DNA damage and radiation dose (219). LNT suggests that radiation-induced DNA damage accumulate over time and increase risk of carcinogenesis. This LNT principle is known as the "collective dose" concept, or "dose additivity", which assumes that risk can only increase with additional exposure (169). LNT also assumes that cellular defense mechanisms are not influenced by dose or dose rate and that the mechanisms of carcinogenesis are the same for both HDR and LDR.

However, an increasing amount of evidence questions the validity of the LNT model. Alternatives to the LNT model include the linear threshold model, in which there is a lower-limit radiation threshold below which there is no detectible risk (257, 262), and a non-linear model with decreased risk at LD levels, which takes into account the phenomena of hormesis. According to hormesis, low levels of radiation exposure can actually reduce risk to radiation-induced detrimental outcomes, such as cancer, while the risk at higher doses of radiation is linearly correlated with dose (79). Numerous studies have shown that exposure to a low dose of radiation prior to a high dose actually decreases risk (65, 109, 232, 297), which is in direct opposition to the "dose additivity" tenant of the LNT model. In contrast, other radiation effects,

such as transmissible genome instability and bystander effects (both discussed below), could result in an increase cancer risk at low doses, and therefore, the LNT would under-estimate LDR risks (141). Accurate assessment of risks from LDR exposure is essential for the development of adequate radiation exposure limits imposed by governments.

The LDR Research Program provides funds to projects which directly test the mechanisms and pathways involved in low dose radiation response at a systems level in order to ascertain the radiation-induced perturbations of normal physiology. The overall goal is to characterize an organism's radiation response through all levels of biological organization, from genes and genomes to cells, tissues, and the organism as a whole. From these data, low dose radiation risk can be more easily and accurately predicted for an individual as opposed to a simple, linear extrapolation from high dose radiation risk.

CT scan debate

As mentioned above, the American population is exposed to an ever increasing amount of radiation through medical imaging procedures. This has raised concern over the increased cancer risk from diagnostic radiology, especially that of CT scanning. In a 2007 landmark (and very controversial) report published in The New England Journal of Medicine (NEJM), Brenner & Hall concluded that within a few decades, 1.5-2% of all cancers within the U.S. population could be caused by the current rates of diagnostic CT (33). This conclusion was reached by using a LNT model of extrapolating LD from atomic bomb survivor data (229). They also point out that children exposed to IR from medical imaging are at higher risk than adults. The results of this article were made known to the general public through large media outlets, and a heated debate within the professional radiation research and medical fields ensued. Those who argued against the conclusions of Brenner & Hall's results cited errors in the methodology used to estimate the risk. Shortly after the original publication, The NEJM published three letters to the

editor from leading radiation researchers who questioned the validity of the LNT extrapolation model used to compute risk (78, 187, 263). In addition, Scott et al. published a lengthy editorial in which they critique the assumptions and methods used by Brenner & Hall (229). Scott et al. focused on the adaptive responses of humans to IR, a topic which is discussed in detail later, and concluded that there is evidence that radiation exposure from CT scans could reduce the risk of cancer development among irradiated adults. While they do concede that the impact of diagnostic radiation exposure on children is less clear, Scott et al. discount the validity of the LNT model-based risks estimates derived for children by the extrapolation from atomic bomb survivors. In a very recent editorial in The NEJM, Brenner emphasizes that CT imaging is overused, and effective non-radiological imaging methods (i.e., magnetic resonance imaging, MRI) are sufficient diagnostic tools in many situations (31).

Responses to LDR

Non-targeted effects and adaptive responses modulate cellular responses to both HDR and LDR (176). Here these effects are discussed within the context of shaping the dose-response curve at low doses of IR.

Non-targeted effects: Genomic instability and bystander effects

Radiation's carcinogenic potential is not just a result of DNA damage and subsequent misrepair of the damage as once believed, but it is also a result of non-targeted effects in that biological effects of radiation exposure can be observed in cells whose nuclei were never directly irradiated (174, 175). These non-targeted effects, also known as epigenetic effects, are heritable genetic changes that are not primarily a result of DNA sequence modification (276). Non-targeted effects include genomic instability and bystander effects, both of which can exaggerate the effects of LDR and result in a supralinear dose-response curve at low doses.

Radiation-induced genomic instability (RIGI) is a delayed, long-lasting effect of IR exposure that is characterized by a high levels of non-clonal mutations in the apparently healthy cells which survived the radiation exposure (183). The genetic alterations include mutations, deletions, chromosomal rearrangements, micronuclei formation gene amplification, and cell killing. Chromosomal instability is probably the most obvious alteration and the best characterized. Genomic instability is evident in most cancers and is observed in pre-malignant states, and thus appears to play a role in carcinogenisis (148). Understanding the initiation and perpetuation of RIGI may reveal some of the mechanisms of radiation-induced cancer formation (119).

Genomic instability following low dose radiation exposure is thought to involve bystander effects. Radiation-induced bystander effect (BSE) is a non-targeted effect where non-irradiated cells exhibit typical radiation responses, e.g., chromosomal instability (RIGI), cell death, DNA damage response signaling, etc. (183). Considerable inter-individual variability in the elicitation and response to RIGI has been observed (182). Proposed mechanisms for RIGI effect involve gap junction communication and the release of soluble factors by irradiated cells.

Bystander effects are studied in vitro by a variety of methods including co-culturing irradiated and non-irradiated cells, transferring media from irradiated cells to non-irradiated cells, using very low doses of α-particles such that not every cell receives an α-particle, or using a focused microbeam irradiator (183). Bystander effects were first demonstrated in vivo using *Patched* heterozygous mice, which are susceptible to cerebellar tumor formation which is accelerated with irradiation (160). When Mancuso and colleagues developed a lead shield to protect the brains of the mice during irradiation of the skin, there was an unexpected enhancement of cerebellar tumor formation. DSBs and apoptotic cells were observed within the shielded cerebella. They provided evidence of gap-junctional intercellular communication of the bystander effects in the central nervous system (160). Wright and colleagues demonstrated a

genotype-dependent bystander effect by exposing normal hemaopoietic clonogenic stem cells to bone marrow-conditioned medium from irradiated mice (151). The descendants of the hemaopoietic cells demonstrated chromosomal instability while the descendants of the directly irradiated cells did not. This effect was genotype-dependent because it was observed in bone marrow cells from CBA/Ca mice, who are susceptible to radiation-induced acute myeloid leukemia (r-AML), but not in C57BL/6 mice, who are resistant to r-AML. The source of the bystander effect was determined to be macrophages through a signaling mechanism which involved tumor necrosis factor-α, nitric oxide, and superoxide (151). Other data supports mechanisms involving cytokine signaling, specifically transforming growth factor-β (165) and oxidative stress due to mitochondrial dysfunction (119). Interestingly, irradiation of cell culture medium alone (e.g. in the absence of cells) with alpha particles can also induce bystander effects (138).

Adaptive responses

A sub-lethal exposure to radiation which is above background elicits stress responses and stimulates adaption. The adaptive responses can provide protection for the cell/organism, e.g., the hormesis effect. Adaptive protection develops within a few hours after exposure but may last for several months or weeks depending on the mechanisms and tissues involved and appear to have maximum effectiveness at about 10cGy total dose (Fig. 2.3) (79). Adaptive responses to radiation involve molecular scavenging, molecular repair, and removal of damaged cells (79, 80). Molecular scavenging involves oxidative stress response, and molecular repair mainly involves DNA repair (see *Radiation-induced cell damage and repair* section above). Adaptive protection is discussed in terms of hormesis. There are three main types of hormesis (40, 228):

- *Radiation conditioning hormesis*: A small radiation dose activates protective processes which suppress harm form a subsequent, larger radiation dose

A

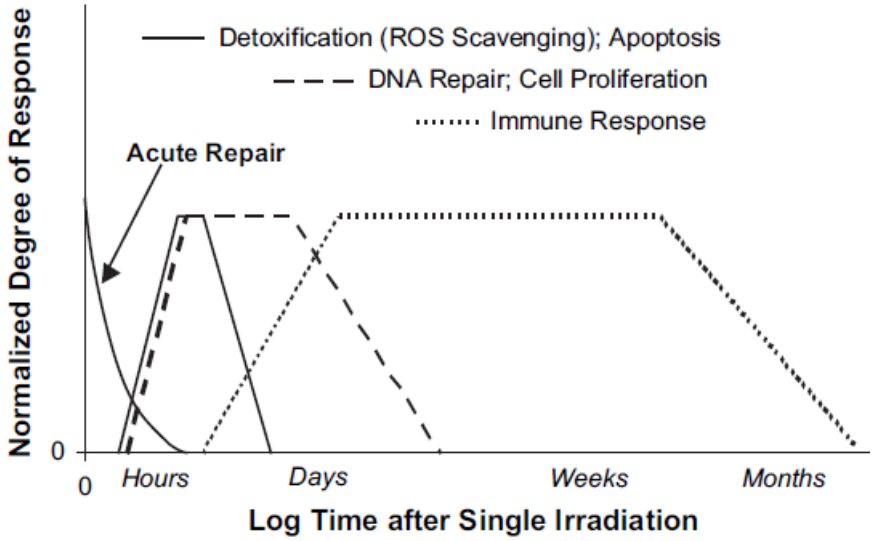

B

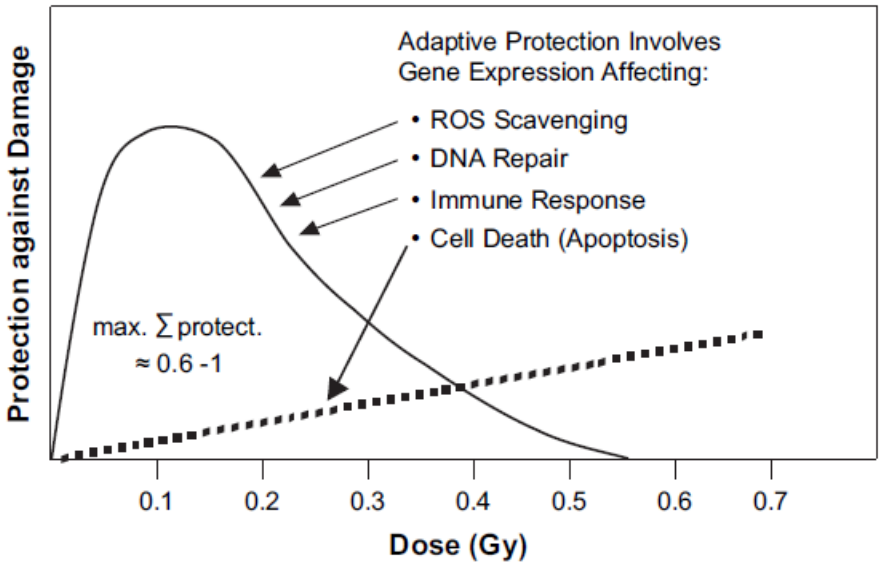

Figure 2-3. Adaptive protection from low dose (low-LET) induced adaptive protection. (A) LDR may induce adaptive responses affecting various levels of biological organization which can occur within hours of exposure and last for several months. (B) DNA damage and apoptosis increase linearly with dose, but other adaptive protections have maximum effectiveness around 0.1Gy. Image courtesy of Feinendegen, 2005 (79).

- *Radiation hormesis*: A small radiation dose activates protective processes and reduces harm below the spontaneous level.
- *Radiation post-exposure conditioning hormesis*: harm caused by a large radiation dose (or another agent) is reduced when a subsequent small radiation dose is administered.

Generally, discussions of “adaptive responses” are referring to *radiation conditioning hormesis*. The first demonstration of *radiation conditioning hormesis* was published in 1984 (198). Olivieri et al. reported that when human lymphocytes were cultured with radioactive thymidine (a source of low-level β-radiation at a total dose of 150cGy) prior to a 1.5Gy x-ray exposure, fewer chromatid aberrations were observed compared to lymphocytes not pre-cultured with radioactive thymidine. The authors speculated that cellular defenses or repair was increased following the low dose exposure, or “priming dose”, which protected the cells from the higher dose, or “challenge dose”. This effect has also been demonstrated in vivo (65, 112, 170, 171). The protective effect is time-dependent and dose-dependent. For example, when a 50mGy priming dose was given to C57BL/6J mice prior to a mid-lethal (5.9Gy) challenge dose, the protective effect (e.g., increased survival) was observed when the challenge dose was given 1, 3, or 7 days later but not 6 hours or 3.5 weeks later. A variety of priming doses were tested (50-400mGy), but the hormetic effect was only observed at the 50mGy dose (112). However, priming doses as low as 0.001mGy have been observed to induce adaptive responses prior to a 1Gy challenge dose (65). Interestingly, the adaptive response was also evident if given when the high dose was given prior to the low dose (65), an example of *radiation post-exposure conditioning hormesis.* These adaptive responses have also been described in the lymphocytes of people exposed to clinical radiation (173) , and occupational radiation (18), as well as those exposed in the Chernobyl accident (200). It is important to note that there is considerable

variability in the adaptive response between individuals (25, 215), and it is clear that dose rate as well as absorbed dose and radiation quality are primary variables.

The first demonstration of a pronounced *radiation hormesis* effect was more that 30 years ago (267). Gamma irradiation was shown to decrease neoplastic transformation in RFM mice, which have a high rate of spontaneous lung-cancer and exhibit high genomic instability burdens, but evidently the authors attributed the results to systematic errors in their lung cancer detection methodology (228). The first report of in vitro radiation hormesis was by Edouard Azzam in 1996 (13). Mouse embryo fibroblasts had a three- to four-fold decrease in the rate of spontaneous neoplastic formation when exposed to a single LD x-ray exposure (as low as 0.1cGy). This finding suggested that LDR can induce cellular processes which protect the cell from naturally occurring alterations which lead to cellular transformation. Since then, numerous studies have demonstrated a radiation-induced cancer protection (41, 98, 101, 122, 143, 170, 194). Many of these effects are thought to involve radiation-induced modulation of the immune system, which is discussed in detail below.

Impact on LDR-response models

Both bystander effects and adaptive responses are potential modifiers of low dose radiation risk, neither of which is taken into account in linear extrapolation of risk from HDR data. However, the two phenomena appear to have conflicting effects on LDR risk. BSE tends to exaggerate the effects of LDR by eliciting detrimental effects to non-irradiated cells, while adaptive responses following LDR are protective. Both effects can impact the shape of the dose response curve at low doses, but how these two phenomena interact and effect overall LDR risk is unclear.

An example of the interaction between a particular BSE and adaptive response in human–hamster hybrid A_L cells was reported by Zhou et al. (303). A priming dose of x-rays given 4 hours before α-particle irradiation with a microbeam significantly decreased bystander

mutagenic response in the nearby cells which did not receive the α-particle irradiation. Therefore, the adaptive response decreased the bystander mutagenesis. However, bystander cells demonstrated an increased sensitivity following an additional challenge with x-rays. The authors concluded that LDR biological responses are a result of a complex interaction between directly induced radiation effects, bystander effects, and adaptive responses. Because these interactions are poorly understood, some radiation biologists believe it is premature to determine if the LNT model overestimates or underestimates the risk at low doses of radiation (176).

LD enhancement of immunity

There is no doubt that high doses of radiation results in immunosupression, which is often attributed to lymphocytes being particularly sensitive to radiation-induced apoptosis (166). However, numerous studies have indicated that LDR can actually be immunostimulatory. In humans, this is demonstrated in the treatment of chronic lymphocytic leukemia and low-grade non-Hodgkin's lymphoma (222). Typical treatment regiments include low dose fractions (0.1 – 0.25Gy) which are given several times a week for a total dose of approximately 1.5Gy. This low dose rate is as effective in inducing long-term remission as chemotherapy treatment (113). Generally high doses of radiation are given during radiotherapy treatments because HDR is much more effective at cell killing. The effectiveness of the LDR treatment in these cancers therefore appears contradictory. It has been proposed that the efficacy of the LDR treatment is not due to direct cell killing, but rather an enhancement of immune system function (222). In other words, the LDR stimulates the immune system to recognize and kill the cancerous cells. There are numerous studies in experimental rodents which demonstrate a similar effect in that LDR can protect against tumor growth and metastasis in an immune-mediated fashion (41, 98,

101, 122, 143, 194). As mentioned above, these studies demonstrate *radiation hormesis*. The immune system enhancement has been demonstrated through (77, 222) :

- The augmentation of immune cell proliferation in response to a mitogenic stimulus (8, 111, 192, 201, 234)
- The alteration of cytokine release (98, 104)
- Changes in expression of receptors on immune cells (144, 145)
- Enhancing signal transduction pathways in lymphocytes (146)

The modulation of immune response by LDR is dependent upon a number of factors including total dose (145), dose rate (109), and genetic background (234). In addition, the biological parameter of interest likely demonstrates a temporal relationship with the other factors (143). The dose-response curve can also be vastly different between various target cells. For example, lymphocytes and their related functions usually follow a “J” shaped curve, while macrophage activation may demonstrate a curve with one or more peaks across a given dose range (143). Therefore, experimental design is key when assessing the dose-response relationship of immunological parameters (143).

The immune system response is the result of a complicated interaction between multiple cell types within the context of the organism. We begin with a brief overview of the anti-tumor and ant-metastasis effects of LDR, followed by a review of the reported LDR effects on particular immune cell populations.

Anti-tumor & anti-metastasis effects of LDR

As mentioned above, LDR has been shown to protect against tumor growth and/or metastasis in a number of in vivo mouse models. There are three general experimental models used to test for these effects.

The first experimental design takes advantage of mice models which have a high spontaneous cancer, such as Trp53(-/+) mice. These mice have a high incidence of lymphomas and osteosarcomas. Mitchel et al. measured the effects of a single LD (1 or 10cGy) γ-irradiation on lymphoma and osteosarcoma frequency and latency in Trp53(-/+) (171). Radiation exposure had no effect on tumor frequency, which indicated that the radiation treatment had no effect on tumor initiation and thus all tumors were assumed to have formed spontaneously. Mice which received the lower radiation dose (1cGy) had significantly increased tumor latency for both lymphoma and osteosarcoma compared with control, indicating that the LD exposure reduced the rate of malignancy in the spontaneously-initiated tumors. Interestingly, the higher dose (10cGy) delayed lymphoma latency longer than the lower dose, but it decreased osteosarcoma latency compared to controls. This study suggested that the 10cGy dose could increase or reduce risk of *metastasis*, depending on the tumor type. Therefore, increased tumor surveillance could have been enhanced by the LDR.

Another common experimental design involves the injection of tumor cells into LDR-treated mice. For example, a study by Hosoi & Sakamoto demonstrated that mice which received low doses of radiation prior to or just after tail injection of squamous cell carcinoma cells developed a significantly fewer lung tumors compared to controls (101). The effect was observed for doses of 15 – 20cGy given from 9 hours before to 3 hours after the tumor cell injection. A similar suppressive effect was also observed in the spontaneous lung metastasis (101).

Lastly, there are a few examples in which high dose cancer induction was suppressed by pre-irradiation with LDR. In one such study, Ina et al. monitored the induction of thymic lymphomas following exposure to high doses of fractioned X radiation (totaling 7.2Gy) in C57BL/6 mice which were pre-irradiated with 7.5cGy x-rays given 6 hours prior to each high dose irradiation (109). Sixty-three percent of the mice which received LDR prior to each HD

irradiation developed thymic lymphomas, compared to 90% of the mice who only received the HD irradiations. The lymphoma frequency was further suppressed to 43% in mice which received continuous γ-radiation (at 1.2mGy/hr) beginning 35 days prior to the first challenge dose. These results demonstrate a LDR-mediated decrease in *tumor induction*. Enhanced immune activities, as measured by increases in B cells, $CD4^+$ T cells, and antibody-producing cells in the spleen following immunization with sheep red blood cells, were observed in the continuously-irradiated mice (109). While tumor immunity is a very complex process, the parallel between tumor suppression and enhanced immune function suggests the involvement of immune activation in tumor suppression by low dose radiation (109), although the specific mechanisms involved remain to be determined.

It is hypothesized that immune system activation plays a key role in the LDR-induced suppression of tumor induction and metastasis. Numerous studies have looked at the effect of LDR on specific immune cell populations (i.e., T cells, B cells, macrophages, etc.), as discussed below.

LDR effects on T cells

Cells of the immune system are some of the most radiosensitive cells in the body (96). Radiation exposure results in alterations in lymphocyte counts, but it appears that lymphocytes within the mouse spleen are affected differently than those in the blood (206). Specifically, the numbers of $CD3^+$ T cells decrease in the blood of mice in a dose-dependent manner at moderate and high doses (0.5 – 3Gy γ-rays), while splenic T cell counts are only decreased with high doses. $CD19^+$ B cell counts are depressed in both the blood and the spleen at high and moderate doses (206). Interestingly, it appears that some radiation-induced changes in lymphocytes can persist chronically in humans, as is seen in atomic bomb survivors (high dose and high dose rate). Flow cytometry analysis of peripheral blood of survivors demonstrate

significant reductions in T helper (T_h) cells, but not T cytotoxic (T_c) cells or B cells (129). Others have demonstrated a decrease in T cell reactivity to mitogens and allogenic cells (2), and in the frequency of cells which secrete type 1 cytokines (128) in survivors. Depression or dysfunction of these lymphocytes can lead to serious health consequences, even increasing the risk for cancer (95). However, as mentioned above, there is evidence that exposure to low doses of radiation can stimulate the immune system, particularly T cells, which are perhaps the most studied target cell of the LDR effect on immune system function.

One of the first demonstrations of LDR-induced augmentation of immune cell proliferation in response to a mitogen was reported in 1982 by Anderson & Troup (8). Splenocytes from LDR-exposed mice showed an increased response to various mitogens, and the authors suggested that T cells were the most responsive. Later it was confirmed that T cells were the primary cellular target of the LDR-induced proliferation augmentation (192). It was also shown that these target T cells expressed high levels of heat-shock proteins (Hsp-70 and Hsp-72) compared to those of controls. Furthermore, the T cells from LD-irradiated mice responded to stimulation by anti-CD3 antibodies by further up-regulation of these genes and proliferating more extensively compared to the T cell of sham-irradiated mice (192). Chronic exposure to low dose radiation has also been shown to activate lymphocytes. In mice exposed to a low-dose-rate (1.2mGy/ hour) of γ-radiation, $CD4^+$ T cells and CD8 expression on $CD8^+$ T cells were significantly increased, while B cells were significantly decreased (108). It has been suggested that the increase in “pro-mitogenic” effects which are evident following LDR are masked at higher doses due to an increase in thymocyte apoptosis (164).

One of the proposed mechanisms for the LDR enhancement and HDR inhibition of T cell activation involves alterations in signal transduction in lymphocytes. Total-body LDR has been shown to increase expression of TCR/CD3 molecules, up-regulation of the transcription factors *c-fos* and *c-jun*, and increase expression of interleukin-2 receptor (IL2R) on thymocytes (144).

LDR has also been shown to up-regulate the CD28 receptor on T cells (145). The CD28 receptor binds to the B7 ligand on antigen presenting cells (APCs), which is itself up-regulated following exposure to LDR or HDR. The interaction between CD28 on the T cell and B7 on the APCs leads to activation of the T cell, and therefore, immune function enhancement. In contrast, HDR exposure results in a down-regulation of CD28 and an up-regulation of CTLA-4, another B7 receptor which can lead to the down-regulation of T cell proliferation.

There is evidence that $CD4^+$ T cells are especially vulnerable to radiation exposure (94, 206). In a recent paper, Gridley et al. analyzed the effects of low dose rate photons at low dosages (1cGy, 5cGy, and 10cGy) on lymphocytes in the blood and spleen of mice following total body exposure (96). Interestingly, T cells, B cells, natural killer (NK), $CD4^+$ T cells, and CD4:CD8 T cell ratio in the spleen were depressed at all doses 21 days post-irradiation, but total T cells, $CD4^+$ T cells and NK cells were increased in the blood. The greatest effect was seen in the $CD4^+$ subpopulation in the 1cGy group. The authors speculate that low $CD4^+$ cell number in the spleen triggered homeostatic mechanisms in order to regain balance in the subsets. The authors also performed gene expression analysis on the $CD4^+$ cells isolated from spleen 1 – 2 hours post-irradiation, and found LDR results in a significant down-regulation of *Inha*, the gene which encodes the alpha subunit of inhibin, a member of the transforming growth factor beta (TGF-β) superfamily. Inhibin “inhibits” interferon-γ (IFN- γ) and interleukin-12 (IL-12) production by Th1 and dendritic cells, and it increases IL-4 and IL-10 production in Th2 cells. Thus, down-regulation of *Inha* suggests a shift in the Th1/Th2 balance towards the Th1 phenotype. Because Th1 cells are involved in cell-mediated immunity, low dose radiation exposure could enhance responses against virus-infected and enhance tumor immunity (95). Conversely, HDR has been shown to shift the Th1/Th2 balance towards the Th2 phenotype (284).

The effect of LDR on lymphocytes has also been shown to be dependent upon genetic background. Shankar, et al. demonstrated different reactivities in the splenocytes of C57BL/6J and DBA/2J mice following LDR (234). Spleenocytes, particularly $CD8^+$ T cells, from LDR-exposed C57BL/6J mice showed an augmented response to Concanavalin A (Con A) compared to controls, while the opposite effect was demonstrated in LDR-exposed DBA/2J mice. The Con A-stimulated spleenocytes from C57BL/6J irradiated mice demonstrated a reduction in p53 expression and reduced apoptosis compared to those from DBA/2J mice. Interestingly, the responses were shown to be dependent upon the mitogen used. When spleenocytes were challenged with *Mycobacterium vaccae*, C57BL/6J LDR-exposed mice demonstrated a suppressed response while BALB/c LDR-exposed mice had an augmented response. Thus, the LDR-induced alteration in lymphocyte activation appears to dependent upon antigen and genetic background. It also appears that p53 expression and induction of apoptosis appears to be involved in the differential responses (234).

Natural killer (NK) cells also play a key role in tumor immunity (127). High doses of radiation have been shown to impair NK cell activity (202), while LDR has been shown to increase NK activity (122). The enhancement of NK activity by LDR has been shown to delay tumor growth. The induction of antioxidant mechanisms, particularly glutathione, may play a role in the modulation of NK activity (122).

LDR effects on macrophages

The effect of low dose radiation on macrophage function is not as well characterized as the effects on lymphocytes, and there have been conflicting reports on whether LDR increases or decreases macrophage-mediated inflammation. Irradiation with a moderate radiation dose (0.5Gy) of x-rays has been shown to decrease macrophage oxidative burst in vitro, which could translate into reduced inflammation following radiation exposure in vivo (227). This effect,

however, is likely to be dose-dependent, and “low” doses (e.g., ≤10cGy) were not examined in that study. In contrast, LDR has also been shown to enhance the phagocytic activity of peritoneal macrophages (201), which could result in increased protection from a subsequent infection, for example. It has also been shown that macrophages isolated from LDR-exposed mice have enhanced cytolytic activity, as measured by the ability to kill L1 sarcoma or P815 mastocytoma cell targets in vitro (194). This enhancement may be at least partially due to increased amounts of nitric oxide released into tumor cell targets. This modulation of macrophage function could play a role in the LDR-induced inhibition of tumor metastasis, as the LDR-exposed mice also had suppressed development of experimental tumor colonies (194).

It has been demonstrated that total-body irradiation across a wide range of doses (0.05 – 6Gy) activates the Toll signaling pathway in peritoneal macrophages, which results in sustained stimulation of the pro-inflammatory cytokines IL-12 and IL-18 (233), as well as TNFα and IL-1β (252). The expression of the surface molecules CD80 and CD86 on macrophages is also increased following exposure to both low and high doses of radiation (116). Because macrophages respond similarly to radiation exposure regardless of dose, it is assumed that differential changes in immunity following LDR and HDR does not reside in the direct response of macrophages (233).

Other studies have suggested that the effects of LDR on macrophages are mainly indirect in that they are dependent upon interactions with other cells. Liu et al. investigated the interaction between spleenocytes and peritoneal macrophages from mice exposed to 7.5cGy x-rays (147). They reported a suppression of IL-10 expression in spleenocytes and a simultaneous increase in IL-12 expression by macrophages, which could contribute to a shift of the immune response in favor of Th1 differentiation. These data support the mechanism proposed by Gridley et al. using proton-radiation data (95). Another study suggested that LDR induces the release of IL-1β by irradiated macrophages which stimulates neighboring cells

(such as lymphocytes). These stimulated neighboring cells either release cytokines or interact directly with the macrophages to further stimulate them (104). This mechanism would also lead to the increased proliferation of lymphocytes.

LDR effects on dendritic cells

Additional support for the Th1 shift in response to LDR involves the role of dendritic cells. In one study, splenic dendritic cells (DCs) were pre-irradiated with 0.02-1Gy of γ-radiation and were cultured with allogenic T cells (236). The DCs which were pre-irradiated with 5cGy radiation demonstrated the highest proliferation capacity of T cells. Dendritic cells were shown to have increased production of Th1 cytokines, including IL-2, IL-12, and IFN-γ, which suggests that the LDR augments T cell activation capacity through the increased cytokine production by DCs. The authors speculate that LDR effects on DCs might cause a shift in naïve T helper cells to Th1 cells.

Systems Genetics Approach to LDR

Introduction to systems genetics

As described above, exposure to LDR results in a variety of changes within the organism. Ionizing radiation can damage DNA, alter gene expression, activate signal transduction pathways, alter intracellular oxidative status, etc. which can, in turn, result in systems level changes such as altered immune function. All of these responses are anchored to heritable variation which predisposes an individual to particular radiation outcomes. Studying each of these biochemical, cellular, and genetic factors in isolation is very useful in understanding particular radiation responses. However, to borrow the words of Aristotle, “The whole is more than the sum of its parts.” In this case, a comprehensive characterization of the health effects of LDR cannot be constructed without a holistic approach within the context of the

organism. Here, we use a systems genetics approach to characterize the genetic effects which modulate LDR-induced immune responses.

Systems genetics is an emerging branch of systems biology in which complex traits are analyzed using multi-scale phenotype data that is assembled into complex molecular and phenotypic networks in the context of genetic variation. The basic premise is that variations in DNA which associate with a particular disease or response (LDR in this case) impact the physiological processes involved with the response through molecular, cellular, tissue, and organism networks (238). Statistical methods and computational algorithms are employed to identify correlations between the multi-level phenotypes and the underlying genetic variants.

Reference populations and QTL mapping

Central to the experimental design of dissecting complex traits though a systems genetics approach is the use of a genetically heterogeneous population. Often genetic reference populations are used because they are genetically stable and therefore reproducible, allowing direct comparison of various treatments among genetically identical individuals. As a result, phenotypic data can be obtained over time from various experiments and investigators and integrated together. Once a sufficient number of polymorphisms within the population are identified and the data made publicly available, researchers do not have to undergo the arduous and costly task of genotyping individuals for each experiment.

Recombinant inbred (RI) mouse strains are valuable genetic reference populations. A RI panel is created from the intercross and subsequent sibling mating of (typically) two inbred mouse strains (called “parental strains” or “parentals”), but as many as eight parental strains have been used, as seen in the Collaborative Cross (53). The generation of RI lines from two parental strains is initiated with the formation of F1 progeny from crossing of the two parentals (Fig. 2-4). When the F1 progeny are crossed to produce the F2 generation, the original parental

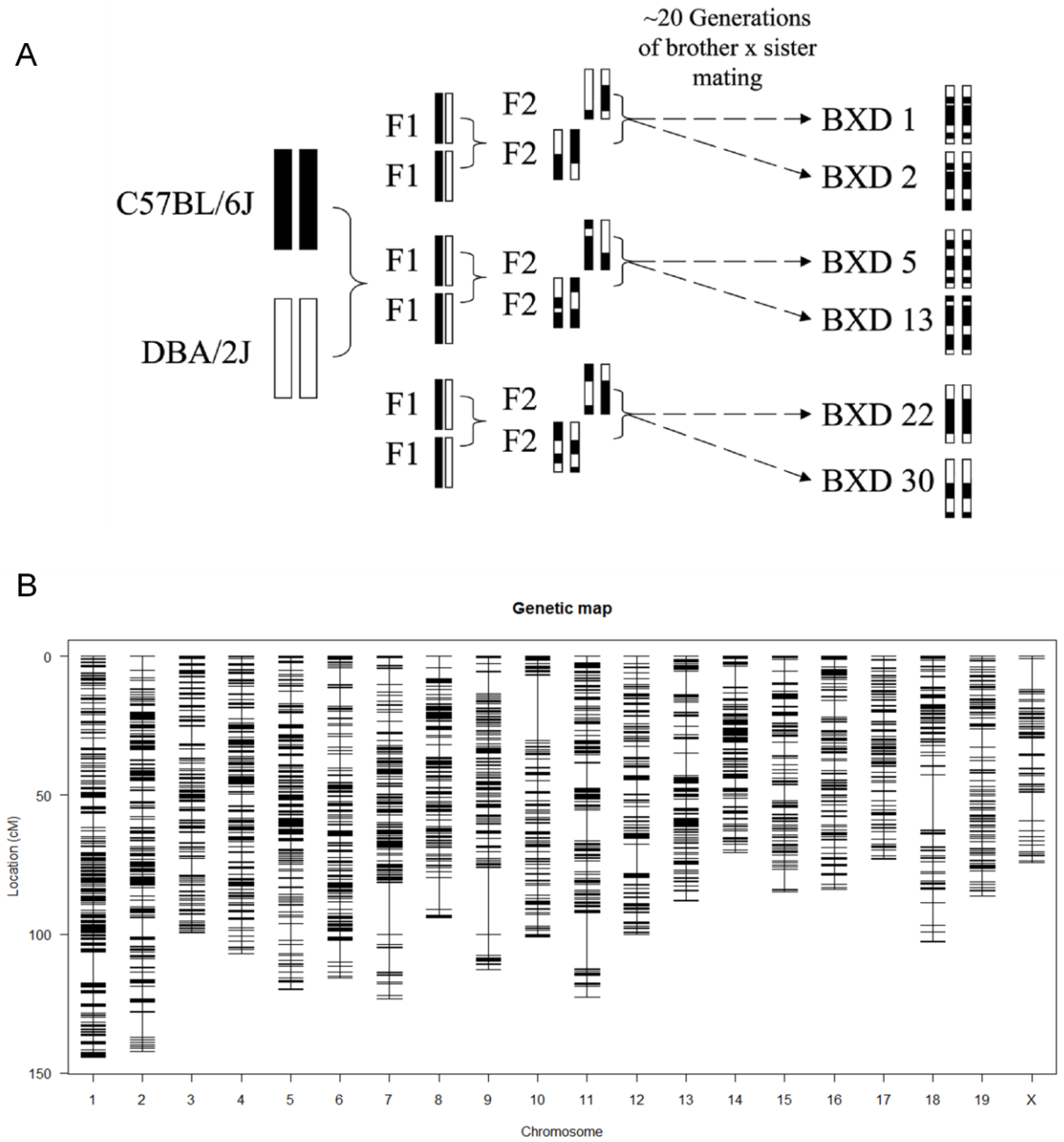

Figure 2-4. BXD recombinant inbred mice. (A) Mating scheme for the creation of the BXD recombinant inbred (RI) panel. The parental strains (C57BL/6J and DBA/2J) are mated to produce an F1 generation. F1 mating produces the F2 generation whose genome is a mixture of the parental strains. Brother-sister mating for more than 20 generations leads to a fixation of the genome. The resulting RI strains are genetically different from one another as each strain has a unique combination of loci from the parental genomes. (B) Genome locations of the ~3,800 polymorphic markers in the BXD RI panel. R/QTL (34) was used to produce a genetic map using the markers downloaded from GeneNetwork (http://www.genenetwork.org/).

genomes are shuffled due to meiotic recombination. Pairs from the F2 generation are randomly chosen and continuous brother-sister mating for more than 20 generations results in the fixation of the genome. The resulting recombinant inbred lines have a unique combination of loci as a result of the meiotic recombination in the crossing of the F1 generation. RI strains are valuable resources for mapping of Mendalian and quantitative traits. One of largest mouse RI panels is the BXD (C57BL/6J X DBA/2J) strain panel, which consists of 81 extant strains (207, 259, 260). The publically available genotype data for the BXD panel consists of nearly 3,800 informative single-nucleotide polymorphisms (SNPs) and microsatellite markers throughout the genome (235). These markers are distributed throughout the genome (Fig. 2-4B) and make identification of loci responsible for quantitative traits relatively straightforward and rapid. Within the next year, additional markers for the BXD panel will be made available based on informative SNPs identified using the Affymetrix-based Mouse Diversity array (293) and will include ~580,000 SNPs (RW Williams, University of Tennessee Health Science Center, personal communication).

Quantitative trait loci (QTLs) are stretches of DNA which are closely linked to genes which underlie a phenotype of interest. Typically QTL analysis is performed on complex traits, or traits whose variability is due to the interactions of multiple loci. A large number of polymorphic markers throughout the genome of the reference population are needed to have sufficient power for informative mapping. QTL mapping is based on the premise that individuals with different alleles at the QTL marker locus will have different phenotypic means (131). This process has been used to identify genomic regions underlying a variety of human diseases (70) and radiation phenotypes (63, 282).

Transcriptomics and genetical genomics

Transcript levels also vary genetically and somatically within populations and are quantitative traits, with the loci associated with their abundance called expression QTLs (eQTLs) (48, 225, 226). Genetical genomics combines transcriptomics with standard QTL mapping to identify loci responsible for regulating gene expression (115). Transcriptomics, or the simultaneous quantification of all expressed transcripts within a cell or tissue, is made possible by technologies such as microarrays.

Genome-wide transcriptional profiling can be used to identify genes whose expression is differentially regulated following radiation exposure, which can reveal the mechanistic responses employed by the cell to respond to the challenge. These responses are temporally regulated and have been shown to be tissue-specific (136), dose-specific (69), and genetic-background dependent (60). By performing semi-quantitative reverse transcriptase PCR, Lee et. al demonstrated that the induction of LDR-responsive genes varied greatly between tissues of C57BL/6J mice following whole-body irradiation, indicated that genetic modifiers of radiation-induced gene expression act differently in different tissues (136). The expression of some p53-regulated genes, such as *Cdkn1a*, *Gadd45a*, and *Mdm2*, appears to up-regulated in response both LDR and HDR, but the magnitude of induction is dependent upon dose (4). Indeed, overall expression profiles following radiation exposure appear to be dose-specific (6, 69, 83, 149, 237). For example, Ding et al. compared gene expression changes following low dose (2cGy) and high doses (4Gy) of x-ray radiation in normal human skin fibroblasts (69). They reported quantitative and qualitative differences in gene expression patterns between the two doses and dose rates (20cGy/min for LDR and 2Gy/min for HDR). The genes which responded to LDR involved functions relating to cell-to-cell signaling, signal transduction, and DNA damage repair. In contrast, those which responded to HDR were involved in apoptosis and cell proliferation. These dose-specific responses in cultured cells support a non-linear correlation between the

biological effects of high and low dose radiation exposures. In addition to being tissue-specific and dose-specific, radiation-induced gene expression varies depending on genetic background. Our lab performed spleen transcriptional profiling in six strains of mice following whole-body LD x-ray exposure and identified significant differences in the both number of genes exhibiting radiation responsiveness and in the pathways in which the genes function (BH Voy, et al., unpublished data). Others have described differences in expression depending on genetic variability in response to HDR (60, 241). A study which integrated global gene expression and various radiation survival parameters (including apoptosis) across the 60 cell lines of the National Cancer Institute Anticancer Drug Screen (NCI-60) demonstrated that a set of radiation-induced cell cycle genes were commonly regulated across the panel, representing penetrant gene expression responses (5). Interestingly, they noted that radiosensitive and resistant lines were well discriminated by their basal expression patterns. They suggested that the basal expression could be even more informative of radiosensitivity than the radiation response signatures (5). Similarly, our lab analyzed differences in baseline spleen expression for correlation with various radiation outcomes.

Data integration

One of the advantages of using microarrays to assess transcript abundance is that the expression levels of all the genes are measured simultaneously allowing for the identification of genes whose expressions are correlated with each other. Genes with similar expression patterns are assumed to participate in common cellular pathways or functions, a concept termed “guilt by association” (75, 287). Computational algorithms can be used to identify interconnected genes and build gene networks. Gene correlation networks can be altered by LDR exposure, representing potential molecular pathways that mediate the radiation response (277).

Cumulating genotype data, expression data, and low dose radiation phenotype data may provide insights into LDR response, but the true power in a systems-genetic approach lies in the integration of these data together in a comprehensive fashion to reveal associations between DNA variation and LDR sensitivity and the molecular networks which drive those associations. Systems biology involves the integration of information through a hierarchy of networks beginning with genetic networks (genomics) that drive molecular networks (including RNA and protein expression networks) which are components of cellular networks that are interconnected to form tissue networks that define living systems (238). Complex phenotypes, such as low dose radiation responses, arise from the complex interactions of these networks.

CHAPTER III

GENETIC ARCHITECTURE OF BXD IMMUNOPHENOTYPES

This chapter is adapted from the following publication:

Lynch RM, Naswa S, Rogers GL, Jr., Kania SA, Das S, Chesler EJ, Saxton AM, Langston MA, and Voy BH. *Physiol Genomics* 2010.

The immune system plays a pivotal role in the susceptibility to and progression of a variety of diseases. Due to its strong genetic basis, heritable differences in immune function may contribute to differential disease susceptibility between individuals. Genetic reference populations, such as the BXD (C57BL/6J X DBA/2J) panel of recombinant inbred (RI) mouse strains, provide unique models through which to integrate baseline phenotypes in healthy individuals with heritable risk for disease because of the ability to combine data collected from these populations across both multiple studies and time. We performed basic immunophenotyping (e.g., percentage of circulating B and T lymphocytes and $CD4^+$ and $CD8^+$ T cell subpopulations) in peripheral blood of healthy mice from 41 BXD RI strains to define the immunophenotypic variation in this strain panel and to characterize the genetic architecture that underlies these traits. Significant QTL models that explained the majority (50 – 77%) of phenotypic variance were derived for each trait and for the T:B cell and CD4+:CD8+ ratios. Combining QTL mapping with spleen gene expression data uncovered two quantitative trait transcripts (QTTs), *Ptprk* and *Acp1*, as candidates for heritable differences in the relative abundance of helper and cytotoxic T cells. These data will be valuable in extracting genetic correlates of the immune system in the BXD panel. In addition, they will be a useful resource for prospective, phenotype-driven model selection to test hypotheses about differential disease or environmental susceptibility between individuals with baseline differences in the composition of the immune system.

Introduction

Systems genetics takes a top-down approach to disease susceptibility by seeking to identify relationships between genetic variants, intermediate molecular, biochemical and cellular pathways, and overlying systems-level phenotypes from large-scale molecular and phenotypic analyses. Typically, putative interconnections are built through correlational analyses of diverse data types collected across genetically heterogeneous populations. These data are often obtained using genetic reference populations, i.e., populations that are genetically stable and thus reproducible, allowing data integration across time and from diverse studies and creating the possibility to uncover novel relationships among genes, pathways and diseases. A number of genetic reference populations exist for mouse, the largest of which is the BXD (C57BL/6J X DBA/2J) recombinant inbred (RI) strain panel, consisting of 81 extant strains for which genotype data are publicly available (207). As the depth of phenotyping for a reference panel like the BXD strain set increases, so does the ability to interconnect physiological systems through genetic correlation of phenotypes. Such discoveries can be valuable for determining the molecular basis for a phenotype, for identifying biomarkers for disease processes, and for elucidating interconnections between apparently divergent physiological systems.

The burgeoning evidence that inflammation either initiates or fuels a wide variety of diseases and pathologies suggests that immune system components are likely to emerge in many systems-level networks of disease susceptibility. Disorders not traditionally linked with the immune system such as obesity and insulin resistance are now causally linked to inflammatory processes and mobilization of immune cells (100, 191, 283). While the abundance of specific lymphocyte subpopulations is altered by numerous environmental factors such as infection and diet (14, 261, 302), these traits are also under tight genetic control (3, 55, 125). The involvement of immune processes in myriad diseases, many of which have a genetic risk, coupled with a strong genetic basis for immune function, raises the possibility that genetic variation in immune

phenotypes *per se* may contribute to differential disease susceptibility between individuals. Supportive of this concept is a recent report by Dendrou et al., using the Cambridge BioResource, which is the human equivalent of a genetic reference population, consisting of ~5,000 healthy, genotyped individuals living near Cambridge, UK who agreed to be studied repeatedly over time (67). Dendrou and colleagues linked a specific T cell phenotype – relative expression of CD25 on the surface of $CD4^+$ memory T cells – with a haplotype previously shown to confer protection from type I diabetes. Understanding the genetic basis of specific immunophenotypes may therefore be valuable in understanding susceptibilities and/or progression of diseases, such as multiple sclerosis and rheumatoid arthritis, which are characterized by dysregulation or imbalances of distinct immune cell populations (59, 99, 240, 253).

As a first step toward determining the heritable differences in immunophenotypes that may predict outcomes of disease and environmental exposures, we profiled the abundance of major lymphocyte subpopulations ($CD79^+$, $CD3^+$, $CD4^+$ and $CD8^+$) in peripheral blood of healthy, unperturbed mice from the BXD strain panel. These data were integrated with existing genotype data in quantitative trait loci (QTL) mapping to characterize the genetic architecture that underlie these traits. They were further combined with microarray data we collected from spleens of the same strain panel to highlight potential candidate genes within significant QTL. Graph algorithms were used to identify gene expression networks that correlate with and are potential mediators of immunophenotypes, and are thus potential targets for environmental stimuli that act on the immune system. Herein we present evidence that peripheral immunophenotypes are under significant genetic control in the BXD population and describe genes and coexpression networks linking genetic variation to immunophenotypic diversity.

Methods

Animals

C57BL/6J, DBA/2J, and BXD RI stocks from strains 6 – 42 were obtained from The Jackson Laboratory (Bar Harbor, ME). BXD RI stocks from strains 43 – 100 were obtained from Dr. Lu Lu and Dr. Robert Williams from the University of Tennessee Health Science Center (UTHSC, Memphis, TN). BXD RI lines were housed and propagated in the specific-pathogen-free (SPF) Russell Vivarium at Oak Ridge National Laboratory (ORNL). Mice received irradiated Purina Diet #5083 and chlorinated water *ad libitum*. The housing conditions were maintained at 70 ± 2 °F and 40-60% humidity. A total of 45 BXD strains were used for spleen expression profiling, immunophenotyping, or both. This subset of the BXD panel was chosen from the set of strains maintained at ORNL based on consistent breeding performance and to represent a balanced combination of the original BXD strains developed at The Jackson Laboratory (259, 260) and the advanced intercross strains developed at the UTHSC (207). Between 10-12 weeks of age, mice were sacrificed by cervical dislocation and either blood was collected for immunophenotyping or the spleens were harvested for RNA expression profiling. All studies were approved by the Animal Care & Use Committee at Oak Ridge National Laboratory.

Immunophenotyping

Flow cytometry was used for the immunophenotyping of male and female mice (average of four mice/sex/strain) from 41 BXD strains and the parental strains. Blood was collected by retro-orbital sinus puncture into EDTA tubes and red blood cells were lysed using lysis buffer (Sigma-Aldrich, St. Louis, MO). Following centrifugation, the white blood cell pellet was suspended in buffer (PBS, 0.2% sodium azide, 0.02% heat-inactivated FBS) and divided into four aliquots for each set of monoclonal antibodies and a blank negative control. Lymphocytes were stained with the appropriate antibody or antibodies for 45 minutes at 4°C.

The negative control was incubated with PBS. One tube was dual-stained with anti-CD3 (PE, clone 17A2) and anti-CD79b (FITC, clone HM79b). Another tube was dual-stained with anti-CD4 (PE, clone H129.19) and anti-CD8a (FITC, clone 53-6.7). The remaining tube was stained with anti-MHC Class II (R-PE, clone NIMR-4). Antibodies were purchased from BD Biosciences (Franklin Lakes, NJ), except MHC Class II-RPE which was purchased from Southern Biotech (Birmingham, AL). Following incubation, the samples were centrifuged and suspended in PBS. All samples were stored on ice in the dark until analyzed by flow cytometry. At least 10,000 cells per sample were analyzed using a Beckman Coulter Epics XL flow cytometer (Brea, CA). Data were analyzed using EXPO32 ADC Software (Beckman Coulter). Lymphocytes were gated for analysis based on forward and side scattering profiles. The immunophenotypes (IPs) measured included the proportion of circulating T cells (%CD3), B cells (%CD79), $CD4^+$ T cells (%CD4), $CD8^+$ T cells (%CD8), as well as the median expression of major histocompatibility complex II (MHCII Median) on $MHCII^+$ lymphocytes (%MHCII).

Identification of immunophenotype QTL

Flow cytometric data were analyzed for quality based on efficient staining of lymphocytes and within-individual consistency (e.g., %CD79 approximately equaling %MHCII and sum of %CD4 plus %CD8 approximately equaling %CD3). Only high quality immunophenotype data were used for further analysis, resulting in an average of 3.3 males and 3.2 females per strain for each IP. T cell to B cell ratio, $CD4^+$ to $CD8^+$ ratio, and MHCII median fluorescence were normalized using natural log transformation (i.e., LN T:B, LN CD4:CD8, LN MHCII).

QTL analysis was performed using genotype data obtained from GeneNetwork (http://www.genenetwork.org/dbdoc/BXDGeno.html). This database contains nearly 3,800 informative single-nucleotide polymorphisms (SNPs) and microsatellite markers originally

reported by Shifman, et al. (235) that have been re-aligned with National Center for Biotechnology Information (NCBI) Build 36. QTL for each IP were identified using the QTL package (34) in R (http://www.r-project.org). The multiple imputation method of Sen and Churchill (230) was used to perform single-QTL genome-wide scans. Genome-wide significance thresholds were calculated based on 1,000 permutations (54). The cut-off *p*-values for significant and suggestive loci were $P = 0.05$ and $P = 0.63$, respectively (130).The ± 1 LOD support intervals for each QTL were calculated using the lodint function in R/QTL. Multiple-QTL modeling was performed using stepwise linear regression in SAS (SAS Institute, Cary, NC); a *p*-value of 0.05 was used as the threshold for terms to remain in the final model.

Expression profiling

Transcriptome profiling was performed in spleens from an independent set of mice representing 38 BXD strains (34 of which were immunophenotyped). Total spleen RNA was isolated from spleens stabilized in RNAlater (Sigma-Aldrich) using RNeasy Mini Kits (Qiagen, Valencia, CA). RNA concentration and quality were assessed using Experion RNA StdSens Chips on the Experion system (Bio-Rad, Hercules, CA). Each BXD sample profiled consisted of a pool of equal amounts of RNA from either two males or two females per strain. Expression profiling was performed by Genome Quebec (Montreal, Canada) using the Mouse WG-6 v1.1 BeadChip on the Illumina platform (San Diego, CA). Six strains were analyzed per chip. The data were normalized using Variance Stabilizing Transformation (VST) followed by Robust Spline Normalization (RSN) using the R/lumi package (74) in Bioconductor (87). Raw and normalized microarray data have been uploaded to NCBI's GEO database (http://www.ncbi.nlm.nih.gov/projects/geo; Accession GSE19935) according to MIAME standards (29). Expression data, along with all IP data, are also available through GeneNetwork (http://www.genenetwork.org).

Transcriptome Map and eQTL analysis

Of the 34,492 probes on the Illumina arrays, 11,445 transcripts demonstrated variable expression across the panel (coefficient of variation > 0.01) and were used for expression QTL (eQTL) analysis. QTL Reaper (http://www.genenetwork.org/qtlreaper.html) was used to identify the maximum likelihood ratio statistic (LRS) and a permuted *p*-value (1,000 permutations) for each transcript. QTL Reaper performs Haley-Knott regression for QTL analysis, with an adaptive permutation by transcript which runs an increased number of permutations for those traits with significant results to ensure precise *p*-value estimation at the low end of the *p*-distribution. This method is fast and sufficient for high density marker maps as are available for the BXD RI lines. At a *p*-value threshold of 0.05 over the entire array, 1881 transcripts were associated with 686 loci. These eQTLs were classified as *cis* or *trans* according to their genomic positions (located within or beyond 10Mb of transcription start site, respectively). Permutation testing was used to define the maximum number of transcripts likely to be associated by chance in *trans* with an eQTL. The 1881 transcripts were randomly assigned to the 686 significant loci; in 10 million permutations, the maximum number of transcripts associated in *trans* with a single marker was 19. Therefore we analyzed only the *trans*-eQTL bands in which a single marker was associated with 20 or more transcripts.

Statistical modeling and graph algorithm

MGI (http://www.informatics.jax.org) was used to extract genes located within the ± 1 LOD support intervals for the two significant QTLs identified for the CD4:CD8 immunophenotype. Stepwise linear regression in SAS was used to model the CD4:CD8 ratio using the expression of these genes. Graph algorithms were performed as described previously (277), and all source codes are available from the authors. Graphs were created from microarray data by computing all pair-wise Pearson correlations between expressed transcripts

and then filtering the matrix to retain only statistically significant correlations based on a false discovery rate of 5% (q-value < 0.05; (250)). Maximal cliques were extracted and anchored cliques identified as previously described (277). A bipartite graph was created with one partition being the expressed transcripts and the second partition being a set of five immunophenotypes (CD3%, LN T:B, CD4%, CD8%, LN CD4:CD8). Pearson correlations were computed between each possible pairing of transcript expression and immunophenotype. Edges in the bipartite graph were filtered to retain correlations of interest ($P < 0.001$) and maximal bicliques were then extracted. Gene ontology (GO) enrichment analysis was performed using DAVID (102); Benjamini-Hochberg false discovery rate-corrected *p*-values are reported (19).

Results

We began by profiling a panel of immunophenotypes (IPs) in male and female C57BL/6J and DBA/2J mice to define baseline differences in the two BXD parental strains. Peripheral blood was analyzed for proportion of circulating T cells ($CD3^+$), B cells ($CD79^+$), T helper cells ($CD4^+$), cytotoxic T cells ($CD8^+$), and expression of major histocompatibility complex II (MHCII) on $MHCII^+$ lymphocytes using flow cytometry. As shown in Table 3-1, the parental strains differ significantly in each of these traits ($P < 0.05$) except for $CD3^+$ cells ($P = 0.184$) and $CD8^+$ T cells ($P = 0.064$). C57BL/6J mice demonstrate a higher percentage of circulating B cells and $CD8^+$ T cells and lower levels of $CD4^+$ T cells compared with DBA/2J mice, which is consistent with previous reports (46, 186, 272).

The same panel of immunophenotypes was profiled across a set of 41 BXD strains to establish the immunophenotypic diversity in this RI panel and to model the genetic regulation of each trait. ANOVA indicated a significant effect of strain on each IP ($P < 0.0001$), manifested as broad ranges for each of the traits across the strains. For example, the percentage of T lymphocytes varies over 5-fold (10.3 – 56.1%) while the percentages of $CD4^+$ and $CD8^+$

Table 3-1. **Differences in peripheral blood immunophenotypes in C57BL/6J and DBA/2J mice.**

Immunophenotype	**C57BL/6J Mean**	**DBA/2J Mean**	***p*-value**
% CD3 Lymphocytes	32.06 ± 1.03	35.60 ± 2.21	0.1840
% CD79 Lymphocytes	61.40 ± 0.98	53.86 ± 2.73	0.0352*
LN T:B	-0.65 ± 0.03	-0.42 ± 0.09	0.0392*
% CD4 Lymphocytes	23.84 ± 1.64	31.56 ± 2.41	0.0190*
% CD8 Lymphocytes	7.98 ± 0.56	6.50 ± 0.47	0.0636
LN CD4:CD8	1.10 ± 0.10	1.58 ± 0.07	0.0012†
% MHCII Lymphocytes	61.62 ± 1.87	51.22 ± 2.64	0.0194*
LN MHCII Density	3.53 ± 0.16	4.31 ± 0.08	0.0003†

Data shown as mean ± SEM of 5 to 9 mice per strain. *P*-value indicates significance of strain effect (* $P < 0.05$, † $P < 0.01$).

lymphocytes vary over 6 fold (5.6 – 35.6% and 4.4 – 26.4%, respectively) (Fig. 3-1). These ranges relative to those of the parentals illustrate the genetic complexity of the traits and are within the range of the phenotypic diversity found in a survey of 32 standard inbred strains of diverse origin (22, 209). There is also a significant strain*sex interaction effect for each immunophenotype ($P < 0.05$), but the effect is much smaller (F statistic < 30%) than that of the main strain effects. Thus, overall strain effects were modeled for each immunophenotype.

QTL analysis was performed on each IP as well as the T:B and CD4:CD8 ratios to identify overlapping and unique loci associated with each trait. We began with MHCII density as a reference trait with a defined genetic basis on Chromosome (Chr) 17, a region in which the BXD parental strains carry different haplotypes (C57BL/6J carries the H-2^b haplotype and DBA/2J carries the H-2^d). Not surprisingly, the genotype at the H2 locus is the largest factor in explaining median expression of MHCII on MHCII-expressing lymphocytes (Fig. 3-2A). The locus itself accounts for 57% of the variance within the BXD panel (LOD = 7.52, $P < 0.001$), with the DBA/2J genotype increasing MHCII expression. A suggestive secondary locus, Chr 10 @ 114Mb, accounts for an additional 4.5% of the variance. The genetic basis for variation in the remaining immunophenotypes was modeled by first performing single model genome-wide scans (Fig. 3-2B,C) and then using suggestive and significant loci from those scans in multi-locus regression to allow for additive and interactive contributions of multiple loci. A 9Mb region on Chr 17 spanning the H2 locus was identified as either suggestive or significant for single model scans of each trait except for the CD4:CD8 ratio (Fig. 3-3). The majority of variance (50.1 – 77.5%) for each trait is explained by models incorporating the Chr 17 region in combination with at most three additional loci (Table 3-2). T and B cells were measured as a percentage of total gated lymphocytes and collectively represent the majority of this population, making these two measurements highly inversely correlated. Accordingly, the QTL models for each trait are very similar. The relative abundance between these two cell types (natural log transformed T:B

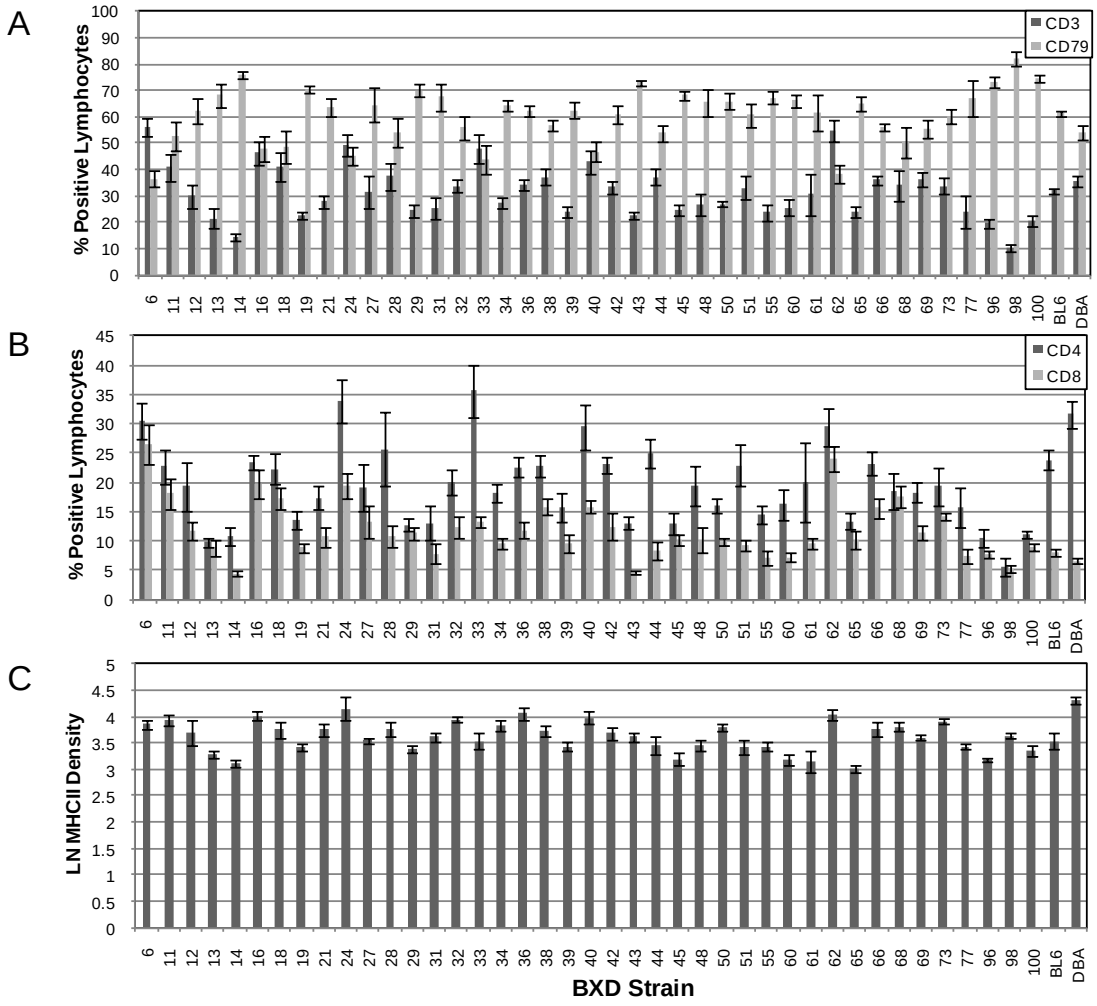

Figure 3-1. Peripheral blood lymphocyte subpopulations of BXD and parental strains. (A) %CD3 and %CD79 lymphocytes, (B) %CD4 and %CD8 lymphocytes, and (C) and MHCII density on MHCII+ lymphocytes (LN of median MHCII fluorescence). Data shown as mean ± SEM of at least 3 males and 3 females per strain.

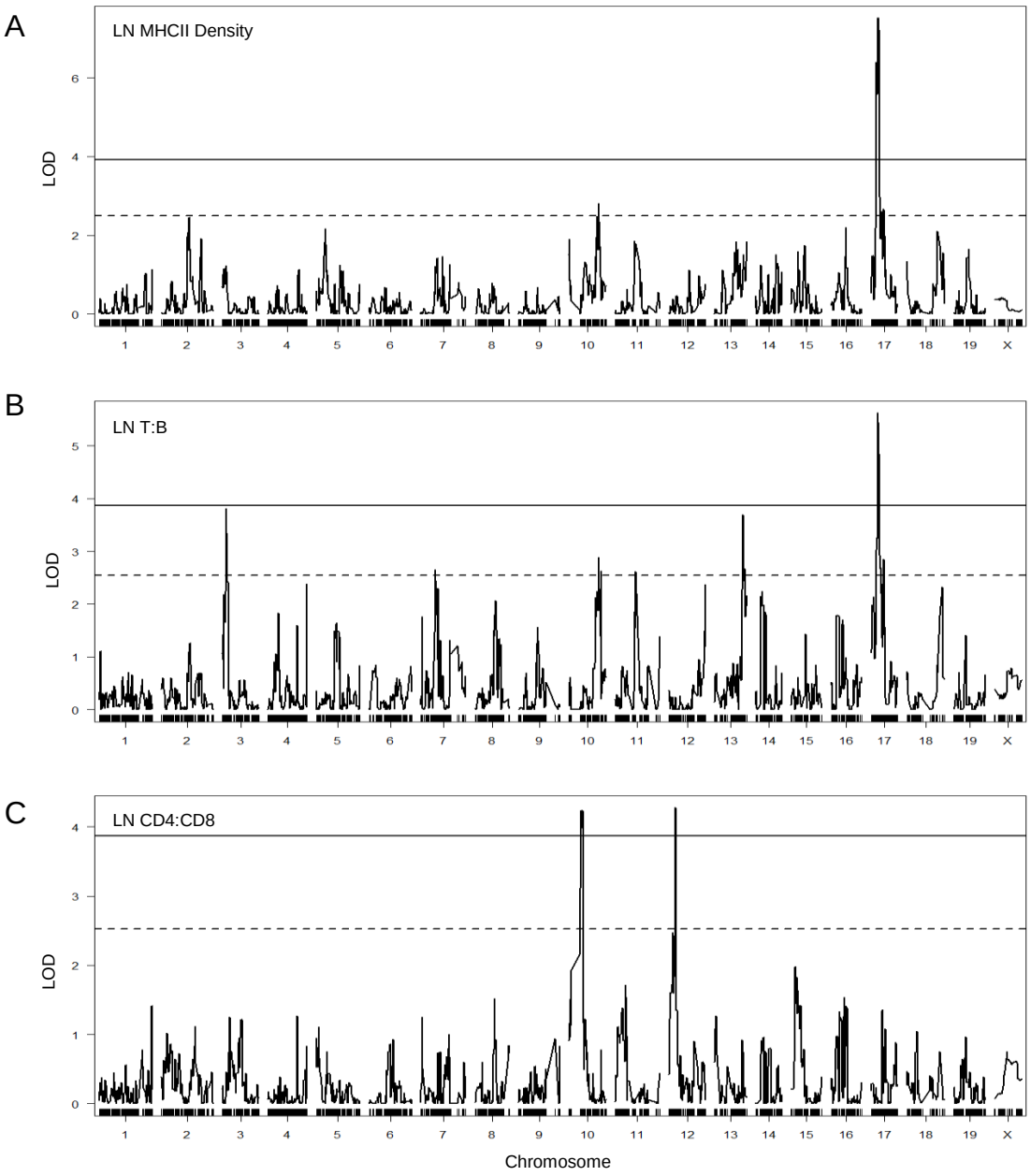

Figure 3-2. Genome-wide scans for peripheral blood immunophenotypes of 41 BXD strains. (A) MHCII density as measured by the LN of the median fluorescence of MHCII on MHCII^{+} lymphocytes, (B) T:B ratio as measured by the LN of the ratio of %CD3 to %CD79 lymphocytes. (C) CD4:CD8 as measured by the LN of the ratio of %CD4 to %CD8 lymphocytes. Solid horizontal lines represent genome-wide significance at $P < 0.05$, and the dashed lines represent $P < 0.63$, based on 1,000 permutations. LOD indicates logarithm of odds scores.

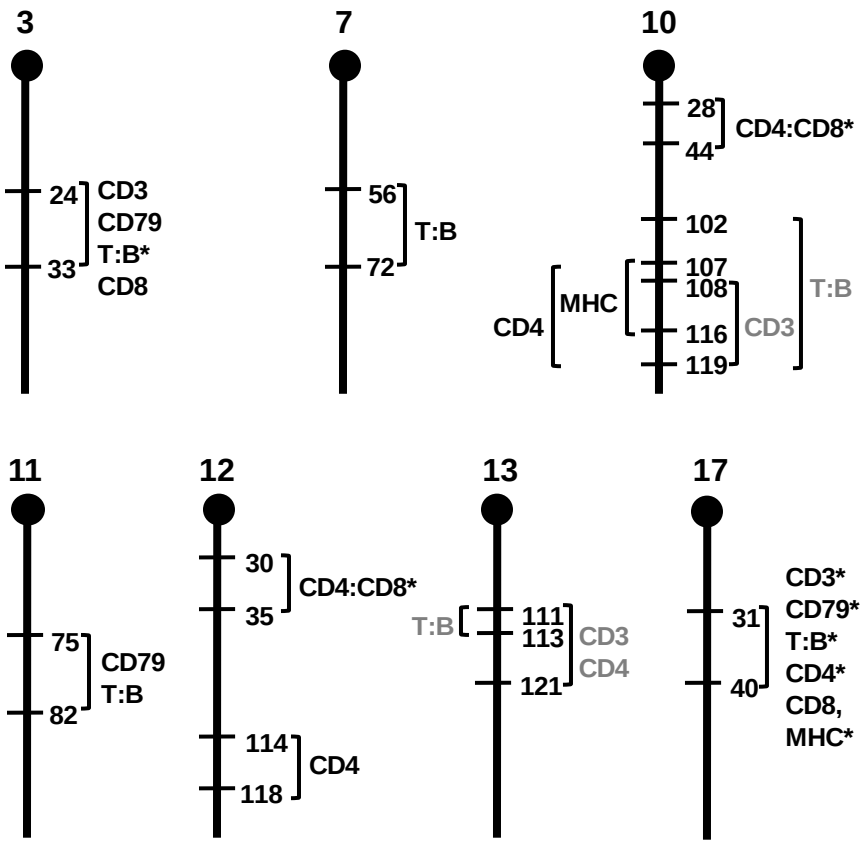

Figure 3-3. Summary of BXD immunophenotype (IP) QTLs. The ranges indicate the ± 1 LOD support intervals for each significant and suggestive QTL, in Mb. Immunophenotypes are %CD3 lymphocytes (CD3), %CD79 lymphocytes (CD79), LN of CD3:CD79 (T:B), %CD4 lymphocytes (CD4), %CD8 lymphocytes (CD8), LN of CD4:CD8 (CD4:CD8), and LN of MHCII median expression on MHCII^{+} lymphocytes (MHC). * indicates significant QTL ($P < .05$) in single-locus genome-wide scan. IP labels in black are QTLs that are significant in the final model ($P < .05$); gray IP labels are not significant in final model.

Table 3-2. Summary of final QTL models for BXD immunophenotypes.

Immuno-phenotype	Final Model	Variance Explained (%)	QTLs				
				Marker	Chr	Position	LOD
%CD3	Loc1*2 + Loc2	58.9	Loc1	rs13477026	3	27 Mb	3.72*
			Loc2	rs13482963	17	35 Mb	5.28*
%CD79	Loc1 + Loc2 + Loc3	67.2	Loc1	rs13477026	3	27 Mb	4.17*
			Loc2	rs13481119	11	79 Mb	2.54
			Loc3	rs13482947	17	31 Mb	5.41*
LN T:B	Loc1*2 + Loc1*4 + Loc3+ Loc4	77.5	Loc1	rs13477026	3	27 Mb	3.81
			Loc2	rs13479274	7	58 Mb	2.64
			Loc3	rs13481119	11	79 Mb	2.61
			Loc4	rs13482947	17	31 Mb	5.62*
%CD4	Loc1*2 + Loc3	50.1	Loc1	rs3690259	10	114 Mb	3.10
			Loc2	rs3694890	12	118 Mb	2.70
			Loc3	rs13482963	17	35 Mb	4.07*
%CD8	Loc1*2 + Loc2	56.6	Loc1	rs13477030	3	28 Mb	3.82*
			Loc2	rs3672987	17	33 Mb	3.79*
LN CD4:CD8	Loc1 + Loc2	53.8	Loc1	rs13480570	10	31 Mb	4.24*
			Loc2	rs6225272	12	31 Mb	4.28*
LN MHC Median	Loc1 + Loc2	61.5	Loc1	rs3690259	10	114 Mb	2.81
			Loc2	rs13482947	17	31 Mb	7.52*

Models were analyzed using significant and suggestive QTLs from single locus genome-wide scans. Representative SNP markers for each locus in the final models are reported; genome locations are according to NCBI Build 36. LOD indicates logarithm of odds scores based on single locus models. * indicates significant QTLs; all others are suggestive.

ratio, or LN T:B) was mapped to identify loci that may be involved in lymphocyte maturation. The T:B phenotype is partially explained by interactions between loci on Chrs 3 and 7 and between the Chr 3 locus and H2 locus. In combination with the additive effects of the H2 locus and an additional region on Chr 11, this model explains 77.5% of the variation in the T:B ratio. The only locus important in modeling the T:B ratio that was not identified for either lymphocyte population separately (i.e., %CD3 and %CD79) is the locus on Chr 7. The complete set of significant and suggestive QTLs for each immunophenotype is depicted in Fig. 3-3.

Genetic control of T cell abundance was further probed by mapping loci that contribute to variance in the major T cell subpopulations, $CD4^+$ and $CD8^+$ T cells. While QTL analysis identified the H2 locus as contributing to both %CD4 and %CD8 (LOD of 4.07 and 3.79, respectively), the remaining QTLs were unique to the particular T cell subpopulations (Fig. 3-3). A multi-locus model consisting of three loci (on Chrs 10, 12, and the H2 locus) explains 50.1% of the variance in %CD4, while a model consisting of a locus on Chr 3 with the H2 locus explains 56.6% of the variance in %CD8. The ratio of $CD4^+$ to $CD8^+$ cells was used in QTL analysis after normalization using natural log transformation (LN CD4:CD8). Two loci (Chr 10 @ 31Mb, LOD = 4.24 and Chr 12 @ 31Mb, LOD = 4.28) were identified as significant, independent contributors to this trait (Fig. 3-2C, Table 3-2). At both loci, the DBA/2J allele shifts the ratio in favor of $CD4^+$ cells, consistent with the increased abundance of $CD4^+$ cells in the DBA/2J parents (Table 3-1). These two loci explain nearly 54% of the variation in the CD4:CD8 ratio. Interestingly, neither region is implicated in control of either T cell subtype as analyzed independently, suggesting that these two regions contain genetic variation that contributes to a differentiation process in which one cell type is retained at the expense of the other.

Expression QTL (eQTL) profiling has emerged as a means to identify loci linked directly or indirectly to regulation of gene expression (30, 71, 115, 226). We performed eQTL mapping using spleen microarray data to determine whether the QTL regions identified for IP traits also

harbored *trans*-eQTL bands, loci that are linked to expression of multiple genes and could thus be implicated in mechanistic control of the trait(s) through coordinated transcriptional regulation. Spleen was chosen because it contains abundant levels of both B and T lymphocytes and contributes to multiple aspects of immune function. Two *trans*-bands exceeded the maximal size of 18 transcripts obtained by permutation testing, consisting of 42 and 30 transcripts located on Chrs 4 (@ 139.0 Mb) and 12 (@ 15.8 Mb), respectively (Fig. 3-4). Neither *trans*-band co-localized with IP QTLs, nor were the transcripts associated with each *trans*-band enriched for functions suggestive of IP regulation. Both bands did, however, contain an abundance of genes involved in cell cycle, cell division and DNA replication, which may have general relevance for heritable regulation of gene expression in the BXD panel.

We further exploited the microarray data to identify potential IP candidate genes by determining if expression of one or more genes within the QTL intervals were correlated with the overlying trait(s), a strategy that has been used successfully for other traits (17, 152, 203). We identified quantitative trait transcripts (QTTs), transcripts whose expression is correlated with a phenotype (203), for the T:B and CD4:CD8 ratios. We focused on these two traits because they capture relative abundance of multiple cell types and have significant QTLs. Pearson's correlation coefficients were calculated between expression levels of genes residing within the ± 1 LOD support intervals for each QTL and the immunophenotype data. Of the 517 genes located within these intervals for T:B ratio, 88 showed significant correlation with the phenotype ($P < 0.05$). GO enrichment analysis indicated that this set of genes was significantly enriched in processes related to antigen presentation and processing, as expected from the fact that many of these genes lie within the H2 locus on Chr 17. This set also contains a small number of genes (30 genes) that are highly correlated with T:B but reside on other chromosomes, the strongest of which are mitofusin 1 ($r = 0.626$, $P < 0.0001$) and phospholipase D1 ($r = -0.563$, $P = 0.0005$), both of which are within the QTL on Chr 3. Mitofusins are mitochondrial fusion proteins

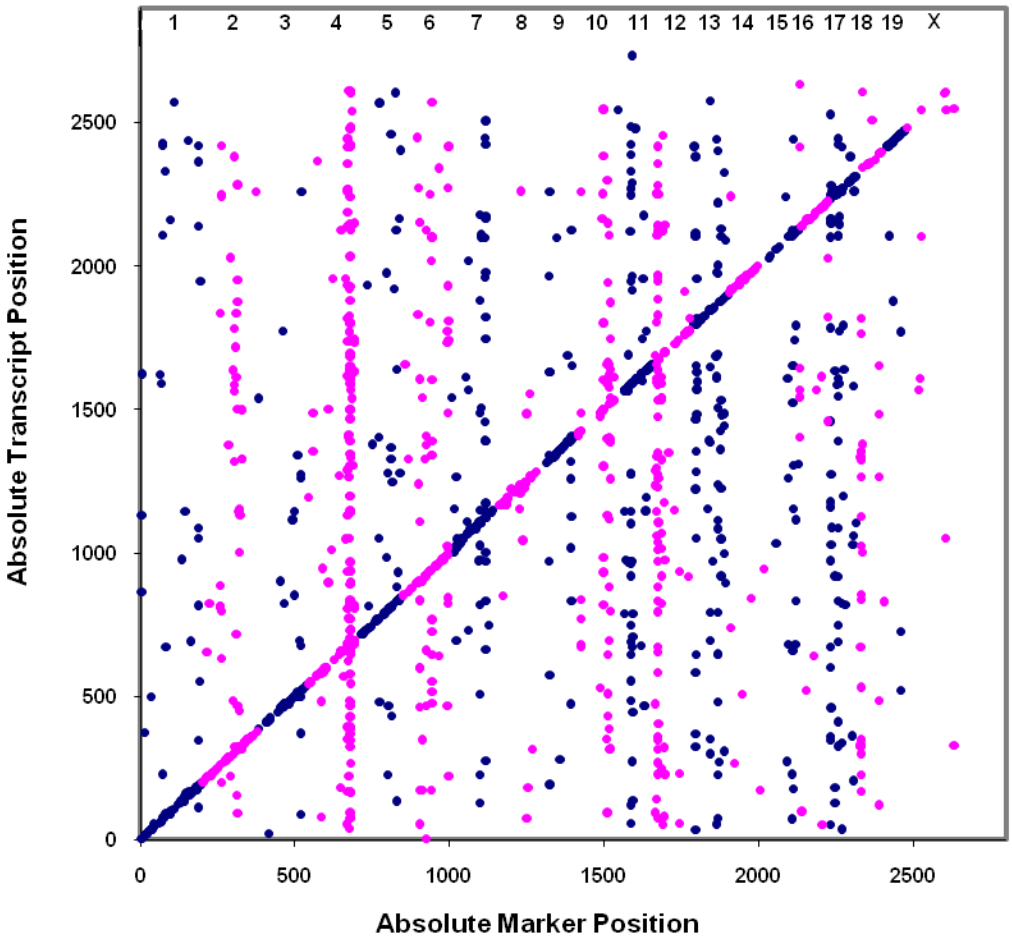

Figure 3-4. Spleen transcriptome map based on 38 BXD strains. The horizontal axis represents the genomic locations of the SNP markers/ QTL locations in Mb (chromosomes are in alternating colors), and the vertical axis represents the genomic location of each transcript in Mb. Each data point represents the maximum eQTL for each of the 1,881 transcripts that had a permuted *p*-value < 0.05.

that have recently been linked to the innate antiviral defense system (295). Phospholipase D1 was shown to be critical for coordination of inflammatory signaling through TNF-alpha in leukocytes (231).

Similar analysis of the QTL regions for the CD4:CD8 phenotype highlights a smaller set of potential candidate genes for this trait in the BXD panel. Of the 115 genes located within the QTL intervals for CD4:CD8 ratio, only 9 (7.8%) were significantly correlated with the CD4:CD8 phenotype. Of these, the most highly correlated QTT (r = 0.575; P = 0.0004) is the transcript for protein tyrosine phosphatase, receptor type, K (*Ptprk*), a phosphatase expressed in spleen and other tissues (294) . Loss of *Ptprk* due to a spontaneous deletion in Long Evans Cinnamon (LEC) rats was recently shown to underlie the deficiency in $CD4^+$ T cells in this model (124). Conversely, our data link increased expression of *Ptprk* with elevated levels of $CD4^+$ cells. Stepwise linear regression of *Ptprk* and the eight other QTL interval genes correlated with the CD4:CD8 ratio was used to estimate the amount of trait variance explained by expression of these genes. A model containing *Ptprk* along with acid phosphatase 1 (*Acp1*; also known as low molecular weight protein tyrosine phosphatase) and laminin B-1 (*Lamb1-1*) explains 61% of variance in the CD4:CD8 phenotype (P < 0.0001). Like *Ptprk*, *Acp1* is also a strong candidate gene for heritable variation in CD4:CD8 in the BXD panel. Polymorphisms in the human ACP1 gene have been correlated with susceptibility to a number of inflammatory and autoimmune disorders such as type I diabetes, allergy and atherosclerosis, all disorders in which CD4 and/or CD8 cells are implicated in pathogenesis (20, 37, 162). *Lamb1-1* has not been linked specifically to immune function but is widely expressed in spleen (154).

Our group has developed a number of graph algorithms based on the extraction of cliques and other dense subgraphs to identify putative gene coexpression networks from large scale ‘omics data (16, 24, 47, 133, 277, 300). Here we use the concept of anchored clique to extract networks of genes co-expressed with *Acp1* and *Ptprk* that may provide insight into the

mechanisms linking each gene to the CD4:CD8 phenotype. Both genes encode phosphatases and have been linked through genetic association studies to a number of inflammatory conditions, but relatively little is known about the cellular pathways in which each gene functions. The largest clique containing *Acp1* in a graph thresholded at q-value = 0.05 (with corresponding *P* = 0.0026) consisted of a total of 500 transcripts. The correlations of genes within this clique range from |r| = 0.550 to 0.917. Gene Ontology enrichment revealed that this *Acp1* coexpression network is highly enriched for genes involved in cell cycle (*P* = 2.0e-22, Benjamini = 1.1e-18), cell division (*P* = 1.6e-20, Benjamini = 4.2e-17), and DNA replication (*P* = 2.4e-18, Benjamini = 3.2e-15). To insure that this high degree of GO enrichment was not somehow an artifact of our specific dataset, we identified genetic correlates of *Acp1* expression in an independent spleen array dataset from 24 BXD strains within GeneNetwork (64). As with our data, *Acp1* expression was highly significantly correlated with genes involved in cell cycle and related processes (e.g., GO term M phase, Benjamini = 1.13e-18). The cell cycle enrichment in our *Acp1* anchored clique is also represented in the KEGG pathway for cell cycle control (*P* = 3.3e-12, Benjamini = 6.5e-10). Interestingly, of the 20 genes included in the KEGG pathway and co-expressed with *Acp1*, 18 are regulated by phosphorylation. These results suggest that abundance of the *Acp1* transcript *per se* may regulate phosphorylation status of cell cycle targets, either directly or indirectly, in the spleen. Similar analysis was performed for the maximal anchored clique of 135 genes containing *Ptprk*, but significant GO enrichment was not observed.

One of our long term interests is to identify gene coexpression networks linked to immune function in healthy individuals and to determine how these networks are perturbed by environmental factors that promote inflammation and/or alter immune function. To visualize the intersection between gene networks associated with IPs, we used a biclique algorithm to identify the largest set of transcripts in which each member is significantly correlated with each other

and one or more phenotypes. Pearson correlations were computed between each transcript and five immunophenotype measurements (%CD4, %CD3, LN T:B, %CD8, and LN CD4:CD8), and the matrix was thresholded to retain only those correlations most likely to symbolize true relationships ($P < 0.001$), leaving a total of 218 transcripts that are significantly correlated with one or more IPs. The relationship between gene expression and IPs are represented in Fig. 3.5, and as expected significant overlap exists between the sets of genes associated with each trait. For example, *Notch4* is correlated with %CD3, LN T:B, %CD4, and %CD8. *Notch4* is part of the highly conserved Notch family which play important roles in lymphocyte lineage commitment (256) and other cell-fate decisions (10). Specifically, there is evidence to support the role of *Notch4* in the differentiation and expansion of hematopoietic stem cells and in lymphomogenesis (275, 296). These data provide a starting point from which to test the impact of specific environmental variables on networks of genes linked to IPs of interest.

Discussion

Systems genetics enables the detection of QTLs and the identification of putative candidate genes for further testing and validation. In parallel, it produces phenomic data that can be mined in the context of the system by integrating it with all of the other multi-scale and diverse data types obtained from the same population. At a total of 79 strains, the BXD RI strain panel is the largest inbred mouse RI panel, and one for which an abundance of genomic resources now exist (207). We characterized the range of variation and the genetic architecture of immunophenotypes in the BXD RI panel to produce a baseline profile of the immune system that can be integrated into systems genetics studies with this population. These data are relevant for genetic susceptibility to the plethora of environmental factors and disorders that invoke the immune system, e.g., ionizing radiation exposure and diet-induced obesity.

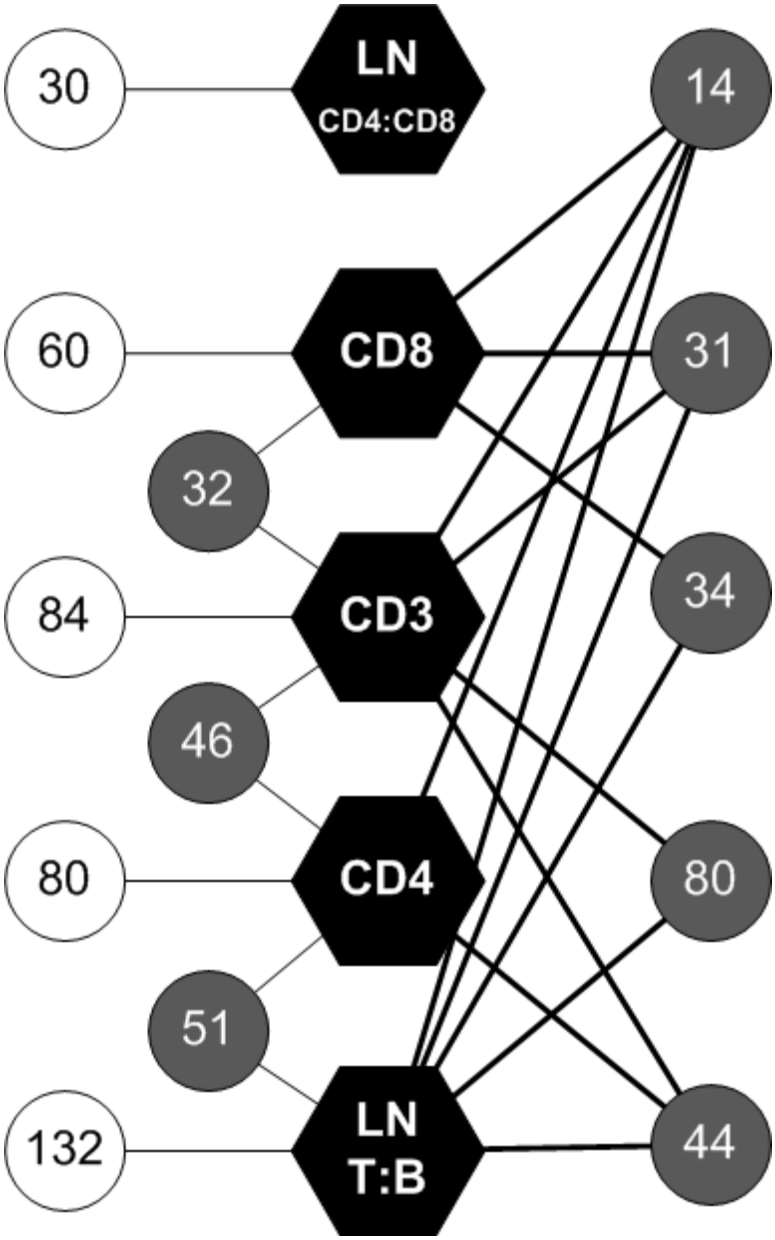

Figure 3-5. Bipartite graph demonstrating the connectivity of 5 immunophenotypes (IPs) and transcript expression. IPs are listed in the center of the graph and are symbolized by hexagons. The numbers of transcripts correlated ($P < 0.001$) with the IP(s) are depicted in the circles. The transcript sets symbolized by white circles create a maximal biclique with a single IP, while the transcript sets that create a maximal biclique with more than one IP are symbolized with gray circles.

We found that genetic models explain the majority of variation in each of the immunophenotypes, which is consistent with reports from humans and other species that lymphocyte subpopulations in healthy individuals are under strong genetic control. Three of the immunophenotypes (proportions of B, $CD4^+$ and $CD8^+$ lymphocytes in peripheral blood) were previously profiled in 22 of the same BXD lines included in our study (46). Two of the three IPs are significantly correlated with our data (%B lymphocytes, $r^2 = 0.530$, $P = 0.010$; %CD8 lymphocytes, $r^2 = 0.437$, $P = 0.041$) despite the passage of several years between studies and the use of independent BXD breeding colonies and institutions, highlighting the genetic stability of these phenotypes. The QTLs identified for these three traits differ between the two studies, likely because the Chen and Harrison (46) study relied on 35 BXD strains from the original BXD panel (strains 1 – 42) and a limited number of genetic markers, while ours was balanced between the original BXD set and the advanced recombinant inbred set produced by Peirce, et al. (207). Recent polymorphisms in this population (235) have been shown to influence the location and direction of QTL effects in these populations (210). In addition, a significant increase in the number of informative genetic markers are now available for the BXD panel and were used herein, which also may contribute to the discrepancy in QTL positions. Our reported QTL intervals (and those for many other traits mapped using the BXD panel) will likely be further refined with upcoming availability of genotype data across a panel of 580,000 SNPs, data that will soon be available through the GeneNetwork website (RW Williams, UTHSC, personal communication).

Identifying QTLs is relatively straightforward and rapid when using genetic reference panels such as BXD for which genotype data are readily available; cloning the causative polymorphism and confirming its role in phenotypic determination is a much more elusive target and one that we have not attempted. However, by combining QTL mapping with gene expression data, we have winnowed the list of potential candidate genes for traits of interest to a

manageable number for further study. This approach produced two particularly compelling candidate genes – *Ptprk* and *Acp1* – within the two significant QTLs associated with CD4:CD8, a trait used clinically as a marker for the prognosis of human immunodeficiency virus (HIV) (156), rheumatoid arthritis (81), and other diseases. *Ptprk* encodes a receptor-type protein-tyrosine phosphatase with no specific properties that link it to lymphocyte development. However, a potential role for Ptprk in $CD4^+$ T cell development was serendipitously uncovered in studies of the LEC rat, a model of Wilson's disease (due to a mutation in the copper transporting ATPase gene) that also had been noted to be deficient in $CD4^+$ T cells (1). Recently, two groups (11, 124) used linkage analysis to identify a deletion containing *Ptprk* in LEC rats and confirmed that loss of Ptprk is responsible for defective $CD4^+$ T cell development. Clinically, deletions of the chromosomal region containing PTPRK (chromosome 6q22-23) are frequently present in high-grade non-Hodgkin's lymphoma (188, 301), and loss of this region is also predictive of poor prognosis in CNS lymphoma (39), implicating this phosphatase in oncogenesis of the immune system. We used coexpression analysis in an attempt to gain insight into Ptprk function in spleen, based on the concept of genetic correlation. However, many of the transcripts with which *Ptprk* is most tightly co-expressed are un- or poorly- annotated, and no specific functions showed statistical enrichment. On the other hand, *Acp1*, the second candidate gene of interest for the CD4:CD8 phenotype, is part of a large clique of 500 transcripts that is highly enriched in functions related to cell cycle. *Acp1*, also known as low molecular weight protein tyrosine phosphatase, regulates phosphorylation status of a number of proliferative signaling molecules (244) and is up-regulated in several types of cancers (158, 163). Genetic screens in humans link polymorphisms in or near the ACP1 locus to a variety of inflammatory diseases including allergy, asthma and obesity (26), and Acp1 is involved in activation, adhesion, and differentiation of T cells (27, 88). The QTLs containing *Acp1* and *Ptprk* reside on separate chromosomes that showed significant independent and additive linkage with the CD4:CD8

phenotype, suggesting that genes within each locus may interact to affect CD4:CD8 ratio. At the molecular level Ptprk positively regulates the protein tyrosine kinase Src (280), which in turn phosphorylates and activates Acp1 (36, 254). Whether these events occur in the same cell type, and in one relevant to T cell development, is unknown but is worthy of further experimentation. It is worth noting that both Acp1 and Ptprk have been linked through genetic screens to colon cancer susceptibility (245, 249). Germane to our overarching interest in radiation sensitivity is the fact that both Acp1 and Ptprk have been shown to be altered by radiation exposure (89, 290).

Although Ptprk and Acp1 emerge as attractive candidates for the CD4:CD8 phenotype, a potential limitation of our study is that the tissue (spleen) used to highlight these QTTs is not the site of T lymphocyte lineage commitment and selection, processes thought to primarily occur within the thymus (38). However, it has been suggested that there are compensatory adjustments that occur within peripheral immune organs (i.e., spleen and lymph nodes) and alters the T cell peripheral population (186). Therefore, it is possible that the expression levels of *Ptprk* and *Acp1* in the thymus and spleen are regulated through similar mechanisms, or that the genetic polymorphisms that cause variation between strains exert similar effects in both tissues. If so, the relationship between trait values and expression levels would be predicted, even though the specific tissue profiled is not the primary tissue involved in the process of interest. Alternatively, the causative polymorphisms within the QTL intervals, whether in *Ptprk* and *Acp1* or other genes or regulatory elements, may act on processes that occur in the periphery, such as T cell proliferation. However, the mice used in this study were not exposed to any known immune challenges and were maintained in an SPF facility, and we would expect peripheral proliferation of T cells to be minimal in these animals. It is also possible that, despite convergent evidence to support their contribution to CD4:CD8, the causative polymorphism for variation in this trait do not act through either Acp1 or Ptprk.

Genetic correlations between immunophenotypes in the BXD panel and disease susceptibility would be enriched by more detailed characterization of T cell subpopulations beyond the classification as either Th ($CD4^+$) or Tc ($CD8^+$). For example, additional surface markers could be used to further classify $CD4^+$ cells as Th1, Th2, Th17, regulatory T (Treg), follicular helper T (Tfh), γδ T cells, etc. Each of these cell types play important roles in host defense and autoimmune diseases, and understanding the genetic basis of T cell subpopulation distributions would be invaluable in elucidating susceptibilities to T cell-mediated disorders, such as rheumatoid arthritis (123, 139, 291) .

One of the advantages of using BXD strains as a reference population is the wealth of genotypic, phenotypic, and gene expression information available for the panel, much of which is freely available through the online database GeneNetwork. For example, we transiently uploaded our data into GeneNetwork to scan for genetic correlation between our immunophenotypes and other traits measured on the BXD population. This *ad hoc* analysis revealed an association between the baseline T:B ratio profiled in our study and outcomes of *Chlamydia psittaci* exposure as measured by Miyairi and colleagues (172). Among BXD strains that persisted 30 days post-infection, both spleen weight and pathogen load in spleen (GeneNetwork records 11025 and 11026) are significantly correlated ($r = -0.811$, $P < 0.001$, and $r = -0.728$, $P = 0.003$, respectively) with the T:B phenotype. The opportunity for such integrative analyses provided by the use of genetic reference populations such as the BXD panel highlights the strengths of systems genetics, namely the ability to assimilate genetic susceptibility to disease or the environment in the context of the healthy state through the stable genetic basis of the population. As the BXD strain continues to be phenotyped, the ability to connect seemingly disparate phenotypes grows proportionally. The Collaborative Cross, an idealized genetic reference population, should also be widely available within the next few years for expanded systems genetics studies (50).

In summary, we have characterized the genetic architecture of a set of basic but informative immunophenotypes in the BXD panel. We have uncovered potential candidate genes that contribute to genetic variation in the relative abundance of helper and cytotoxic T cells, and follow-on studies to test the roles of both Ptprk and Acp1 can now be initiated. Beyond the classical follow-ups to QTL mapping, these data can be a useful resource in choosing BXD strains with a particular baseline immunoprofile for the study of a particular disease susceptibility or progression. For example, we have gene expression data from spleen suggesting that low dose radiation exposure differentially impacts T cell subpopulations in a way that depends on genetic background (BH Voy et al., unpublished data). We can now use these BXD data to select strain subsets based on differences in T cell subpopulations and prospectively test if heritable differences in immunophenotypes alter radiation effects on immune function.

CHAPTER IV

IDENTIFYING GENETIC DIFFERENCES UNDERLYING DIFFERENTIAL LOW DOSE RADIATION RESPONSES

This manuscript will be submitted to *Radiation Research* with the following author list:

Lynch RM, Naswa S, Rogers GL, Jr., Kania SA, Das S, Chesler EJ,
Saxton AM, Langston MA, Bogard JS, and Voy BH

The immune system illustrates the challenges of assigning risk to low dose radiation (LDR) exposure in a population. While high radiation doses clearly suppress immune function, a number of studies have shown that LDR affects immune cell subpopulations in ways that could be beneficial. In the intact organism, defining the consequences of LDR is further complicated by the impact of genetic background, particularly in systems such as the immune system for which both radiosensitivity and genetic effects are profound. We employed a systems genetics approach to test for heritable differences in LDR responses. Mice from 39 BXD recombinant inbred (RI) strains were exposed to 10cGy gamma radiation to determine effects on immune function and oxidative stress 48h after irradiation. LDR significantly enhanced neutrophil phagocytosis in a manner that was independent of genetic background. In contrast, genetic background significantly impacted LDR-induced changes in spleen superoxide dismutase activity. Transcriptome data from spleens of the BXD parental strains highlighted the impact of genetic background on LDR responses and also indicate that genetic variation in radiosensitivity is further unmasked at low radiation doses. Taken together, these data highlight the need to consider genetic variation when assessing LDR outcomes.

Introduction

Average levels of radiation exposure over the past thirty years are estimated to have doubled, largely due to the widespread use of diagnostic imaging procedures such as computed tomography (190). Physically, the likelihood of an individual cell receiving a radiation track is proportional to dose, and the current model used to predict dose-dependent risk is based on linear extrapolation from high dose effects. Biologically, however, low doses of ionizing radiation elicit responses that are not necessarily observed at higher doses. A number of microarray studies have reported dose-specific gene expression profiles using mouse and human cell lines irradiated in vitro (6, 69, 83, 149, 237). Higher order phenotypes, such as reactive oxygen species (ROS) scavenging (292), DNA damage and repair (299), and immune responses (79), have also been shown to exhibit non-linear responses to increasing radiation dose (79). Therefore the physiological consequences of exposure to low doses of radiation (LDR, ≤10cGy) are not easily extrapolated from the responses characteristic of high dose radiation (HDR) exposure (79, 228, 262, 264).

The immune system, which is known for its radiosensitivity, illustrates the challenges in delineating health effects of radiation exposure at low doses. High radiation doses (>1Gy) clearly suppress immune function through destruction of myeloid and lymphoid cell populations in bone marrow. In contrast, several studies of various immune cell types suggests that low doses of radiation enhances cellular functions that could be viewed as beneficial to the organism (143). For example, LDR has been shown to increase mitogen-induced lymphocyte proliferation (8, 111, 192, 201, 234), macrophage and natural killer cell activation (104, 147, 194, 201, 233), and tumor surveillance (41, 98, 101, 122, 143, 194). At the molecular level, LDR alters gene expression (95), cytokine secretion (94, 104, 145), expression of surface molecules on immune cells (145, 146), and apoptosis (234), which can lead to LDR-induced modification of leukocyte distribution (96). Relatively little is known, however, about how this sensitivity

translates into efficacy of immune system, and if LDR alters the organism's ability to respond to invading pathogens.

Classical studies of radiation sensitivity in mice illustrate the importance of considering genetic variation when ascribing biological consequences of radiation dose. In 1963, Roderick characterized survival times of 27 inbred mouse strains following daily exposure to 1Gy of x-ray radiation (high dose delivered at a high dose rate). The most susceptible strains, including CBA/J and BALB/cJ, succumbed to the radiation in approximately 16 days, while the most resistant strains, such as 129/J, survived more than twice as long. Since then, differences between strains at sublethal radiation doses have been reported for a number of outcomes, including radiation-induced apoptosis (178-181, 279) and carcinogenesis (157, 177, 266, 298). With respect to carcinogenesis, differences between strains have been described even though most are not inherently sensitive to radio-carcinogenesis. Given that genetic variation alters the effects of lethal doses, it is reasonable to suspect that evidence for radiation sensitivity would be even more apparent at low doses that present a more subtle challenge to cells and tissues. A limited number of studies have reported differential effects of low radiation doses in inbred mouse strains and in cell lines derived from a panel of human donors (117, 285).

Incorporating genetic variation into models of environmental susceptibility in humans is challenging even for prevalent factors such as high fat diets or cigarette smoke. Population-based mouse models, such as outbred crosses or recombinant inbred strain panels provide a means to address the impact of genetic variation on responses to environmental stimuli, such as radiation, for which large, controlled study populations or purposeful exposures are not available in humans. We describe the results of using BXD (C57BL/6J X DBA/2J) recombinant inbred (RI) mouse strains as a population-based model to assess the impact of genetic variation on response to LDR and to test the hypothesis that LDR alters aspects of immune function. The BXD recombinant inbred (RI) strain panel was used as a genetically characterized reference

population in which the parental strains (C57BL/6J and DBA/2J) exhibit known differences in baseline immune function and differential sensitivities and responses to LDR exposure (153, 172, 281). Part of our overarching hypothesis is that the immunological effects of LDR exposure within a population depend in part on the individual's baseline immunoprofile and gene expression which are ultimately dependent upon genetic background. We utilize our previously published baseline peripheral blood immunophenotype and spleen expression data in the BXD panel to identify correlations with LDR responses. We focused our efforts on a limited number of biochemical and functional endpoints that could be efficiently assayed across a large number of mice. Transcriptomic profiling of spleen from the BXD parental strains was used to assess differential sensitivity to low dose radiation at the molecular level, and to test the hypothesis that genetic variation in the radiation response is more apparent at low doses. Here we show that LDR enhances neutrophil phagocytosis across the BXD panel, while spleen superoxide dismutase activity and spleen gene expression changes in response to LDR exposure vary significantly depending upon genetic background.

Methods

Radiation exposure

C57BL/6J, DBA/2J, and BXD RI stocks from strains 6 – 42 were obtained from The Jackson Laboratory (Bar Harbor, ME). BXD RI stocks from strains 43 – 100 were obtained from Dr. Lu Lu and Dr. Robert Williams from the University of Tennessee Health Science Center (UTHSC, Memphis, TN). Mice were housed and propagated in the specific-pathogen-free (SPF) Russell Vivarium at Oak Ridge National Laboratory (ORNL) as previously described (153). Approximately 10 week-old mice from a balanced subset of 39 BXD strains selected from the original Jackson Laboratory strains (259, 260) and the advanced intercross strains developed at UTHSC (207) were exposed to a single dose of 10cGy radiation from a ^{137}Cs source delivered

at a rate of ~9cGy/h. Each strain*treatment group consisted of an average of 4 irradiated or 4 sham-exposed control mice per strain, and each group was balanced between males and females. Only 2 mice (1 irradiated and 1 sham control) per strain were exposed on any given day, and strains were randomized across the study. Following radiation or sham exposure, mice were housed for 48h in a satellite facility prior to dissection. Blood was collected by retro-orbital sinus puncture into heprinized tubes for neutrophil function assays. Spleens were harvested and snap-frozen in liquid nitrogen and stored at -80°C for subsequent biochemical assays.

For spleen expression profiling, male C57BL/6J and DBA/2J mice were exposed to either a low dose (10cGy, as described above), or a high dose (1Gy) of γ-radiation delivered by a ^{60}Co source with a dose rate of ~6Gy/min. Mice were sacrificed 24 following exposure, and spleens were stabilized in RNAlater (Sigma-Aldrich, St. Louis, MO) until RNA was extracted. All studies were approved by the Animal Care & Use Committee at Oak Ridge National Laboratory.

Neutrophil functional assays

Flow cytometry was used to assay neutrophil function in peripheral blood from 34 BXD strains 48h after sham or radiation exposure. For both assays, red blood cells in the blood samples were lysed and leukocytes were fixed prior to flow cytometric analysis. DNA staining was used to distinguish between aggregation artifacts and murine cells. At least 10,000 leukocytes per sample were analyzed using a Beckman Coulter Epics XL flow cytometer and EXPO32 ADC Software (Beckman Coulter, Brea, CA). Neutrophils were gated for analysis based on forward and side scattering profiles. Gating based on fluorescence was set on unstimulated samples from each mouse to include approximately 10% of the evaluated cell population, and the same gating parameters were used to evaluate percentage and median channel fluorescence (MCF) of stimulated neutrophils exhibiting phagocytic or oxidative burst activity. Neutrophil phagocytosis (Phagotest Kit, Orpegen Pharma, Heidelberg, Germany) and

oxidative burst assays (Phagoburst Kit, Orpegen Pharma) were performed as previously described (135).

Biochemical assays

Response to oxidative stress was assayed by quantification of superoxide dismutase (SOD) activity, glutathione (GSH), and oxidized glutathione (GSSG) in spleens from 39 BXD strains. Spleens were homogenized in 1mL of cold HEPES buffer (20mM HEPES, pH 7.2, with 1mM EGTA, 210mM mannitol, and 70mM sucrose). The homogenate was aliquoted for SOD, GSH, and Bradford assays. SOD activity was measured in the spleen extracts using an enzymatic assay (Cayman Chemical Company, Ann Arbor, MI) that reflects the combined activity levels of all three SOD isoforms (SOD1, SOD2, and SOD3), normalized to the protein concentration of the spleen extract (Bio-Rad, Hercules, CA), and reported as the units of SOD activity per mg of protein (U/mg). The percentage of GSSG to total GSH in deproteinated spleen extracts was determined with a kit which utilizes an enzymatic recycling method using glutathione reductase (Cayman Chemical Company). GSSG levels were assayed separately from the determination of total GSH levels; both were assayed according to manufacturer's instructions using the end-point method. The percentage of GSSG to total GSH was determined, as well as the GSSG and total GSH concentration normalized to the protein concentration of the original spleen lysate.

QTL mapping

Quantitative trait loci (QTL) mapping was performed on SOD activity in sham and LDR-exposed BXD mice. Estimates from the models described above were used for QTL mapping. QTL analysis was performed using nearly 3,8000 single-nucleotide polymorphisms (SNPs) and microsatellite markers for the BXD panel obtained from GeneNetwork database (http://www.genenetwork.org/dbdoc/BXDGeno.html). The genotype information was based on

the markers originally reported by Shifman et al. (235) which were re-aligned with National Center for Biotechnology Information (NCBI) Build 36. QTLs were identified using WebQTL (49), which creates a linkage map using a mixture mapping algorithm combining simple marker regression, linear interpolation, and standard Haley-Knott interval mapping. Genome-wide significance thresholds were calculated based on 1,000 permutations (54), and the cut-off *p*-values for significant and suggestive loci were $P = 0.05$ and $P = 0.63$, respectively (130). Multiple-QTL modeling was performed using stepwise linear regression in SAS; a *p*-value of 0.05 was used as the threshold for terms to remain in the final model.

Parental gene expression profiling

Transcriptome profiling in C57BL/6J and DBA/2J spleens was performed by Genome Quebec (Montreal, Canada) using the Mouse WG-6 v1.1 BeadChip on the Illumina platform (San Diego, CA). as previously described (153). Quantitative polymerase chain reaction (Q-PCR) was used to confirm the microarray results of myeloperoxidase (*Mpo*) differential expression in the parental strains following radiation exposure. Reverse transcription was performed on 500ng of RNA using the Bio-Rad iScript cDNA Synthesis kit from Bio-Rad. QuantiTect primers were used in conjunction with the QuantiTect SYBR Green PCR kit (Qiagen) on a CFX96 real-time PCR detection system (Bio-Rad). All samples were analyzed in triplicate; *Mpo* expression was normalized to hypoxanthine guanine phosphoribosyl transferase (*Hprt)* expression. Fold changes were calculated based on the ΔΔCt method and differences between groups were tested using ANOVA.

Statistical testing

Statistical testing was performed using SAS (SAS Institute, Cary, NC). For biochemical and neutrophil function assays, Proc Mixed was used to test for strain, radiation, and strain*radiation interaction effects, using the assay date as a random variable. If the

strain*radiation term was not significant (*P* = 0.05), then a reduced model was rerun using only the strain and radiation terms. All neutrophil function and biochemical data reported are least squares means from the Proc Mixed model.

Expression data from Illumina bead chips were normalized using Variance Stabilizing Transformation (VST) followed by Robust Spline Normalization (RSN) using the R/Bioconductor (87) package lumi (74). Fold changes were calculated after reverse transforming the data using inverseVST function of lumi package. Raw and normalized expression data are available through NCBI's GEO database (http://www.ncbi.nlm.nih.gov/projects/geo). SAS procedure GLM (General Linear Model) was used for analysis of variance (ANOVA) to test the effects of strain, dose and their interaction on expression (expression ~ strain + dose + strain*dose). Post ANOVA contrast tests were used to compare the groups C57BL/6J LD and C57BL/6J HD vs. C57BL/6J control, DBA/2J LD and DBA/2J HD vs. DBA/2J control, strain*LD interaction and strain*HD interaction. An alpha of 0.05 was used for all statistical tests. False discoveries due to multiple comparison testing were controlled by using q-value (250). Differential expression was considered significant if both p and q values were < 0.05 and fold change > 1.5. DAVID (68, 102) was used for gene ontology (GO) enrichment analysis of differentially expressed genes. Benjamini-Hochberg false discovery rate-corrected p-values are reported (19).

Results

Neutrophil Function

Across the panel of BXD strains, LDR exposure significantly increased both the percentage of phagocytic neutrophils (i.e., phagocytosis of one or more FITC-labeled bacteria per cell; *P* = 0.0437) and the median channel fluorescence (MCF) of phagocytic neutrophils, reflecting the number of bacteria phagocytosed per *E.coli*-positive cell (*P* = 0.0193, Fig. 4-1). The radiation effect translates into approximately a 4% increase in the number of cells

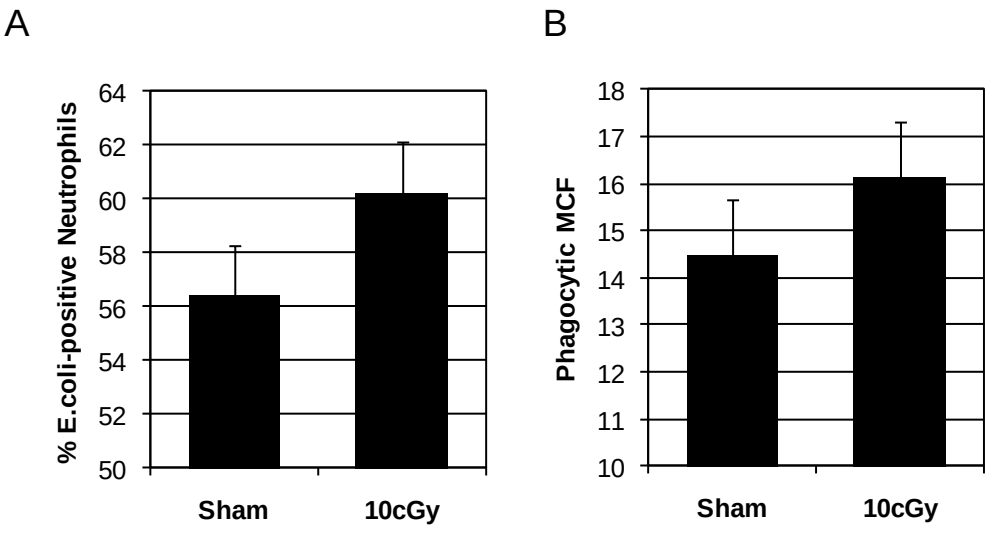

Figure 4-1. Effect of radiation on neutrophil function. Peripheral neutrophils were assayed using flow cytometry 48h after irradiation; N ≥ 66 mice / group (A) A greater percentage of neutrophils from radiation-exposed mice engulfed FITC-labeled *E. coli* compared to those of controls ($p = 0.044$). (B) *E. coli*-positive neutrophils from radiation-exposed mice had a greater median channel fluorescence (Phagocytic MCF, indicating more bacteria engulfed per cell) compared to those of control ($p = 0.019$). Error bars reflect the SEM.

undergoing phagocytosis and an 11% increase in the number of bacteria engulfed by those cells, relative to sham controls. In addition to a main effect of radiation, both measures of phagocytic activity showed significant effects of strain (% Phagocytic Neutrophils, $P < 0.001$ and Phagocytic MCF, $P = 0.0023$), reflecting the impact of genetic variation on phagocytic function in the BXD panel. Despite the wide range of baseline variation across strains, there was no significant interaction between strain and radiation exposure (% Phagocytic Neutrophils, $P = 0.99$ and Phagocytic MCF, $P = 0.38$). These results demonstrate for the first time using an *in vivo* model that low dose radiation alters neutrophil function.

Flow cytometry also was used to measure the generation of intracellular reactive oxygen species (ROS) generated during oxidative burst. The percentage of oxidative burst-positive neutrophils (%OB Neutrophils) was analyzed as well as the MCF of positive neutrophils (measurement of enzymatic activity). While both %OB Neutrophils and OB MCF varied significantly by strain ($P = 0.020$ and $P < 0.001$, respectively), radiation and strain*radiation interaction effects were not significant ($P = 0.66$ and $P = 0.54$, respectively).

Anti-oxidant defense system

Total SOD activity in spleen varied significantly across the BXD strain panel ($P < 0.001$), reflecting the impact of genetic background on baseline SOD activity. Genetic background further altered the SOD response to LDR, as indicated by the very significant strain*radiation interaction ($P < 0.001$). Unlike for phagocytosis, the main effect of radiation was not significant ($P = 0.32$). Neither the GSSG levels nor percentage of oxidized (GSSG) to total glutathione (GSH) levels significantly differed among strains or between radiation and sham-exposed mice within strains (all *P*-values > 0.1). When total GSH levels were normalized to the protein concentration in the spleen lysate, a significant strain effect was observed ($P = 0.0014$), but there was no radiation main effect ($P = 0.21$) or strain*radiation interaction effect ($P = 0.97$).

The significant interactive effect of strain and radiation on SOD activity demonstrates that genetic factors play a pivotal role in the antioxidant response to low dose exposure. We performed QTL analysis to identify loci associated with this differential response to LDR, using genotype data readily available for the BXD panel (235). QTL analysis (Fig. 4-2) revealed a significant QTL on Chromosome (Chr) 15 (@ 74Mb, LOD = 3.54), as well two suggestive QTLs on Chr 16 (@ 69Mb, LOD = 2.34 and @ 93Mb, LOD = 2.80), that are linked to SOD activity in unexposed controls. The QTL on distal Chr 16 encompasses the *Sod1* gene. In contrast, QTL analysis of LDR SOD activity identified a locus on Chr 17 (@ 76Mb, LOD = 1.17) which was not present in analyses of control SOD activity, suggesting that this locus mediates the SOD response to LDR but not baseline SOD activity. Further, the Chr 16 locus containing *Sod1* was not present in the LDR QTL model. A multi-locus regression model which includes additive effects of the Chr 15, which were present in both models, and the Chr 17 loci explains 24% of the variance in SOD activity in the spleens of LDR-exposed mice.

Correlations between baseline IP and gene expression with radiation outcomes

The concept of genetic correlation (210) was applied to search for relationships between baseline traits in unexposed mice and low dose radiation responses, which may identify genes that are involved in or biomarkers of differential low dose response. Transcriptomic and immunophenotype data from spleens of an overlapping set of BXD strains were integrated with SOD activity and neutrophil function data, and all possible pair-wise Pearson correlations were computed between expressed transcripts, immunophenotypes and SOD activity in sham and LDR-exposed BXD strains. Spleen microarray data and immunophenotypes (e.g., $CD79^+$, $CD3^+$, $CD4^+$ and $CD8^+$ lymphocytes) in peripheral blood were collected as described previously (153). We were particularly interested in genes for which baseline expression levels were significantly correlated with post-radiation SOD activity but not with sham SOD activity. Interestingly, these

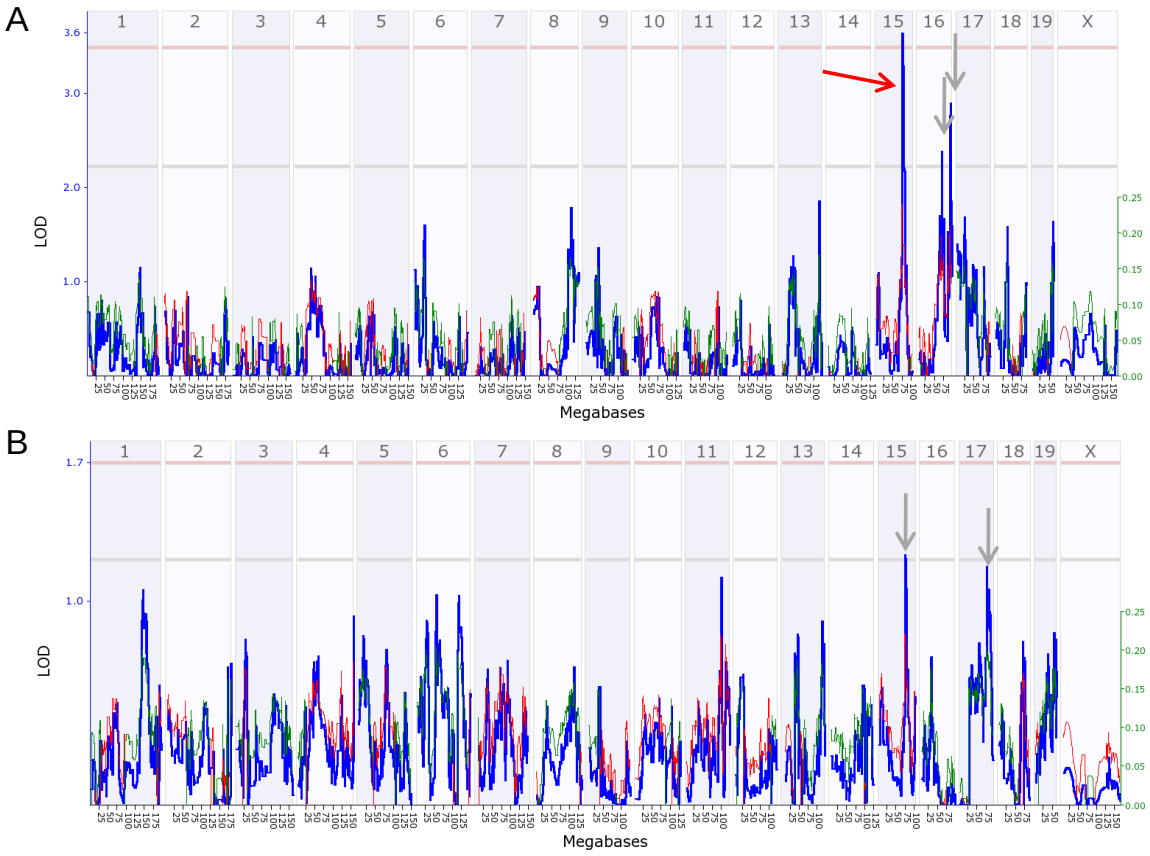

Figure 4-2. SOD activity QTL analysis. WebQTL interval mapping of spleen SOD activity in sham (A) and radiation-exposed (B) BXD mice. The mouse genome is portrayed along the horizontal axis, while the vertical axis shows the logarithm of odds (LOD). Significant and suggestive levels of association were determined based on permutation testing and are depicted by horizontal red and gray lines, respectively. Significant and suggestive loci are indicated by red and gray arrows, respectively. LOD scores are indicated by the blue line across the genome; the red line indicates that the C57BL/6J allele at the marker increases the SOD activity, while the green line indicates the DBA/2J allele increases activity. Strength of additive effects is indicated by the scale on the right.

parameters include expression of *Sod2* which was significantly correlated with LDR SOD activity (r = 0.47, *P* = 0.0026) but not with sham SOD activity (r = 0.030, *P* = 0.86). In addition to *Sod2*, baseline expression of apoptosis-inducing factor, mitochondrion-associated 2 (*Aifm2*) was differentially correlated with LRD SOD activity (r = 0.55, *P* < 0.001) but not sham SOD activity (r = 0.16, *P* = 0.35). AIFM2 is a DNA-binding protein with oxidoreductase activity (161) and was originally described as a caspase-independent inducer of apoptosis (289), functions that have clear relevance to radiation response. With respect to immunophenotypes, we found a significant and inverse correlation between % Phagocytic Neutrophils and the CD4:CD8 ratio (r = -0.48, *P* = 0.0082, N = 29 strains) in LDR but not control mice which was largely due to an inverse correlation with the percentage of $CD4^+$ lymphocytes (r = -0.33, *P* = 0.078) (Fig. 4-3).

Spleen gene expression

We used microarrays to compare and contrast effects of LDR in the two BXD parental strains based on differences in gene expression profiles. A higher dose (1Gy) exposure was included to determine if the effects of genetic variation, based on molecular phenotypes, were more apparent at a lower level of radiation exposure. Low dose radiation significantly altered the expression of 74 genes in both C57BL/6J and DBA/2J mice (q-value < 0.05 and fold change > 1.5). This gene set is highly enriched in immune-related functions, including the Gene Ontology (GO) terms “response to wounding” (15 genes, Benjamini = 7.1E-8) and “defense response” (13 genes, Benjamini = 2.9E-5). GO enrichment highlighted qualitative differences in the response of each strain. Genes differentially expressed in C57Bl/6J but not DBA/2J (N = 138) were significantly enriched in heme biosynthesis, while DBA/2J-specific LDR genes (N = 752) were enriched in various immune processes, including lymphocyte activation (Table 4-1). In total, 1200 genes showed a significant strain*LDR interaction, reflecting genes for which the response to LDR depends upon genetic background. Consistent with previous reports of differential

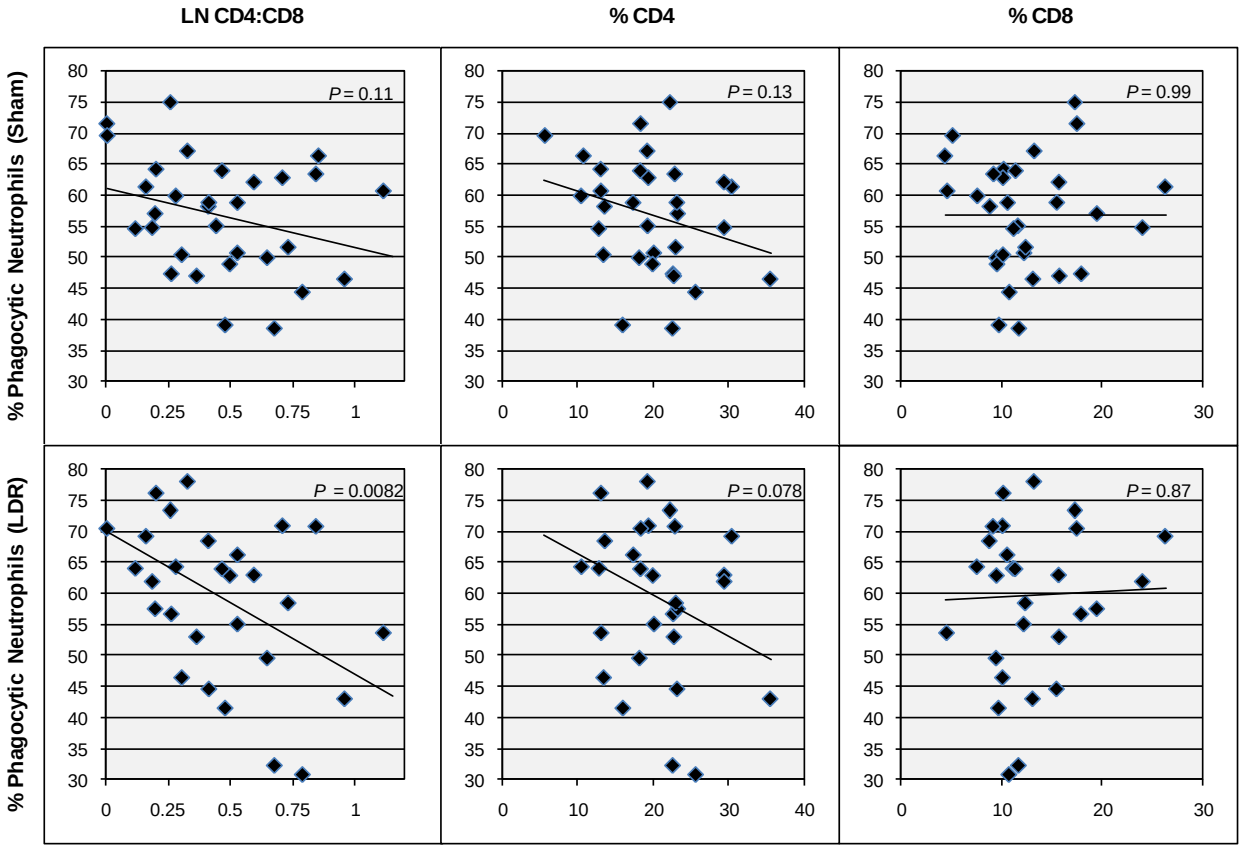

Figure 4-3. Scatterplots of neutrophil phagocytosis of BXD mice with baseline immunophenotypes. Percent phagocytic neutrophils in low dose radiation-exposed mice (LDR) is significantly (P = 0.0082) correlated with the natural log of the CD4:CD8 ratio (LN CD4:CD8), which is largely due to the correlation with %CD4-positive lymphocytes (%CD4) and not %CD8-positive lymphocytes (%CD8).

Table 4-1. GO enrichment of genes demonstrating a LDR*Strain interaction.

GO Biological Process[a]	# of Genes[b]	Bonferroni
hemopoietic or lymphoid organ development	44	4.21E-08
M phase	41	1.18E-06
DNA metabolic process	43	7.58E-04
nucleosome organization	17	1.13E-04
regulation of apoptosis	47	1.33E-02
hemopoiesis	37	2.66E-06
heme biosynthetic process[†]	8	1.32E-04
B cell activation[‡]	14	4.57E-03
T cell activation[‡]	16	1.87E-02
antigen receptor-mediated signaling pathway[‡]	8	4.50E-02
antigen processing and presentation of exogenous peptide antigen via MHC class II[‡]	10	3.33E-06

[a]Selection of enriched GO biological processes, level 5
[b]Number of genes with significant LDR*Strain interaction (q-value < 0.05)
[†]Significant GO process unique to C57BL/6J low dose
[†]Significant GO process unique to DBA/2J low dose

apoptotic responses in irradiated C57BL/6J and DBA/2J strains (44, 89), the list of significant LDR*strain interaction genes includes 50 genes involved in apoptosis regulation.

The list of genes with the most significant LDR*strain interactions was further probed to identify specific cellular functions that manifested the strongest genetic differences in LDR response. After sorting the list based on q-value, 14 of the top 15 genes were found to be involved in varying aspects of neutrophil function (9, 35, 56, 58, 110, 114, 118, 137, 142, 159, 255) (Table 4-2), all of which showed an inverse response to radiation between strains. Q-PCR was used to validate differential effects of LDR on *Mpo*, which confirmed significant down-regulation in C57BL/6J (4.8-fold; $P < 0.001$) and up-regulation in DBA/2J (3.3-fold; $P < 0.001$). We used the text mining tool FABLE (http://fable.chop.edu) to query the entire LDR*strain interaction list for correlations with neutrophil function. A total of 157 genes were found in 10 or more PubMed articles relating to neutrophils, suggesting that LDR had differential effects on aspects of neutrophil function, depending upon genetic background.

We compared the molecular responses to 10cGy (LDR) vs. 1Gy (high dose radiation, HDR) exposures in C57BL/6J and DBA/2J mice to determine if a more subtle environmental stimulus unmasked genetic variation that was less apparent with a higher dose. ANOVA identified a total of 562 genes differentially expressed in HDR mice, regardless of strain. As expected, this set of genes was significantly enriched in KEGG pathways for cell cycle (17 genes, Benjamini = 2.4E-5), p53 signaling (10 genes, Benjamini = 7.3E-3), and DNA replication (7 genes, Benjamini = 0.011). Out of the 562 HDR and 964 LDR genes, 307 had altered expression in response to both radiation doses. This set of overlapping genes was significantly enriched in functions related to various biological processes including hemostasis (10 genes, Benjamini = 3.8E-04), chromatin assembly (8 genes, Benjamini = 0.0093), and immune system development (14 genes, Benjamini = 0.023). In contrast to LDR, in which a total of 1200 genes showed significant LDR*strain interaction, only five genes demonstrated differential HDR

Table 4-2. Top 15 genes demonstrating the most significant LDR*Strain interaction effects.

Gene Symbol	Gene Name	q-value[a]	C57BL/6J Fold Change[b]	DBA/2J Fold Change
Prtn3	proteinase 3	1.7E-05	-14.9	12.2
Ltb4r1	leukotriene B4 receptor 1	1.7E-05	-2.4	4.3
Mpo	myeloperoxidase	1.7E-05	-14.2	9.0
Elane	elastase, neutrophil expressed	1.7E-05	-12.8	9.8
Tmem180	transmembrane protein 180	1.7E-05	-1.3	1.9
Mt1	metallothionein 1	2.2E-05	-1.3	2.4
Fcnb	ficolin B	2.2E-05	-3.9	5.0
Cebpe	CCAAT/enhancer binding protein (C/EBP), epsilon	3.5E-05	-3.3	4.6
Mt2	metallothionein 2	3.8E-05	-1.2	2.9
Camp	cathelicidin antimicrobial peptide	4.9E-05	-9.0	5.9
Ltf	lactotransferrin	5.5E-05	-12.5	6.4
Lcn2	lipocalin 2	7.2E-05	-8.3	7.6
F5	coagulation factor V	7.2E-05	-1.7	1.9
Pglyrp1	peptidoglycan recognition protein 1	7.2E-05	-1.5	3.6
Chi3l1	chitinase 3-like 1	7.2E-05	-2.9	4.3

[a]ANOVA q-value for LDR*Strain interaction term
[b]Estimated by reverse transformation of normalized microarray data

response between strains (q-value < 0.05 for interaction effect). These results suggest that while C57BL/6J and DBA respond to high dose radiation in a qualitatively similar manner at the level of gene expression, their responses diverge at a lower dose exposure.

Discussion

We assessed the impact of LDR on the immune system by measuring the response of neutrophils to bacteria, a functional endpoint of the innate immune system. We demonstrated that across the BXD population, a single exposure to 10cGy of radiation significantly enhanced both the numbers of cells that engaged in phagocytosis and the phagocytic activity of those cells. These data suggest that, at least acutely, LDR increases the ability to respond to invading pathogens. Our findings are consistent with a study of immune function in residents of two villages in Iran, Taleshmahaleh and Chaparsar, who are exposed to background radiation levels 13 times greater than normal due to elevated natural levels of radiation exposure. Residents of these two villages were shown to have increased neutrophil phagocytosis and motility, as well as differences in circulating cytokines such as IL-2, IL-4 and IL-10 (12). It is important to note, however, that both radiation quality and dose rate differ significantly between these two studies. One limitation of our study is that only one time point was analyzed (48 hours post-exposure), which was chosen to fit the overall study design characterizing LDR-effects that are downstream of the initial radiation stress. This time point may not be optimal for this phenotype; greater enhancement of phagocytosis might be observed at earlier or later time points following irradiation. Because the half-life of murine neutrophils in peripheral blood is approximately 8 hours (150), the cells assayed by flow cytometry were irradiated while undergoing maturation in bone marrow. Therefore the mechanism of increased phagocytosis could include maturational effects on cells prior to their release into circulation. Alternatively, LDR may have increased phagocytosis by altering levels of cytokines and chemokines such as TNFα, IL-8, and IFNγ that

act on neutrophils in circulation (85, 94, 104). Phagocytosis is one of a series of steps that lead to bacterial killing, and only phagocytosis and oxidative burst (which was not affected by LDR) were measured in this study. Follow-up studies are necessary to more broadly define the functional effects of LDR on neutrophils. Our microarray data collected from the BXD parental strains further support significant effects of LDR on neutrophils, as indicated by the abundance of neutrophil-related genes with significant strain*radiation interaction effects (Table 4-2). Moreover, they suggest that these effects differ markedly between the two strains, as indicated by the inverse patterns of gene expression. Mature neutrophils were once thought to be transcriptionally inert, but are now known to respond to a number of stressors and cellular signals through changes in gene expression (rev. in (121)). We do not have parallel functional data in these two strains and thus cannot determine if phagocytosis was also differentially impacted by LDR in C57BL/6J and DBA/2J. Current efforts are directed to collecting these data and expanding the scope of LDR-induced neutrophil phenotypes, including chemotaxis and cell killing. We should also point out that the expression data were collected in spleen rather than in isolated neutrophils or in bone marrow, and divergent effects of LDR on gene expression could be due to indirect effects, such as differential neutrophil migration into spleen or clearance of apoptotic neutrophils. Further experiments will be necessary to test these hypotheses.

In contrast to phagocytosis, SOD activity in response to LDR varied significantly between strains. SOD activity increases after radiation exposure to mitigate oxidative stress resulting from the radiolysis of intracellular water, a response that is largely due to increased activity of mitochondrial SOD (SOD2) (97, 199). We interpret the significant interaction between strain and treatment to reflect genetic differences in the kinetics of SOD activity and its repletion following radiation stress, as opposed to opposite regulation of the enzyme across strains. Increased SOD activity in spleen occurs within hours of LDR-exposure (292), but less is known about the persistence of the response over time. Our data indicate that certain individuals within

a population mount a more persistent antioxidant defense to LDR, or that the supply of SOD available is rapidly depleted in some individuals, while others have intrinsically greater response to oxidative LDR stress. The significant genetic correlation we observed between *Sod2* expression in spleen of unexposed mice and SOD activity after LDR exposure further supports this relationship. This relationship is consistent with results seen from genetically engineered Sod2 deficient mice, in which heterozygous C57BL/6J *Sod2*(+/-) mice have increased radiation sensitivity compared to wild type *Sod2*(+/+) controls (76). It would now be interesting to determine if BXD strains with the highest heritable levels of *Sod2* expression are less susceptible to LDR responses that have been shown to be influenced by SOD2 activity, including adaptive radio-resistance and DNA damage (66).

QTL mapping using existing resources for the BXD strain panel allowed us to identify a region on Chr 17 associated with LDR-induced but not control SOD activity. To our knowledge, this is the first identification of a QTL for differential responses to LDR. The gene encoding *Sod2* is located on Chr 17, but is positioned >60Mb downstream of the maximum LDR SOD activity QTL. Therefore it does not appear that genetic variation within the *Sod2* locus itself, or in proximal regulatory regions, contributes to the LDR SOD variation between strains. In contrast, a QTL for control SOD activity encompassed the position of the *Sod1* enzyme locus. Using previously collected microarray data from BXD spleens (153) we identified a gene, xanthine dehydrogenase (*Xdh*), that is located approximately 2Mb upstream of the maximum LOD, and has expression levels that are significantly correlated with LDR-induced but not sham control SOD activity ($r = -0.34$, $P = 0.041$ and $r = -0.19$, $P = 0.26$, respectively). XDH, along with xanthine oxidase, forms the xanthine oxidoreductase (XOD) system. XDH can be converted to the superoxide-generating enzyme xanthine oxidase (XO) by reversible sulfhydryl oxidation or irreversibly by proteolytic modification (248), a process that has been shown to occur in response to high (>3Gy) doses of ionizing radiation, potentiating tissue oxidative stress beyond

the initial radiochemical reactions (247). Whether variation in activity of the XOD system could potentially alter SOD activity upon radiation remains to be determined. Access to high density SNP-based genotypes, which will soon be available for the BXD panel, should allow us to narrow the QTL interval and facilitate the search for causal polymorphisms linked to differential SOD activity with LDR.

Differences in radiation sensitivity between the BXD parental strains were first described by Roderick more than 45 years ago, with DBA/2J succumbing more quickly than C57BL/6J to a lethal dose of radiation (217). At more modest doses, C57BL/6J mice were shown to be more resistant to radiation-induced genomic instability than DBA/2J (193, 281, 288). Wright and colleagues described differential apoptotic responses between the two strains after 1Gy radiation, with C57BL/6J favoring apoptosis through rapid induction of p53 and up-regulation of pro-apoptotic *Bax*, and DBA/2J having a delayed but prolonged p53 activation with more emphasis on p21 activation and cell cycle arrest (57, 140, 279). Our microarray data collected from spleen further illustrates that genetic variation plays a major role in how these two strains respond to radiation, particularly at low doses. Based on the strain*radiation interaction term in the ANOVA model, 1200 genes showed evidence for response to LDR that depended upon genetic background. This set of genes is enriched for numerous GO terms, including aspects of cell maintenance and immune defense (Table 4-1). In general, genes altered by LDR in DBA/2J were more closely related to lymphocyte functions (e.g., B cell and T cell activation) than were genes responsive to LDR in C57BL/6J mice, which showed differential enrichment in processes related to erythropoiesis.

How these distinct expression profiles manifest in differential immune consequences of LDR remains to be determined, but they do further confirm that genetic background plays a key role in LDR response.

In stark contrast to LDR exposure, only five genes showed a significant interaction between strain and radiation after a 1Gy exposure. These differential effects across a rather modest (10-fold) increase in dose suggest that above a certain threshold, the response to radiation between individuals qualitatively becomes more similar as the demand to abate damage overrides other less critical processes. As dose is lowered to a level that imposes oxidative stress rather than immediate damage, genetic variation in mechanisms for coping with stress and the consequential effects on other pathways begin to emerge. Our array data also support the concept that the mechanisms of LDR response are not simply a subset of those enlisted with higher radiation exposures. Only 32% (307 of 964 genes) of the genes differentially expressed following LDR-exposure were also changed in response to HDR. Taken together, these array data highlight the need to consider genetic variation when assessing LDR outcomes, perhaps even more so than for higher radiation doses.

Using a genetically stable reference population for this study allowed us to go beyond QTL analysis and exploit genetic correlation as a means to identify other phenotypes correlated with, and potential functionally related to, LDR response. With respect to SOD activity, this enabled the discovery that *Sod2* expression in the baseline, un-irradiated state is positively correlated with SOD activity after LDR exposure, using microarray data that we previously generated from spleens of BXD strains (153). Similar relationships between baseline gene expression and radiation sensitivity were reported by Amundson et al. using the National Cancer Institute Anticancer Drug Screen (NCI-60) panel of cell lines (5). In our case, *Sod2* was an obvious candidate because of its known role in LDR adaptation, but nonetheless it was identified using a method that did not require *a priori* knowledge about what genes might be uncovered. Genetic correlation also uncovered a significant inverse relationship between neutrophil phagocytosis following LDR exposure and the CD4:CD8 lymphocyte ratio in un-irradiated mice. Whether this relationship stems from a common regulator of T cell maturation

and radiation effects on phagocytosis or from an indirect association remains to be determined. Nonetheless, these relationships illustrate how systems genetics provides a framework for extracting interrelationships between phenotypes that might not otherwise be suspected. Mechanistically, this approach can uncover potential functional relationships that can be further tested, resulting in fundamental advances in physiology. At the translational level, systems genetics can potentially improve the assessment of risk through identification of phenotypes, whether they be molecular, cellular or biochemical, that signal differential sensitivity to radiation and other environmental challenges of concern.

In summary, our results show both responses to low dose exposure that are robust to genetic variation (enhanced neutrophil phagocytosis) and those from which genetic background significantly impacts the response (SOD activity). By integrating these results with our previous analyses of BXD RI strains, we have demonstrated that heritable differences in baseline expression and immunophenotypes can correlate with various low dose radiation responses. These data provide the groundwork for predicting LDR responses using baseline expression, immunophenotypes, and/or genotype.

CHAPTER V

FUTURE STUDIES

This dissertation research has demonstrated that the BXD recombinant inbred (RI) strain panel is a powerful reference population for analyzing the effects of low dose radiation (LDR) on immune function. To our knowledge, this is the first report showing that neutrophil function can be enhanced following in vivo LDR exposure. Future studies will focus on further characterization of neutrophil function and the mechanisms behind the LDR induced stimulatory effects. While we have shown that phagocytosis of bacteria is enhanced following LDR, other important steps in neutrophil-mediated innate defense will need to be analyzed. For example, does LDR lead to an increase in bacterial recognition by the neutrophils? Are the stimulated neutrophils more efficient at bacteria killing once the bacteria are engulfed? Do chemokines such as IL-8 active neutrophils following LDR? Can a similar response be observed with an in vivo bacterial challenge? These questions need to be answered to have a better understanding of the mechanisms involved in LDR-modulated neutrophil function. It would also need to be determined if other general LDR responses, such as oxidative stress and the induction of apoptosis, are involved in the neutrophil response to exposure. Furthermore, our gene expression profiling highlighted the differential regulation of neutrophil-related genes between the two parental strains following LDR. On-going studies are determining if the expression of these same genes are altered in the bone marrow, the site of neutrophil maturation.

By comparing LDR responses with baseline immunophenotype data, we found a negative correlation between neutrophil phagocytosis following LDR and the percentage of peripheral lymphocytes which are $CD4^+$. Numerous studies have shown that $CD4^+$ cells are particularly responsive/sensitive to LDR. It would be interesting to see if $CD4^+$ cell counts or

gene expression is altered in a genetic-background dependent manner following LDR exposure, or if LDR alters the Th1/Th2 balance.

Our analyses also suggested that baseline expression of mitochondrial SOD (*Sod2*) might be a predictor of SOD activity following radiation exposure. This possibility can be further explored by determining if the BXD strains with the highest *Sod2* expression levels are more resistant to radiation-induced DNA damage.

The results presented here, combined with previously published data, raise some interesting possibilities regarding the effects of low dose radiation exposure in humans. As mentioned above, there is concern over the risks associated with the dramatic increases in radiation exposure from medical diagnostic procedures. Because numerous animal studies have demonstrated that low doses of radiation can suppress harm from a subsequent larger radiation dose ("radiation conditioning hormesis"), it would very useful to determine similar responses can be observed in humans. A low dose radiation exposure, or "priming dose", would be given prior to the larger radiation dose. Of course, in most cases, an individual does not know *a priori* when they will receive a significant radiation dose, but priming doses could possibly be administered prior to certain radiological medical procedures. For instance, would a "priming" chest x-ray administered prior to a CT or PET scan reduce long-term cancer risk? If so, the protective effect of the priming x-rays might be especially important for individuals who undergo multiple diagnostic scans.

The data presented in this dissertation provide intriguing glimpses into the genetic basis of low dose radiation responses. These data provide the groundwork for developing personalized risk assessments of low dose radiation risk based on genetic background.

REFERENCES

1. **Agui T, Oka M, Yamada T, Sakai T, Izumi K, Ishida Y, Himeno K, and Matsumoto K**. Maturational arrest from CD4+8+ to CD4+8- thymocytes in a mutant strain (LEC) of rat. *J Exp Med* 172: 1615-1624, 1990.
2. **Akiyama M, Yamakido M, Kobuke K, Dock DS, Hamilton HB, Awa AA, and Kato H**. Peripheral lymphocyte response to PHA and T cell population among atomic bomb survivors. *Radiat Res* 93: 572-580, 1983.
3. **Amadori A, Zamarchi R, De Silvestro G, Forza G, Cavatton G, Danieli GA, Clementi M, and Chieco-Bianchi L**. Genetic control of the CD4/CD8 T-cell ratio in humans. *Nat Med* 1: 1279-1283, 1995.
4. **Amundson SA, Do KT, and Fornace AJ, Jr.** Induction of stress genes by low doses of gamma rays. *Radiat Res* 152: 225-231, 1999.
5. **Amundson SA, Do KT, Vinikoor LC, Lee RA, Koch-Paiz CA, Ahn J, Reimers M, Chen Y, Scudiero DA, Weinstein JN, Trent JM, Bittner ML, Meltzer PS, and Fornace AJ, Jr.** Integrating global gene expression and radiation survival parameters across the 60 cell lines of the National Cancer Institute Anticancer Drug Screen. *Cancer Res* 68: 415-424, 2008.
6. **Amundson SA, Lee RA, Koch-Paiz CA, Bittner ML, Meltzer P, Trent JM, and Fornace AJ, Jr.** Differential responses of stress genes to low dose-rate gamma irradiation. *Mol Cancer Res* 1: 445-452, 2003.
7. **An J, Huang YC, Xu QZ, Zhou LJ, Shang ZF, Huang B, Wang Y, Liu XD, Wu DC, and Zhou PK**. DNA-PKcs plays a dominant role in the regulation of H2AX phosphorylation in response to DNA damage and cell cycle progression. *BMC Mol Biol* 11: 18.
8. **Anderson RE, and Troup GM**. Effects of irradiation upon the response of murine spleen cells to mitogens. *Am J Pathol* 109: 169-178, 1982.
9. **Arita M, Ohira T, Sun YP, Elangovan S, Chiang N, and Serhan CN**. Resolvin E1 selectively interacts with leukotriene B4 receptor BLT1 and ChemR23 to regulate inflammation. *J Immunol* 178: 3912-3917, 2007.
10. **Artavanis-Tsakonas S, Matsuno K, and Fortini ME**. Notch signaling. *Science* 268: 225-232, 1995.
11. **Asano A, Tsubomatsu K, Jung CG, Sasaki N, and Agui T**. A deletion mutation of the protein tyrosine phosphatase kappa (Ptprk) gene is responsible for T-helper immunodeficiency (thid) in the LEC rat. *Mamm Genome* 18: 779-786, 2007.
12. **Attar M, Molaie Kondolousy Y, and Khansari N**. Effect of high dose natural ionizing radiation on the immune system of the exposed residents of Ramsar Town, Iran. *Iran J Allergy Asthma Immunol* 6: 73-78, 2007.
13. **Azzam EI, de Toledo SM, Raaphorst GP, and Mitchel RE**. Low-dose ionizing radiation decreases the frequency of neoplastic transformation to a level below the spontaneous rate in C3H 10T1/2 cells. *Radiat Res* 146: 369-373, 1996.
14. **Babcock GF, Taylor AF, Hynd BA, Sramkoski RM, and Alexander JW**. Flow cytometric analysis of lymphocyte subset phenotypes comparing normal children and adults. *Diagn Clin Immunol* 5: 175-179, 1987.
15. **Bakkenist CJ, and Kastan MB**. DNA damage activates ATM through intermolecular autophosphorylation and dimer dissociation. *Nature* 421: 499-506, 2003.
16. **Baldwin NE, Chesler EJ, Kirov S, Langston MA, Snoddy JR, Williams RW, and Zhang B**. Computational, integrative, and comparative methods for the elucidation of genetic coexpression networks. *J Biomed Biotechnol* 2005: 172-180, 2005.

17. **Bao L, Peirce JL, Zhou M, Li H, Goldowitz D, Williams RW, Lu L, and Cui Y**. An integrative genomics strategy for systematic characterization of genetic loci modulating phenotypes. *Hum Mol Genet* 16: 1381-1390, 2007.
18. **Barquinero JF, Barrios L, Caballin MR, Miro R, Ribas M, Subias A, and Egozcue J**. Occupational exposure to radiation induces an adaptive response in human lymphocytes. *International journal of radiation biology* 67: 187-191, 1995.
19. **Benjamini Y, and Hochberg Y**. Controlling the False Discovery Rate - a Practical and Powerful Approach to Multiple Testing. *Journal of the Royal Statistical Society Series B-Methodological* 57: 289-300, 1995.
20. **Betts RJ, and Kemeny DM**. CD8+ T cells in asthma: friend or foe? *Pharmacol Ther* 121: 123-131, 2009.
21. **Bhatia S, Robison LL, Oberlin O, Greenberg M, Bunin G, Fossati-Bellani F, and Meadows AT**. Breast cancer and other second neoplasms after childhood Hodgkin's disease. *N Engl J Med* 334: 745-751, 1996.
22. **Bogue MA, Grubb SC, Maddatu TP, and Bult CJ**. Mouse Phenome Database (MPD). *Nucleic Acids Res* 35: D643-649, 2007.
23. **Bond VP, and Cronkite EP**. Effects of radiation on mammals. *Annu Rev Physiol* 19: 299-328, 1957.
24. **Borate BR, Chesler EJ, Langston MA, Saxton AM, and Voy BH**. Comparison of threshold selection methods for microarray gene co-expression matrices. *BMC Res Notes* 2: 240, 2009.
25. **Bosi A, and Olivieri G**. Variability of the adaptive response to ionizing radiations in humans. *Mutat Res* 211: 13-17, 1989.
26. **Bottini N, Bottini E, Gloria-Bottini F, and Mustelin T**. Low-molecular-weight protein tyrosine phosphatase and human disease: in search of biochemical mechanisms. *Arch Immunol Ther Exp (Warsz)* 50: 95-104, 2002.
27. **Bottini N, Stefanini L, Williams S, Alonso A, Jascur T, Abraham RT, Couture C, and Mustelin T**. Activation of ZAP-70 through specific dephosphorylation at the inhibitory Tyr-292 by the low molecular weight phosphotyrosine phosphatase (LMPTP). *J Biol Chem* 277: 24220-24224, 2002.
28. **Boyle JM, Spreadborough A, Greaves MJ, Birch JM, Varley JM, and Scott D**. The relationship between radiation-induced G(1)arrest and chromosome aberrations in Li-Fraumeni fibroblasts with or without germline TP53 mutations. *Br J Cancer* 85: 293-296, 2001.
29. **Brazma A, Hingamp P, Quackenbush J, Sherlock G, Spellman P, Stoeckert C, Aach J, Ansorge W, Ball CA, Causton HC, Gaasterland T, Glenisson P, Holstege FC, Kim IF, Markowitz V, Matese JC, Parkinson H, Robinson A, Sarkans U, Schulze-Kremer S, Stewart J, Taylor R, Vilo J, and Vingron M**. Minimum information about a microarray experiment (MIAME)-toward standards for microarray data. *Nat Genet* 29: 365-371, 2001.
30. **Breitling R, Li Y, Tesson BM, Fu J, Wu C, Wiltshire T, Gerrits A, Bystrykh LV, de Haan G, Su AI, and Jansen RC**. Genetical genomics: spotlight on QTL hotspots. *PLoS Genet* 4: e1000232, 2008.
31. **Brenner DJ**. Medical imaging in the 21st century--getting the best bang for the rad. *N Engl J Med* 362: 943-945, 2010.
32. **Brenner DJ, Doll R, Goodhead DT, Hall EJ, Land CE, Little JB, Lubin JH, Preston DL, Preston RJ, Puskin JS, Ron E, Sachs RK, Samet JM, Setlow RB, and Zaider M**. Cancer risks attributable to low doses of ionizing radiation: assessing what we really know. *Proc Natl Acad Sci U S A* 100: 13761-13766, 2003.
33. **Brenner DJ, and Hall EJ**. Computed tomography--an increasing source of radiation exposure. *N Engl J Med* 357: 2277-2284, 2007.

34. **Broman KW, Wu H, Sen S, and Churchill GA**. R/qtl: QTL mapping in experimental crosses. *Bioinformatics* 19: 889-890, 2003.
35. **Brooks AS, Hammermueller J, DeLay JP, and Hayes MA**. Expression and secretion of ficolin beta by porcine neutrophils. *Biochim Biophys Acta* 1624: 36-45, 2003.
36. **Bucciantini M, Chiarugi P, Cirri P, Taddei L, Stefani M, Raugei G, Nordlund P, and Ramponi G**. The low Mr phosphotyrosine protein phosphatase behaves differently when phosphorylated at Tyr131 or Tyr132 by Src kinase. *FEBS Lett* 456: 73-78, 1999.
37. **Buono C, Binder CJ, Stavrakis G, Witztum JL, Glimcher LH, and Lichtman AH**. T-bet deficiency reduces atherosclerosis and alters plaque antigen-specific immune responses. *Proc Natl Acad Sci U S A* 102: 1596-1601, 2005.
38. **Busslinger M, Nutt SL, and Rolink AG**. Lineage commitment in lymphopoiesis. *Curr Opin Immunol* 12: 151-158, 2000.
39. **Cady FM, O'Neill BP, Law ME, Decker PA, Kurtz DM, Giannini C, Porter AB, Kurtin PJ, Johnston PB, Dogan A, and Remstein ED**. Del(6)(q22) and BCL6 rearrangements in primary CNS lymphoma are indicators of an aggressive clinical course. *J Clin Oncol* 26: 4814-4819, 2008.
40. **Calabrese EJ, Bachmann KA, Bailer AJ, Bolger PM, Borak J, Cai L, Cedergreen N, Cherian MG, Chiueh CC, Clarkson TW, Cook RR, Diamond DM, Doolittle DJ, Dorato MA, Duke SO, Feinendegen L, Gardner DE, Hart RW, Hastings KL, Hayes AW, Hoffmann GR, Ives JA, Jaworowski Z, Johnson TE, Jonas WB, Kaminski NE, Keller JG, Klaunig JE, Knudsen TB, Kozumbo WJ, Lettieri T, Liu SZ, Maisseu A, Maynard KI, Masoro EJ, McClellan RO, Mehendale HM, Mothersill C, Newlin DB, Nigg HN, Oehme FW, Phalen RF, Philbert MA, Rattan SI, Riviere JE, Rodricks J, Sapolsky RM, Scott BR, Seymour C, Sinclair DA, Smith-Sonneborn J, Snow ET, Spear L, Stevenson DE, Thomas Y, Tubiana M, Williams GM, and Mattson MP**. Biological stress response terminology: Integrating the concepts of adaptive response and preconditioning stress within a hormetic dose-response framework. *Toxicol Appl Pharmacol* 222: 122-128, 2007.
41. **Cao ZA, Daniel D, and Hanahan D**. Sub-lethal radiation enhances anti-tumor immunotherapy in a transgenic mouse model of pancreatic cancer. *BMC Cancer* 2: 11, 2002.
42. **Cardis E, Gilbert ES, Carpenter L, Howe G, Kato I, Armstrong BK, Beral V, Cowper G, Douglas A, Fix J, and et al.** Effects of low doses and low dose rates of external ionizing radiation: cancer mortality among nuclear industry workers in three countries. *Radiat Res* 142: 117-132, 1995.
43. **Cardis E, Vrijheid M, Blettner M, Gilbert E, Hakama M, Hill C, Howe G, Kaldor J, Muirhead CR, Schubauer-Berigan M, Yoshimura T, Bermann F, Cowper G, Fix J, Hacker C, Heinmiller B, Marshall M, Thierry-Chef I, Utterback D, Ahn YO, Amoros E, Ashmore P, Auvinen A, Bae JM, Bernar J, Biau A, Combalot E, Deboodt P, Diez Sacristan A, Eklof M, Engels H, Engholm G, Gulis G, Habib RR, Holan K, Hyvonen H, Kerekes A, Kurtinaitis J, Malker H, Martuzzi M, Mastauskas A, Monnet A, Moser M, Pearce MS, Richardson DB, Rodriguez-Artalejo F, Rogel A, Tardy H, Telle-Lamberton M, Turai I, Usel M, and Veress K**. The 15-Country Collaborative Study of Cancer Risk among Radiation Workers in the Nuclear Industry: estimates of radiation-related cancer risks. *Radiat Res* 167: 396-416, 2007.
44. **CDC**. Center for Disease Control and Prevention http://www.bt.cdc.gov/radiation/arsphysicianfactsheet.asp#1. [03/01/10.
45. **Celeste A, Petersen S, Romanienko PJ, Fernandez-Capetillo O, Chen HT, Sedelnikova OA, Reina-San-Martin B, Coppola V, Meffre E, Difilippantonio MJ, Redon C, Pilch DR, Olaru A, Eckhaus M, Camerini-Otero RD, Tessarollo L, Livak F, Manova K, Bonner WM, Nussenzweig MC, and Nussenzweig A**. Genomic instability in mice lacking histone H2AX. *Science* 296: 922-927, 2002.

46. **Chen J, and Harrison DE**. Quantitative trait loci regulating relative lymphocyte proportions in mouse peripheral blood. *Blood* 99: 561-566, 2002.
47. **Chesler EJ, and Langston MA**. Combinatorial genetic regulatory network analysis tools for high throughput transcriptomic data. In: *Systems Biology and Regulatory Genomics*, edited by Eskin ESpringer, 2006, p. 150–165.
48. **Chesler EJ, and Langston MA**. Combinatorial genetic regulatory network analysis tools for high throughput transcriptomic data. In: *Proceedings, RECOMB Satellite Workshop on Systems Biology and Regulatory Genomics*. San Diego: 2005.
49. **Chesler EJ, Lu L, Wang J, Williams RW, and Manly KF**. WebQTL: rapid exploratory analysis of gene expression and genetic networks for brain and behavior. *Nat Neurosci* 7: 485-486, 2004.
50. **Chesler EJ, Miller DR, Branstetter LR, Galloway LD, Jackson BL, Philip VM, Voy BH, Culiat CT, Threadgill DW, Williams RW, Churchill GA, Johnson DK, and Manly KF**. The Collaborative Cross at Oak Ridge National Laboratory: developing a powerful resource for systems genetics. *Mamm Genome* 19: 382-389, 2008.
51. **Chistiakov DA, Voronova NV, and Chistiakov PA**. Genetic variations in DNA repair genes, radiosensitivity to cancer and susceptibility to acute tissue reactions in radiotherapy-treated cancer patients. *Acta Oncol* 47: 809-824, 2008.
52. **Christner JA, Zavaletta VA, Eusemann CD, Walz-Flannigan AI, and McCollough CH**. Dose reduction in helical CT: dynamically adjustable z-axis X-ray beam collimation. *AJR Am J Roentgenol* 194: W49-55.
53. **Churchill GA, Airey DC, Allayee H, Angel JM, Attie AD, Beatty J, Beavis WD, Belknap JK, Bennett B, Berrettini W, Bleich A, Bogue M, Broman KW, Buck KJ, Buckler E, Burmeister M, Chesler EJ, Cheverud JM, Clapcote S, Cook MN, Cox RD, Crabbe JC, Crusio WE, Darvasi A, Deschepper CF, Doerge RW, Farber CR, Forejt J, Gaile D, Garlow SJ, Geiger H, Gershenfeld H, Gordon T, Gu J, Gu W, de Haan G, Hayes NL, Heller C, Himmelbauer H, Hitzemann R, Hunter K, Hsu HC, Iraqi FA, Ivandic B, Jacob HJ, Jansen RC, Jepsen KJ, Johnson DK, Johnson TE, Kempermann G, Kendziorski C, Kotb M, Kooy RF, Llamas B, Lammert F, Lassalle JM, Lowenstein PR, Lu L, Lusis A, Manly KF, Marcucio R, Matthews D, Medrano JF, Miller DR, Mittleman G, Mock BA, Mogil JS, Montagutelli X, Morahan G, Morris DG, Mott R, Nadeau JH, Nagase H, Nowakowski RS, O'Hara BF, Osadchuk AV, Page GP, Paigen B, Paigen K, Palmer AA, Pan HJ, Peltonen-Palotie L, Peirce J, Pomp D, Pravenec M, Prows DR, Qi Z, Reeves RH, Roder J, Rosen GD, Schadt EE, Schalkwyk LC, Seltzer Z, Shimomura K, Shou S, Sillanpaa MJ, Siracusa LD, Snoeck HW, Spearow JL, Svenson K, Tarantino LM, Threadgill D, Toth LA, Valdar W, de Villena FP, Warden C, Whatley S, Williams RW, Wiltshire T, Yi N, Zhang D, Zhang M, and Zou F**. The Collaborative Cross, a community resource for the genetic analysis of complex traits. *Nat Genet* 36: 1133-1137, 2004.
54. **Churchill GA, and Doerge RW**. Empirical threshold values for quantitative trait mapping. *Genetics* 138: 963-971, 1994.
55. **Clementi M, Forabosco P, Amadori A, Zamarchi R, De Silvestro G, Di Gianantonio E, Chieco-Bianchi L, and Tenconi R**. CD4 and CD8 T lymphocyte inheritance. Evidence for major autosomal recessive genes. *Hum Genet* 105: 337-342, 1999.
56. **Cloutier A, Guindi C, Larivee P, Dubois CM, Amrani A, and McDonald PP**. Inflammatory cytokine production by human neutrophils involves C/EBP transcription factors. *J Immunol* 182: 563-571, 2009.
57. **Coates PJ, Lorimore SA, Lindsay KJ, and Wright EG**. Tissue-specific p53 responses to ionizing radiation and their genetic modification: the key to tissue-specific tumour susceptibility? *The Journal of pathology* 201: 377-388, 2003.

58. **Coffman FD**. Chitinase 3-Like-1 (CHI3L1): a putative disease marker at the interface of proteomics and glycomics. *Crit Rev Clin Lab Sci* 45: 531-562, 2008.
59. **Cope AP, Schulze-Koops H, and Aringer M**. The central role of T cells in rheumatoid arthritis. *Clin Exp Rheumatol* 25: S4-11, 2007.
60. **Correa CR, and Cheung VG**. Genetic variation in radiation-induced expression phenotypes. *Am J Hum Genet* 75: 885-890, 2004.
61. **Cronkite EP, Bond VP, Chapman WH, and Lee RH**. Biological effect of atomic bomb gamma radiation. *Science* 122: 148-150, 1955.
62. **Curtis RE FD, Ron E, Ries LAG, Hacker DG, Edwards BK, Tucker MA, Fraumeni JF Jr.** editor. *New Malignancies Among Cancer Survivors: SEER Cancer Registries, 1973-2000.* Bathesda: National Cancer Institute, 2006.
63. **Darakhshan F, Badie C, Moody J, Coster M, Finnon R, Finnon P, Edwards AA, Szluinska M, Skidmore CJ, Yoshida K, Ullrich R, Cox R, and Bouffler SD**. Evidence for complex multigenic inheritance of radiation AML susceptibility in mice revealed using a surrogate phenotypic assay. *Carcinogenesis* 27: 311-318, 2006.
64. **Davies MN, Lawn S, Whatley S, Fernandes C, Williams RW, and Schalkwyk LC**. Is blood a reasonable surrogate for brain in gene expression studies? GeneNetwork Accession: GN277. www.genenetwork.org. [January 7, 2010].
65. **Day TK, Zeng G, Hooker AM, Bhat M, Turner DR, and Sykes PJ**. Extremely low doses of x-radiation can induce adaptive responses in mouse prostate. *Dose Response* 5: 315-322, 2007.
66. **de Toledo SM, Asaad N, Venkatachalam P, Li L, Howell RW, Spitz DR, and Azzam EI**. Adaptive responses to low-dose/low-dose-rate gamma rays in normal human fibroblasts: the role of growth architecture and oxidative metabolism. *Radiat Res* 166: 849-857, 2006.
67. **Dendrou CA, Plagnol V, Fung E, Yang JH, Downes K, Cooper JD, Nutland S, Coleman G, Himsworth M, Hardy M, Burren O, Healy B, Walker NM, Koch K, Ouwehand WH, Bradley JR, Wareham NJ, Todd JA, and Wicker LS**. Cell-specific protein phenotypes for the autoimmune locus IL2RA using a genotype-selectable human bioresource. *Nat Genet* 41: 1011-1015, 2009.
68. **Dennis G, Jr., Sherman BT, Hosack DA, Yang J, Gao W, Lane HC, and Lempicki RA**. DAVID: Database for Annotation, Visualization, and Integrated Discovery. *Genome Biol* 4: P3, 2003.
69. **Ding LH, Shingyoji M, Chen F, Hwang JJ, Burma S, Lee C, Cheng JF, and Chen DJ**. Gene expression profiles of normal human fibroblasts after exposure to ionizing radiation: a comparative study of low and high doses. *Radiat Res* 164: 17-26, 2005.
70. **Donnelly P**. Progress and challenges in genome-wide association studies in humans. *Nature* 456: 728-731, 2008.
71. **Doss S, Schadt EE, Drake TA, and Lusis AJ**. Cis-acting expression quantitative trait loci in mice. *Genome Res* 15: 681-691, 2005.
72. **Dropkin G**. Low dose radiation and cancer in A-bomb survivors: latency and non-linear dose-response in the 1950-90 mortality cohort. *Environ Health* 6: 1, 2007.
73. **Dropkin G**. Reanalysis of cancer mortality in Japanese A-bomb survivors exposed to low doses of radiation: bootstrap and simulation methods. *Environ Health* 8: 56, 2009.
74. **Du P, Kibbe WA, and Lin SM**. lumi: a pipeline for processing Illumina microarray. *Bioinformatics* 24: 1547-1548, 2008.
75. **Eisen MB, Spellman PT, Brown PO, and Botstein D**. Cluster analysis and display of genome-wide expression patterns. *Proc Natl Acad Sci U S A* 95: 14863-14868, 1998.
76. **Epperly MW, Epstein CJ, Travis EL, and Greenberger JS**. Decreased pulmonary radiation resistance of manganese superoxide dismutase (MnSOD)-deficient mice is corrected

by human manganese superoxide dismutase-Plasmid/Liposome (SOD2-PL) intratracheal gene therapy. *Radiat Res* 154: 365-374, 2000.
77. **Fang SP, Tago F, Tanaka T, Simura N, Muto Y, Goto R, and Kojima S**. Repeated irradiations with gamma-rays at a Dose of 0.5 Gy may exacerbate asthma. *J Radiat Res (Tokyo)* 46: 151-156, 2005.
78. **Feinendegen LE**. Computed tomography and radiation exposure. *N Engl J Med* 358: 851; author reply 852-853, 2008.
79. **Feinendegen LE**. Evidence for beneficial low level radiation effects and radiation hormesis. *Br J Radiol* 78: 3-7, 2005.
80. **Feinendegen LE, Pollycove M, and Neumann RD**. Whole-body responses to low-level radiation exposure: new concepts in mammalian radiobiology. *Exp Hematol* 35: 37-46, 2007.
81. **Fekete A, Soos L, Szekanecz Z, Szabo Z, Szodoray P, Barath S, and Lakos G**. Disturbances in B- and T-cell homeostasis in rheumatoid arthritis: suggested relationships with antigen-driven immune responses. *J Autoimmun* 29: 154-163, 2007.
82. **Folley JH, Borges W, and Yamawaki T**. Incidence of leukemia in survivors of the atomic bomb in Hiroshima and Nagasaki, Japan. *Am J Med* 13: 311-321, 1952.
83. **Franco N, Lamartine J, Frouin V, Le Minter P, Petat C, Leplat JJ, Libert F, Gidrol X, and Martin MT**. Low-dose exposure to gamma rays induces specific gene regulations in normal human keratinocytes. *Radiat Res* 163: 623-635, 2005.
84. **Frome EL, Cragle DL, Watkins JP, Wing S, Shy CM, Tankersley WG, and West CM**. A mortality study of employees of the nuclear industry in Oak Ridge, Tennessee. *Radiat Res* 148: 64-80, 1997.
85. **Galdiero M, Cipollaro de l'Ero G, Folgore A, Cappello M, Giobbe A, and Sasso FS**. Effects of irradiation doses on alterations in cytokine release by monocytes and lymphocytes. *J Med* 25: 23-40, 1994.
86. **Gatti RA**. The inherited basis of human radiosensitivity. *Acta Oncol* 40: 702-711, 2001.
87. **Gentleman RC, Carey VJ, Bates DM, Bolstad B, Dettling M, Dudoit S, Ellis B, Gautier L, Ge Y, Gentry J, Hornik K, Hothorn T, Huber W, Iacus S, Irizarry R, Leisch F, Li C, Maechler M, Rossini AJ, Sawitzki G, Smith C, Smyth G, Tierney L, Yang JY, and Zhang J**. Bioconductor: open software development for computational biology and bioinformatics. *Genome Biol* 5: R80, 2004.
88. **Giannoni E, Chiarugi P, Cozzi G, Magnelli L, Taddei ML, Fiaschi T, Buricchi F, Raugei G, and Ramponi G**. Lymphocyte function-associated antigen-1-mediated T cell adhesion is impaired by low molecular weight phosphotyrosine phosphatase-dependent inhibition of FAK activity. *J Biol Chem* 278: 36763-36776, 2003.
89. **Giannoni E, Raugei G, Chiarugi P, and Ramponi G**. A novel redox-based switch: LMW-PTP oxidation enhances Grb2 binding and leads to ERK activation. *Biochem Biophys Res Commun* 348: 367-373, 2006.
90. **Gilbert ES**. Invited commentary: studies of workers exposed to low doses of radiation. *Am J Epidemiol* 153: 319-322; discussion 323-314, 2001.
91. **Gilbert ES, Cragle DL, and Wiggs LD**. Updated analyses of combined mortality data for workers at the Hanford Site, Oak Ridge National Laboratory, and Rocky Flats Weapons Plant. *Radiat Res* 136: 408-421, 1993.
92. **Gilbert ES, Fix JJ, and Baumgartner WV**. An approach to evaluating bias and uncertainty in estimates of external dose obtained from personal dosimeters. *Health Phys* 70: 336-345, 1996.
93. **Gotoff SP, Amirmokri E, and Liebner EJ**. Ataxia telangiectasia. Neoplasia, untoward response to x-irradiation, and tuberous sclerosis. *Am J Dis Child* 114: 617-625, 1967.

94. **Gridley DS, Pecaut MJ, Miller GM, Moyers MF, and Nelson GA**. Dose and dose rate effects of whole-body gamma-irradiation: II. Hematological variables and cytokines. *In Vivo* 15: 209-216, 2001.
95. **Gridley DS, Pecaut MJ, Rizvi A, Coutrakon GB, Luo-Owen X, Makinde AY, and Slater JM**. Low-dose, low-dose-rate proton radiation modulates CD4(+) T cell gene expression. *International journal of radiation biology* 85: 250-261, 2009.
96. **Gridley DS, Rizvi A, Luo-Owen X, Makinde AY, and Pecaut MJ**. Low dose, low dose rate photon radiation modifies leukocyte distribution and gene expression in CD4(+) T cells. *J Radiat Res (Tokyo)* 50: 139-150, 2009.
97. **Guo G, Yan-Sanders Y, Lyn-Cook BD, Wang T, Tamae D, Ogi J, Khaletskiy A, Li Z, Weydert C, Longmate JA, Huang TT, Spitz DR, Oberley LW, and Li JJ**. Manganese superoxide dismutase-mediated gene expression in radiation-induced adaptive responses. *Mol Cell Biol* 23: 2362-2378, 2003.
98. **Hashimoto S, Shirato H, Hosokawa M, Nishioka T, Kuramitsu Y, Matushita K, Kobayashi M, and Miyasaka K**. The suppression of metastases and the change in host immune response after low-dose total-body irradiation in tumor-bearing rats. *Radiat Res* 151: 717-724, 1999.
99. **Hemmer B, Archelos JJ, and Hartung HP**. New concepts in the immunopathogenesis of multiple sclerosis. *Nat Rev Neurosci* 3: 291-301, 2002.
100. **Hevener AL, and Febbraio MA**. The 2009 Stock Conference Report: Inflammation, Obesity and Metabolic Disease. *Obes Rev* 2009.
101. **Hosoi Y, and Sakamoto K**. Suppressive effect of low dose total body irradiation on lung metastasis: dose dependency and effective period. *Radiother Oncol* 26: 177-179, 1993.
102. **Huang da W, Sherman BT, and Lempicki RA**. Systematic and integrative analysis of large gene lists using DAVID bioinformatics resources. *Nat Protoc* 4: 44-57, 2009.
103. **Huertas P**. DNA resection in eukaryotes: deciding how to fix the break. *Nat Struct Mol Biol* 17: 11-16.
104. **Ibuki Y, and Goto R**. Contribution of inflammatory cytokine release to activation of resident peritoneal macrophages after in vivo low-dose gamma-irradiation. *J Radiat Res (Tokyo)* 40: 253-262, 1999.
105. **ICRP**. Recommendations of the International Commission on Radiological Protection Oxford: 1991.
106. **ICRU**. International Commission on Radiological Protection (ICRP): Publication 103: Recommendations of the ICRP. USA: Elsevier, 2007.
107. **ICRU**. Publication 60: Fundamental Quantities and Units for Ionizing Radiation. USA: Elsevier, 1998.
108. **Ina Y, and Sakai K**. Activation of immunological network by chronic low-dose-rate irradiation in wild-type mouse strains: analysis of immune cell populations and surface molecules. *International journal of radiation biology* 81: 721-729, 2005.
109. **Ina Y, Tanooka H, Yamada T, and Sakai K**. Suppression of thymic lymphoma induction by life-long low-dose-rate irradiation accompanied by immune activation in C57BL/6 mice. *Radiat Res* 163: 153-158, 2005.
110. **Inoue K, Takano H, Shimada A, Wada E, Yanagisawa R, Sakurai M, Satoh M, and Yoshikawa T**. Role of metallothionein in coagulatory disturbance and systemic inflammation induced by lipopolysaccharide in mice. *FASEB J* 20: 533-535, 2006.
111. **Ishii K, Yamaoka K, Hosoi Y, Ono T, and Sakamoto K**. Enhanced mitogen-induced proliferation of rat splenocytes by low-dose whole-body X-irradiation. *Physiol Chem Phys Med NMR* 27: 17-23, 1995.

112. **Ito M, Shibamoto Y, Ayakawa S, Tomita N, Sugie C, and Ogino H**. Low-dose whole-body irradiation induced radioadaptive response in C57BL/6 mice. *J Radiat Res (Tokyo)* 48: 455-460, 2007.
113. **Jacobs P, and King HS**. A randomized prospective comparison of chemotherapy to total body irradiation as initial treatment for the indolent lymphoproliferative diseases. *Blood* 69: 1642-1646, 1987.
114. **Jann NJ, Schmaler M, Kristian SA, Radek KA, Gallo RL, Nizet V, Peschel A, and Landmann R**. Neutrophil antimicrobial defense against Staphylococcus aureus is mediated by phagolysosomal but not extracellular trap-associated cathelicidin. *J Leukoc Biol* 86: 1159-1169, 2009.
115. **Jansen RC, and Nap JP**. Genetical genomics: the added value from segregation. *Trends Genet* 17: 388-391, 2001.
116. **Jin SZ, He SJ, and Liu SZ**. Effect of different doses of X-rays on the expression of CD80 and CD86 on mouse macrophages. *J Radiat Res Radiat Proc* 19: 153-157, 2001.
117. **Kataoka T, Mizuguchi Y, Notohara K, Taguchi T, and Yamaoka K**. Histological changes in spleens of radio-sensitive and radio-resistant mice exposed to low-dose X-ray irradiation. *Physiol Chem Phys Med NMR* 38: 21-29, 2006.
118. **Kessenbrock K, Frohlich L, Sixt M, Lammermann T, Pfister H, Bateman A, Belaaouaj A, Ring J, Ollert M, Fassler R, and Jenne DE**. Proteinase 3 and neutrophil elastase enhance inflammation in mice by inactivating antiinflammatory progranulin. *J Clin Invest* 118: 2438-2447, 2008.
119. **Kim GJ, Chandrasekaran K, and Morgan WF**. Mitochondrial dysfunction, persistently elevated levels of reactive oxygen species and radiation-induced genomic instability: a review. *Mutagenesis* 21: 361-367, 2006.
120. **Kleinerman RA, Tucker MA, Tarone RE, Abramson DH, Seddon JM, Stovall M, Li FP, and Fraumeni JF, Jr.** Risk of new cancers after radiotherapy in long-term survivors of retinoblastoma: an extended follow-up. *J Clin Oncol* 23: 2272-2279, 2005.
121. **Kobayashi S, and DeLeo F**. Role of neutrophils in innate immunity: a systems biology-level approach. *WIREs Systems Biology and Medicine* 1: 309-333, 2009.
122. **Kojima S, Nakayama K, and Ishida H**. Low dose gamma-rays activate immune functions via induction of glutathione and delay tumor growth. *J Radiat Res (Tokyo)* 45: 33-39, 2004.
123. **Kolls JK, and Linden A**. Interleukin-17 family members and inflammation. *Immunity* 21: 467-476, 2004.
124. **Kose H, Sakai T, Tsukumo S, Wei K, Yamada T, Yasutomo K, and Matsumoto K**. Maturational arrest of thymocyte development is caused by a deletion in the receptor-like protein tyrosine phosphatase kappa gene in LEC rats. *Genomics* 89: 673-677, 2007.
125. **Kraal G, Weissman IL, and Butcher EC**. Genetic control of T-cell subset representation in inbred mice. *Immunogenetics* 18: 585-592, 1983.
126. **Kraemer KH, Patronas NJ, Schiffmann R, Brooks BP, Tamura D, and DiGiovanna JJ**. Xeroderma pigmentosum, trichothiodystrophy and Cockayne syndrome: a complex genotype-phenotype relationship. *Neuroscience* 145: 1388-1396, 2007.
127. **Kuby J**. *Immunology*. New York: W. H. Freeman and Company, 1997.
128. **Kusunoki Y, Hayashi T, Morishita Y, Yamaoka M, Maki M, Bean MA, Kyoizumi S, Hakoda M, and Kodama K**. T-cell responses to mitogens in atomic bomb survivors: a decreased capacity to produce interleukin 2 characterizes the T cells of heavily irradiated individuals. *Radiat Res* 155: 81-88, 2001.
129. **Kusunoki Y, Kyoizumi S, Hirai Y, Suzuki T, Nakashima E, Kodama K, and Seyama T**. Flow cytometry measurements of subsets of T, B and NK cells in peripheral blood lymphocytes of atomic bomb survivors. *Radiat Res* 150: 227-236, 1998.

130. **Lander E, and Kruglyak L**. Genetic dissection of complex traits: guidelines for interpreting and reporting linkage results. *Nat Genet* 11: 241-247, 1995.
131. **Lander ES, and Botstein D**. Mapping mendelian factors underlying quantitative traits using RFLP linkage maps. *Genetics* 121: 185-199, 1989.
132. **Lane DP**. Cancer. p53, guardian of the genome. *Nature* 358: 15-16, 1992.
133. **Langston MA, Perkins AD, Saxton AM, Scharff JA, and Voy BH**. Innovative computational methods for transcriptomic data analysis: A case study in the use of FPT for practical algorithm design and implementation. *Comput J* 51: 26-38, 2008.
134. **Lavin MF**. Ataxia-telangiectasia: from a rare disorder to a paradigm for cell signalling and cancer. *Nat Rev Mol Cell Biol* 9: 759-769, 2008.
135. **Leblanc CJ, Leblanc AK, Jones MM, Bartges JW, and Kania SA**. Evaluation of peripheral blood neutrophil function in tumor-bearing dogs. *Vet Clin Pathol* 2010.
136. **Lee WJ, Majumder ZR, Jeoung DI, Lee HJ, Kim SH, Bae S, and Lee YS**. Organ-specific gene expressions in C57BL/6 mice after exposure to low-dose radiation. *Radiat Res* 165: 562-569, 2006.
137. **Legrand D, and Mazurier J**. A critical review of the roles of host lactoferrin in immunity. *Biometals*.
138. **Lehnert BE, and Goodwin EH**. A new mechanism for DNA alterations induced by alpha particles such as those emitted by radon and radon progeny. *Environ Health Perspect* 105 Suppl 5: 1095-1101, 1997.
139. **Leipe J, Skapenko A, Lipsky PE, and Schulze-Koops H**. Regulatory T cells in rheumatoid arthritis. *Arthritis Res Ther* 7: 93, 2005.
140. **Lindsay KJ, Coates PJ, Lorimore SA, and Wright EG**. The genetic basis of tissue responses to ionizing radiation. *Br J Radiol* 80 Spec No 1: S2-6, 2007.
141. **Little JB**. Lauriston S. Taylor lecture: nontargeted effects of radiation: implications for low-dose exposures. *Health Phys* 91: 416-426, 2006.
142. **Liu C, Gelius E, Liu G, Steiner H, and Dziarski R**. Mammalian peptidoglycan recognition protein binds peptidoglycan with high affinity, is expressed in neutrophils, and inhibits bacterial growth. *J Biol Chem* 275: 24490-24499, 2000.
143. **Liu SZ**. On radiation hormesis expressed in the immune system. *Crit Rev Toxicol* 33: 431-441, 2003.
144. **Liu SZ, Han ZB, and Liu WH**. Changes in lymphocyte reactivity to modulatory factors following low dose ionizing radiation. *Biomed Environ Sci* 7: 130-135, 1994.
145. **Liu SZ, Jin SZ, Liu XD, and Sun YM**. Role of CD28/B7 costimulation and IL-12/IL-10 interaction in the radiation-induced immune changes. *BMC Immunol* 2: 8, 2001.
146. **Liu SZ, SuXu, Zhang YC, and Zhao Y**. Signal transduction in lymphocytes after low dose radiation. *Chin Med J (Engl)* 107: 431-436, 1994.
147. **Liu XD, Ma SM, and Liu SZ**. Effects of 0.075 Gy x-ray irradiation on the expression of IL-10 and IL-12 in mice. *Phys Med Biol* 48: 2041-2049, 2003.
148. **Loeb LA, Loeb KR, and Anderson JP**. Multiple mutations and cancer. *Proc Natl Acad Sci U S A* 100: 776-781, 2003.
149. **Long XH, Zhao ZQ, He XP, Wang HP, Xu QZ, An J, Bai B, Sui JL, and Zhou PK**. Dose-dependent expression changes of early response genes to ionizing radiation in human lymphoblastoid cells. *Int J Mol Med* 19: 607-615, 2007.
150. **Lord BI, Molineux G, Pojda Z, Souza LM, Mermod JJ, and Dexter TM**. Myeloid cell kinetics in mice treated with recombinant interleukin-3, granulocyte colony-stimulating factor (CSF), or granulocyte-macrophage CSF in vivo. *Blood* 77: 2154-2159, 1991.
151. **Lorimore SA, Chrystal JA, Robinson JI, Coates PJ, and Wright EG**. Chromosomal instability in unirradiated hemaopoietic cells induced by macrophages exposed in vivo to ionizing radiation. *Cancer Res* 68: 8122-8126, 2008.

152. **Lu L, Wei L, Peirce JL, Wang X, Zhou J, Homayouni R, Williams RW, and Airey DC**. Using gene expression databases for classical trait QTL candidate gene discovery in the BXD recombinant inbred genetic reference population: mouse forebrain weight. *BMC Genomics* 9: 444, 2008.
153. **Lynch RM, Naswa S, Rogers GL, Jr., Kania SA, Das S, Chesler EJ, Saxton AM, Langston MA, and Voy BH**. Identifying genetic loci and spleen gene coexpression networks underlying immunophenotypes in BXD recombinant inbred mice. *Physiol Genomics* 2010.
154. **Maatta M, Liakka A, Salo S, Tasanen K, Bruckner-Tuderman L, and Autio-Harmainen H**. Differential expression of basement membrane components in lymphatic tissues. *J Histochem Cytochem* 52: 1073-1081, 2004.
155. **MacCallum DE, Hupp TR, Midgley CA, Stuart D, Campbell SJ, Harper A, Walsh FS, Wright EG, Balmain A, Lane DP, and Hall PA**. The p53 response to ionising radiation in adult and developing murine tissues. *Oncogene* 13: 2575-2587, 1996.
156. **MacDonell KB, Chmiel JS, Poggensee L, Wu S, and Phair JP**. Predicting progression to AIDS: combined usefulness of CD4 lymphocyte counts and p24 antigenemia. *Am J Med* 89: 706-712, 1990.
157. **Major IR, and Mole RH**. Myeloid leukaemia in x-ray irradiated CBA mice. *Nature* 272: 455-456, 1978.
158. **Malentacchi F, Marzocchini R, Gelmini S, Orlando C, Serio M, Ramponi G, and Raugei G**. Up-regulated expression of low molecular weight protein tyrosine phosphatases in different human cancers. *Biochem Biophys Res Commun* 334: 875-883, 2005.
159. **Malle E, Furtmuller PG, Sattler W, and Obinger C**. Myeloperoxidase: a target for new drug development? *Br J Pharmacol* 152: 838-854, 2007.
160. **Mancuso M, Pasquali E, Leonardi S, Tanori M, Rebessi S, Di Majo V, Pazzaglia S, Toni MP, Pimpinella M, Covelli V, and Saran A**. Oncogenic bystander radiation effects in Patched heterozygous mouse cerebellum. *Proc Natl Acad Sci U S A* 105: 12445-12450, 2008.
161. **Marshall KR, Gong M, Wodke L, Lamb JH, Jones DJ, Farmer PB, Scrutton NS, and Munro AW**. The human apoptosis-inducing protein AMID is an oxidoreductase with a modified flavin cofactor and DNA binding activity. *J Biol Chem* 280: 30735-30740, 2005.
162. **Martinuzzi E, Lemonnier FA, Boitard C, and Mallone R**. Measurement of CD8 T cell responses in human type 1 diabetes. *Ann N Y Acad Sci* 1150: 61-67, 2008.
163. **Marzocchini R, Malentacchi F, Biagini M, Cirelli D, Luceri C, Caderni G, and Raugei G**. The expression of low molecular weight protein tyrosine phosphatase is up-regulated in 1,2-dimethylhydrazine-induced colon tumours in rats. *Int J Cancer* 122: 1675-1678, 2008.
164. **Matsubara J, Turcanu V, Poindron P, and Ina Y**. Immune effects of low-dose radiation: short-term induction of thymocyte apoptosis and long-term augmentation of T-cell-dependent immune responses. *Radiat Res* 153: 332-338, 2000.
165. **Maxwell CA, Fleisch MC, Costes SV, Erickson AC, Boissiere A, Gupta R, Ravani SA, Parvin B, and Barcellos-Hoff MH**. Targeted and nontargeted effects of ionizing radiation that impact genomic instability. *Cancer Res* 68: 8304-8311, 2008.
166. **McBride WH, Chiang CS, Olson JL, Wang CC, Hong JH, Pajonk F, Dougherty GJ, Iwamoto KS, Pervan M, and Liao YP**. A sense of danger from radiation. *Radiat Res* 162: 1-19, 2004.
167. **Mettler FA, Jr., Bhargavan M, Faulkner K, Gilley DB, Gray JE, Ibbott GS, Lipoti JA, Mahesh M, McCrohan JL, Stabin MG, Thomadsen BR, and Yoshizumi TT**. Radiologic and nuclear medicine studies in the United States and worldwide: frequency, radiation dose, and comparison with other radiation sources--1950-2007. *Radiology* 253: 520-531, 2009.
168. **Mettler FA, Jr., Gus'kova AK, and Gusev I**. Health effects in those with acute radiation sickness from the Chernobyl accident. *Health Phys* 93: 462-469, 2007.

169. **Mitchel RE**. Cancer and low dose responses in vivo: implications for radiation protection. *Dose Response* 5: 284-291, 2007.
170. **Mitchel RE, Jackson JS, McCann RA, and Boreham DR**. The adaptive response modifies latency for radiation-induced myeloid leukemia in CBA/H mice. *Radiat Res* 152: 273-279, 1999.
171. **Mitchel RE, Jackson JS, Morrison DP, and Carlisle SM**. Low doses of radiation increase the latency of spontaneous lymphomas and spinal osteosarcomas in cancer-prone, radiation-sensitive Trp53 heterozygous mice. *Radiat Res* 159: 320-327, 2003.
172. **Miyairi I, Tatireddigari VR, Mahdi OS, Rose LA, Belland RJ, Lu L, Williams RW, and Byrne GI**. The p47 GTPases Iigp2 and Irgb10 regulate innate immunity and inflammation to murine Chlamydia psittaci infection. *J Immunol* 179: 1814-1824, 2007.
173. **Monsieurs MA, Thierens HM, Vral AM, Van De Wiele C, De Ridder LI, and Dierckx RA**. Adaptive response in patients treated with 131I. *J Nucl Med* 41: 17-22, 2000.
174. **Morgan WF**. Non-targeted and delayed effects of exposure to ionizing radiation: I. Radiation-induced genomic instability and bystander effects in vitro. *Radiat Res* 159: 567-580, 2003.
175. **Morgan WF**. Non-targeted and delayed effects of exposure to ionizing radiation: II. Radiation-induced genomic instability and bystander effects in vivo, clastogenic factors and transgenerational effects. *Radiat Res* 159: 581-596, 2003.
176. **Morgan WF**. Will radiation-induced bystander effects or adaptive responses impact on the shape of the dose response relationships at low doses of ionizing radiation? *Dose Response* 4: 257-262, 2006.
177. **Mori N, Matsumoto Y, Okumoto M, Suzuki N, and Yamate J**. Variations in Prkdc encoding the catalytic subunit of DNA-dependent protein kinase (DNA-PKcs) and susceptibility to radiation-induced apoptosis and lymphomagenesis. *Oncogene* 20: 3609-3619, 2001.
178. **Mori N, Okumoto M, Hart AA, and Demant P**. Apoptosis susceptibility genes on mouse chromosome 9 (Rapop2) and chromosome 3 (Rapop3). *Genomics* 30: 553-557, 1995.
179. **Mori N, Okumoto M, Morimoto J, Imai S, Matsuyama T, Takamori Y, and Yagasaki O**. Genetic analysis of susceptibility to radiation-induced apoptosis of thymocytes in mice. *International journal of radiation biology* 62: 153-159, 1992.
180. **Mori N, Okumoto M, van der Valk MA, Imai S, Haga S, Esaki K, Hart AA, and Demant P**. Genetic dissection of susceptibility to radiation-induced apoptosis of thymocytes and mapping of Rapop1, a novel susceptibility gene. *Genomics* 25: 609-614, 1995.
181. **Mori N, van Wezel T, van der Valk M, Yamate J, Sakuma S, Okumoto M, and Demant P**. Genetics of susceptibility to radiation-induced apoptosis in colon: two loci on chromosomes 9 and 16. *Mamm Genome* 9: 377-380, 1998.
182. **Mothersill C, Rea D, Wright EG, Lorimore SA, Murphy D, Seymour CB, and O'Malley K**. Individual variation in the production of a 'bystander signal' following irradiation of primary cultures of normal human urothelium. *Carcinogenesis* 22: 1465-1471, 2001.
183. **Mothersill C, and Seymour CB**. Radiation-induced bystander effects--implications for cancer. *Nat Rev Cancer* 4: 158-164, 2004.
184. **Mullenders L, Atkinson M, Paretzke H, Sabatier L, and Bouffler S**. Assessing cancer risks of low-dose radiation. *Nat Rev Cancer* 9: 596-604, 2009.
185. **Muller HJ**. Artificial Transmutation of the Gene. *Science* 66: 84-87, 1927.
186. **Myrick C, DiGuisto R, DeWolfe J, Bowen E, Kappler J, Marrack P, and Wakeland EK**. Linkage analysis of variations in CD4:CD8 T cell subsets between C57BL/6 and DBA/2. *Genes Immun* 3: 144-150, 2002.
187. **Nagataki S**. Computed tomography and radiation exposure. *N Engl J Med* 358: 850-851; author reply 852-853, 2008.

188. **Nakamura M, Kishi M, Sakaki T, Hashimoto H, Nakase H, Shimada K, Ishida E, and Konishi N**. Novel tumor suppressor loci on 6q22-23 in primary central nervous system lymphomas. *Cancer Res* 63: 737-741, 2003.
189. **NCRP**. Ionizing radiation exposure of the population of the United States: 2006. NCRP Report No. 160. Bathesda, MD: National Council on Radiation Protection and Measurements., 2009.
190. **NCRP**. National Council on Radiation Protection and Measurements: Evaluation of the Linear-Nonthreshold Dose-Response Model for Ionizing Radiation, Report No. 136. Bathesda, MD: 2001.
191. **Nishimura S, Manabe I, Nagasaki M, Eto K, Yamashita H, Ohsugi M, Otsu M, Hara K, Ueki K, Sugiura S, Yoshimura K, Kadowaki T, and Nagai R**. CD8+ effector T cells contribute to macrophage recruitment and adipose tissue inflammation in obesity. *Nat Med* 15: 914-920, 2009.
192. **Nogami M, Huang JT, Nakamura LT, and Makinodan T**. T cells are the cellular target of the proliferation-augmenting effect of chronic low-dose ionizing radiation in mice. *Radiat Res* 139: 47-52, 1994.
193. **Nomura T, Kinuta M, Hongyo T, Nakajima H, and Hatanaka T**. Programmed cell death in whole body and organ systems by low dose radiation. *J Radiat Res (Tokyo)* 33 Suppl: 109-123, 1992.
194. **Nowosielska EM, Wrembel-Wargocka J, Cheda A, Lisiak E, and Janiak MK**. Enhanced cytotoxic activity of macrophages and suppressed tumor metastases in mice irradiated with low doses of X- rays. *J Radiat Res (Tokyo)* 47: 229-236, 2006.
195. **NRC**. National Research Council's BEIR VII: Health Risks from Exposure to Low Levels of Ionizing Radiation Washington, DC: 2005.
196. **Oberley LW, Lindgren LA, Baker SA, and Stevens RH**. Superoxide Ion as the cause of the oxygen effect. *Radiat Res* 68: 320-328, 1976.
197. **Oberley LW, St Clair DK, Autor AP, and Oberley TD**. Increase in manganese superoxide dismutase activity in the mouse heart after X-irradiation. *Arch Biochem Biophys* 254: 69-80, 1987.
198. **Olivieri G, Bodycote J, and Wolff S**. Adaptive response of human lymphocytes to low concentrations of radioactive thymidine. *Science* 223: 594-597, 1984.
199. **Otsuka K, Koana T, Tauchi H, and Sakai K**. Activation of antioxidative enzymes induced by low-dose-rate whole-body gamma irradiation: adaptive response in terms of initial DNA damage. *Radiat Res* 166: 474-478, 2006.
200. **Padovani L, Appolloni M, Anzidei P, Tedeschi B, Caporossi D, Vernole P, and Mauro F**. Do human lymphocytes exposed to the fallout of the Chernobyl accident exhibit an adaptive response? 1. Challenge with ionizing radiation. *Mutat Res* 332: 33-38, 1995.
201. **Pandey R, Shankar BS, Sharma D, and Sainis KB**. Low dose radiation induced immunomodulation: effect on macrophages and CD8+ T cells. *International journal of radiation biology* 81: 801-812, 2005.
202. **Park HR, Jung U, and Jo SK**. Impairment of natural killer (NK) cells is an important factor in a weak Th1-like response in irradiated mice. *Radiat Res* 168: 446-452, 2007.
203. **Passador-Gurgel G, Hsieh WP, Hunt P, Deighton N, and Gibson G**. Quantitative trait transcripts for nicotine resistance in Drosophila melanogaster. *Nat Genet* 39: 264-268, 2007.
204. **Pathak CM, Avti PK, Kumar S, Khanduja KL, and Sharma SC**. Whole body exposure to low-dose gamma radiation promotes kidney antioxidant status in Balb/c mice. *J Radiat Res (Tokyo)* 48: 113-120, 2007.
205. **Paull TT, and Lee JH**. The Mre11/Rad50/Nbs1 complex and its role as a DNA double-strand break sensor for ATM. *Cell Cycle* 4: 737-740, 2005.

206. **Pecaut MJ, Nelson GA, and Gridley DS**. Dose and dose rate effects of whole-body gamma-irradiation: I. Lymphocytes and lymphoid organs. *In Vivo* 15: 195-208, 2001.
207. **Peirce JL, Lu L, Gu J, Silver LM, and Williams RW**. A new set of BXD recombinant inbred lines from advanced intercross populations in mice. *BMC Genet* 5: 7, 2004.
208. **Peterson RD, Kelly WD, and Good RA**. Ataxia-Telangiectasia. Its Association with a Defective Thymus, Immunological-Deficiency Disease, and Malignancy. *Lancet* 1: 1189-1193, 1964.
209. **Petkova SB, Yuan R, Tsaih SW, Schott W, Roopenian DC, and Paigen B**. Genetic influence on immune phenotype revealed strain-specific variations in peripheral blood lineages. Mouse Phenome Database Project: Petkova1. The Jackson Laboratory. http://www.jax.org/phenome. [January 7, 2010].
210. **Philip VM, Duvvuru S, Gomero B, Ansah TA, Blaha CD, Cook MN, Hamre KM, Lariviere WR, Matthews DB, Mittleman G, Goldowitz D, and Chesler EJ**. High-throughput behavioral phenotyping in the expanded panel of BXD recombinant inbred strains. *Genes Brain Behav* 2009.
211. **Pierce DA, and Preston DL**. Radiation-related cancer risks at low doses among atomic bomb survivors. *Radiat Res* 154: 178-186, 2000.
212. **Ponnaiya B, Cornforth MN, and Ullrich RL**. Radiation-induced chromosomal instability in BALB/c and C57BL/6 mice: the difference is as clear as black and white. *Radiat Res* 147: 121-125, 1997.
213. **Powell CL, Swenberg JA, and Rusyn I**. Expression of base excision DNA repair genes as a biomarker of oxidative DNA damage. *Cancer Lett* 229: 1-11, 2005.
214. **Preston DL, Shimizu Y, Pierce DA, Suyama A, and Mabuchi K**. Studies of mortality of atomic bomb survivors. Report 13: Solid cancer and noncancer disease mortality: 1950-1997. *Radiat Res* 160: 381-407, 2003.
215. **Raaphorst GP, and Boyden S**. Adaptive response and its variation in human normal and tumour cells. *International journal of radiation biology* 75: 865-873, 1999.
216. **Richardson D, Sugiyama H, Nishi N, Sakata R, Shimizu Y, Grant EJ, Soda M, Hsu WL, Suyama A, Kodama K, and Kasagi F**. Ionizing radiation and leukemia mortality among Japanese Atomic Bomb Survivors, 1950-2000. *Radiat Res* 172: 368-382, 2009.
217. **Roderick TH**. The Response Of Twenty-Seven Inbred Strains Of Mice To Daily Doses Of Whole-Body X-Irradiation. *Radiat Res* 20: 631-639, 1963.
218. **Rosse T, Olivier R, Monney L, Rager M, Conus S, Fellay I, Jansen B, and Borner C**. Bcl-2 prolongs cell survival after Bax-induced release of cytochrome c. *Nature* 391: 496-499, 1998.
219. **Rothkamm K, and Lobrich M**. Evidence for a lack of DNA double-strand break repair in human cells exposed to very low x-ray doses. *Proc Natl Acad Sci U S A* 100: 5057-5062, 2003.
220. **Rouse J, and Jackson SP**. Interfaces between the detection, signaling, and repair of DNA damage. *Science* 297: 547-551, 2002.
221. **Rube CE, Grudzenski S, Kuhne M, Dong X, Rief N, Lobrich M, and Rube C**. DNA double-strand break repair of blood lymphocytes and normal tissues analysed in a preclinical mouse model: implications for radiosensitivity testing. *Clin Cancer Res* 14: 6546-6555, 2008.
222. **Safwat A**. The immunobiology of low-dose total-body irradiation: more questions than answers. *Radiat Res* 153: 599-604, 2000.
223. **Saito Y, Ochiai Y, Kodama Y, Tamura Y, Togashi T, Kosugi-Okano H, Miyazawa T, Wakabayashi Y, Hatakeyama K, Wakana S, Niwa O, and Kominami R**. Genetic loci controlling susceptibility to gamma-ray-induced thymic lymphoma. *Oncogene* 20: 5243-5247, 2001.
224. **Savitsky K, Bar-Shira A, Gilad S, Rotman G, Ziv Y, Vanagaite L, Tagle DA, Smith S, Uziel T, Sfez S, Ashkenazi M, Pecker I, Frydman M, Harnik R, Patanjali SR, Simmons A,**

Clines GA, Sartiel A, Gatti RA, Chessa L, Sanal O, Lavin MF, Jaspers NG, Taylor AM, Arlett CF, Miki T, Weissman SM, Lovett M, Collins FS, and Shiloh Y. A single ataxia telangiectasia gene with a product similar to PI-3 kinase. *Science* 268: 1749-1753, 1995.
225. **Schadt EE, Molony C, Chudin E, Hao K, Yang X, Lum PY, Kasarskis A, Zhang B, Wang S, Suver C, Zhu J, Millstein J, Sieberts S, Lamb J, GuhaThakurta D, Derry J, Storey JD, Avila-Campillo I, Kruger MJ, Johnson JM, Rohl CA, van Nas A, Mehrabian M, Drake TA, Lusis AJ, Smith RC, Guengerich FP, Strom SC, Schuetz E, Rushmore TH, and Ulrich R**. Mapping the genetic architecture of gene expression in human liver. *PLoS Biol* 6: e107, 2008.
226. **Schadt EE, Monks SA, Drake TA, Lusis AJ, Che N, Colinayo V, Ruff TG, Milligan SB, Lamb JR, Cavet G, Linsley PS, Mao M, Stoughton RB, and Friend SH**. Genetics of gene expression surveyed in maize, mouse and man. *Nature* 422: 297-302, 2003.
227. **Schaue D, Marples B, and Trott KR**. The effects of low-dose X-irradiation on the oxidative burst in stimulated macrophages. *International journal of radiation biology* 78: 567-576, 2002.
228. **Scott BR**. It's Time for a New Low-Dose-Radiation Risk Assessment Paradigm-One That Acknowledges Hormesis. *Dose Response* 6: 333-351, 2008.
229. **Scott BR, Sanders CL, Mitchel RE, and Boreham DR**. CT scans may reduce rather than increase the risk of cancer. *Journal of American Physicians and Surgeons* 13: 8-11, 2008.
230. **Sen S, and Churchill GA**. A statistical framework for quantitative trait mapping. *Genetics* 159: 371-387, 2001.
231. **Sethu S, Mendez-Corao G, and Melendez AJ**. Phospholipase D1 plays a key role in TNF-alpha signaling. *J Immunol* 180: 6027-6034, 2008.
232. **Shadley JD, Afzal V, and Wolff S**. Characterization of the adaptive response to ionizing radiation induced by low doses of X rays to human lymphocytes. *Radiat Res* 111: 511-517, 1987.
233. **Shan YX, Jin SZ, Liu XD, Liu Y, and Liu SZ**. Ionizing radiation stimulates secretion of pro-inflammatory cytokines: dose-response relationship, mechanisms and implications. *Radiat Environ Biophys* 46: 21-29, 2007.
234. **Shankar B, Premachandran S, Bharambe SD, Sundaresan P, and Sainis KB**. Modification of immune response by low dose ionizing radiation: role of apoptosis. *Immunol Lett* 68: 237-245, 1999.
235. **Shifman S, Bell JT, Copley RR, Taylor MS, Williams RW, Mott R, and Flint J**. A high-resolution single nucleotide polymorphism genetic map of the mouse genome. *PLoS Biol* 4: e395, 2006.
236. **Shigematsu A, Adachi Y, Koike-Kiriyama N, Suzuki Y, Iwasaki M, Koike Y, Nakano K, Mukaide H, Imamura M, and Ikehara S**. Effects of low-dose irradiation on enhancement of immunity by dendritic cells. *J Radiat Res (Tokyo)* 48: 51-55, 2007.
237. **Short SC, Buffa FM, Bourne S, Koritzinsky M, Wouters BG, and Bentzen SM**. Dose- and time-dependent changes in gene expression in human glioma cells after low radiation doses. *Radiat Res* 168: 199-208, 2007.
238. **Sieberts SK, and Schadt EE**. Moving toward a system genetics view of disease. *Mamm Genome* 18: 389-401, 2007.
239. **Sies H**. Oxidative stress: oxidants and antioxidants. *Exp Physiol* 82: 291-295, 1997.
240. **Skapenko A, Leipe J, Lipsky PE, and Schulze-Koops H**. The role of the T cell in autoimmune inflammation. *Arthritis Res Ther* 7 Suppl 2: S4-14, 2005.
241. **Smirnov DA, Morley M, Shin E, Spielman RS, and Cheung VG**. Genetic analysis of radiation-induced changes in human gene expression. *Nature* 459: 587-591, 2009.
242. **Smith GC, and Jackson SP**. The DNA-dependent protein kinase. *Genes Dev* 13: 916-934, 1999.

243. **Sont WN, Zielinski JM, Ashmore JP, Jiang H, Krewski D, Fair ME, Band PR, and Letourneau EG**. First analysis of cancer incidence and occupational radiation exposure based on the National Dose Registry of Canada. *Am J Epidemiol* 153: 309-318, 2001.
244. **Souza AC, Azoubel S, Queiroz KC, Peppelenbosch MP, and Ferreira CV**. From immune response to cancer: a spot on the low molecular weight protein tyrosine phosphatase. *Cell Mol Life Sci* 66: 1140-1153, 2009.
245. **Spina C, Saccucci P, Bottini E, and Gloria-Bottini F**. ACP1 genetic polymorphism and colon cancer. *Cancer Genet Cytogenet* 186: 61-62, 2008.
246. **Spitz DR, Azzam EI, Li JJ, and Gius D**. Metabolic oxidation/reduction reactions and cellular responses to ionizing radiation: a unifying concept in stress response biology. *Cancer Metastasis Rev* 23: 311-322, 2004.
247. **Srivastava M, Chandra D, and Kale RK**. Modulation of radiation-induced changes in the xanthine oxidoreductase system in the livers of mice by its inhibitors. *Radiat Res* 157: 290-297, 2002.
248. **Srivastava M, and Kale RK**. Effect of radiation on the xanthine oxidoreductase system in the liver of mice. *Radiat Res* 152: 257-264, 1999.
249. **Starr TK, Allaei R, Silverstein KA, Staggs RA, Sarver AL, Bergemann TL, Gupta M, O'Sullivan MG, Matise I, Dupuy AJ, Collier LS, Powers S, Oberg AL, Asmann YW, Thibodeau SN, Tessarollo L, Copeland NG, Jenkins NA, Cormier RT, and Largaespada DA**. A transposon-based genetic screen in mice identifies genes altered in colorectal cancer. *Science* 323: 1747-1750, 2009.
250. **Storey JD, and Tibshirani R**. Statistical significance for genomewide studies. *Proc Natl Acad Sci U S A* 100: 9440-9445, 2003.
251. **Summers RW, Maves BV, Reeves RD, Arjes LJ, and Oberley LW**. Irradiation increases superoxide dismutase in rat intestinal smooth muscle. *Free Radic Biol Med* 6: 261-270, 1989.
252. **Sun YM, and Liu SZ**. Changes in mRNA level of TNFa and IL-lb in peritoneal macrophages after whole-body X-irradiation. *J Radiat Res Radiat Proc* 18: 235-239, 1998.
253. **Tada Y, Ho A, Koh DR, and Mak TW**. Collagen-induced arthritis in CD4- or CD8-deficient mice: CD8+ T cells play a role in initiation and regulate recovery phase of collagen-induced arthritis. *J Immunol* 156: 4520-4526, 1996.
254. **Tailor P, Gilman J, Williams S, Couture C, and Mustelin T**. Regulation of the low molecular weight phosphotyrosine phosphatase by phosphorylation at tyrosines 131 and 132. *J Biol Chem* 272: 5371-5374, 1997.
255. **Tang Y, Xu H, Du X, Lit L, Walker W, Lu A, Ran R, Gregg JP, Reilly M, Pancioli A, Khoury JC, Sauerbeck LR, Carrozzella JA, Spilker J, Clark J, Wagner KR, Jauch EC, Chang DJ, Verro P, Broderick JP, and Sharp FR**. Gene expression in blood changes rapidly in neutrophils and monocytes after ischemic stroke in humans: a microarray study. *J Cereb Blood Flow Metab* 26: 1089-1102, 2006.
256. **Tanigaki K, and Honjo T**. Regulation of lymphocyte development by Notch signaling. *Nat Immunol* 8: 451-456, 2007.
257. **Tanooka H**. Threshold dose-response in radiation carcinogenesis: an approach from chronic beta-irradiation experiments and a review of non-tumour doses. *International journal of radiation biology* 77: 541-551, 2001.
258. **Taylor AM, Groom A, and Byrd PJ**. Ataxia-telangiectasia-like disorder (ATLD)-its clinical presentation and molecular basis. *DNA Repair (Amst)* 3: 1219-1225, 2004.
259. **Taylor BA, Bedigian HG, and Meier H**. Genetic studies of the Fv-1 locus of mice: linkage with Gpd-1 in recombinant inbred lines. *J Virol* 23: 106-109, 1977.

260. **Taylor BA, Wnek C, Kotlus BS, Roemer N, MacTaggart T, and Phillips SJ**. Genotyping new BXD recombinant inbred mouse strains and comparison of BXD and consensus maps. *Mamm Genome* 10: 335-348, 1999.
261. **Tripp RA, Hou S, McMickle A, Houston J, and Doherty PC**. Recruitment and proliferation of CD8+ T cells in respiratory virus infections. *J Immunol* 154: 6013-6021, 1995.
262. **Tubiana M**. The 2007 Marie Curie prize: the linear no threshold relationship and advances in our understanding of carcinogenesis. *International Journal of Low Dose Radiation* 5: 173-204, 2008.
263. **Tubiana M**. Computed tomography and radiation exposure. *N Engl J Med* 358: 850; author reply 852-853, 2008.
264. **Tubiana M, Feinendegen LE, Yang C, and Kaminski JM**. The linear no-threshold relationship is inconsistent with radiation biologic and experimental data. *Radiology* 251: 13-22, 2009.
265. **Tyner SD, Venkatachalam S, Choi J, Jones S, Ghebranious N, Igelmann H, Lu X, Soron G, Cooper B, Brayton C, Hee Park S, Thompson T, Karsenty G, Bradley A, and Donehower LA**. p53 mutant mice that display early ageing-associated phenotypes. *Nature* 415: 45-53, 2002.
266. **Ullrich RL, and Preston RJ**. Radiation induced mammary cancer. *J Radiat Res (Tokyo)* 32 Suppl 2: 104-109, 1991.
267. **Ullrich RL, and Storer JB**. Influence of gamma irradiation on the development of neoplastic disease in mice. I. Reticular tissue tumors. *Radiat Res* 80: 303-316, 1979.
268. **UNSCEAR**. United Nations Scientific Committee on the Effects of Atomic Radiation: Sources and effects of ionizing radiation 2000.
269. **Vacchio MS, Olaru A, Livak F, and Hodes RJ**. ATM deficiency impairs thymocyte maturation because of defective resolution of T cell receptor alpha locus coding end breaks. *Proc Natl Acad Sci U S A* 104: 6323-6328, 2007.
270. **Valerie K, Yacoub A, Hagan MP, Curiel DT, Fisher PB, Grant S, and Dent P**. Radiation-induced cell signaling: inside-out and outside-in. *Mol Cancer Ther* 6: 789-801, 2007.
271. **van Gent DC, Hoeijmakers JH, and Kanaar R**. Chromosomal stability and the DNA double-stranded break connection. *Nat Rev Genet* 2: 196-206, 2001.
272. **van Meerwijk JP, Bianchi T, Marguerat S, and MacDonald HR**. Thymic lineage commitment rather than selection causes genetic variations in size of CD4 and CD8 compartments. *J Immunol* 160: 3649-3654, 1998.
273. **Varley JM, Chapman P, McGown G, Thorncroft M, White GR, Greaves MJ, Scott D, Spreadborough A, Tricker KJ, Birch JM, Evans DG, Reddel R, Camplejohn RS, Burn J, and Boyle JM**. Genetic and functional studies of a germline TP53 splicing mutation in a Li-Fraumeni-like family. *Oncogene* 16: 3291-3298, 1998.
274. **Varon R, Vissinga C, Platzer M, Cerosaletti KM, Chrzanowska KH, Saar K, Beckmann G, Seemanova E, Cooper PR, Nowak NJ, Stumm M, Weemaes CM, Gatti RA, Wilson RK, Digweed M, Rosenthal A, Sperling K, Concannon P, and Reis A**. Nibrin, a novel DNA double-strand break repair protein, is mutated in Nijmegen breakage syndrome. *Cell* 93: 467-476, 1998.
275. **Vercauteren SM, and Sutherland HJ**. Constitutively active Notch4 promotes early human hematopoietic progenitor cell maintenance while inhibiting differentiation and causes lymphoid abnormalities in vivo. *Blood* 104: 2315-2322, 2004.
276. **Verma M, Maruvada P, and Srivastava S**. Epigenetics and cancer. *Crit Rev Clin Lab Sci* 41: 585-607, 2004.
277. **Voy BH, Scharff JA, Perkins AD, Saxton AM, Borate B, Chesler EJ, Branstetter LK, and Langston MA**. Extracting gene networks for low-dose radiation using graph theoretical algorithms. *PLoS Comput Biol* 2: e89, 2006.

278. **Vrijheid M, Cardis E, Blettner M, Gilbert E, Hakama M, Hill C, Howe G, Kaldor J, Muirhead CR, Schubauer-Berigan M, Yoshimura T, Ahn YO, Ashmore P, Auvinen A, Bae JM, Engels H, Gulis G, Habib RR, Hosoda Y, Kurtinaitis J, Malker H, Moser M, Rodriguez-Artalejo F, Rogel A, Tardy H, Telle-Lamberton M, Turai I, Usel M, and Veress K**. The 15-Country Collaborative Study of Cancer Risk Among Radiation Workers in the Nuclear Industry: design, epidemiological methods and descriptive results. *Radiat Res* 167: 361-379, 2007.
279. **Wallace M, Coates PJ, Wright EG, and Ball KL**. Differential post-translational modification of the tumour suppressor proteins Rb and p53 modulate the rates of radiation-induced apoptosis in vivo. *Oncogene* 20: 3597-3608, 2001.
280. **Wang SE, Wu FY, Shin I, Qu S, and Arteaga CL**. Transforming growth factor {beta} (TGF-{beta})-Smad target gene protein tyrosine phosphatase receptor type kappa is required for TGF-{beta} function. *Mol Cell Biol* 25: 4703-4715, 2005.
281. **Watson GE, Lorimore SA, Clutton SM, Kadhim MA, and Wright EG**. Genetic factors influencing alpha-particle-induced chromosomal instability. *International journal of radiation biology* 71: 497-503, 1997.
282. **Weil MM, Xia C, Xia X, Gu X, Amos CI, and Mason KA**. A chromosome 15 quantitative trait locus controls levels of radiation-induced jejunal crypt cell apoptosis in mice. *Genomics* 72: 73-77, 2001.
283. **Weisberg SP, Hunter D, Huber R, Lemieux J, Slaymaker S, Vaddi K, Charo I, Leibel RL, and Ferrante AW, Jr.** CCR2 modulates inflammatory and metabolic effects of high-fat feeding. *J Clin Invest* 116: 115-124, 2006.
284. **Westermann W, Schobl R, Rieber EP, and Frank KH**. Th2 cells as effectors in postirradiation pulmonary damage preceding fibrosis in the rat. *International journal of radiation biology* 75: 629-638, 1999.
285. **Wilson PF, Nham PB, Urbin SS, Hinz JM, Jones IM, and Thompson LH**. Inter-individual variation in DNA double-strand break repair in human fibroblasts before and after exposure to low doses of ionizing radiation. *Mutat Res* 683: 91-97, 2010.
286. **Wing S, Shy CM, Wood JL, Wolf S, Cragle DL, and Frome EL**. Mortality among workers at Oak Ridge National Laboratory. Evidence of radiation effects in follow-up through 1984. *JAMA* 265: 1397-1402, 1991.
287. **Wolfe CJ, Kohane IS, and Butte AJ**. Systematic survey reveals general applicability of "guilt-by-association" within gene coexpression networks. *BMC Bioinformatics* 6: 227, 2005.
288. **Wright EG**. Radiation-induced genomic instability in haemopoietic cells. *International journal of radiation biology* 74: 681-687, 1998.
289. **Wu M, Xu LG, Su T, Tian Y, Zhai Z, and Shu HB**. AMID is a p53-inducible gene downregulated in tumors. *Oncogene* 23: 6815-6819, 2004.
290. **Xu Y, Shao Y, Voorhees JJ, and Fisher GJ**. Oxidative inhibition of receptor-type protein-tyrosine phosphatase kappa by ultraviolet irradiation activates epidermal growth factor receptor in human keratinocytes. *J Biol Chem* 281: 27389-27397, 2006.
291. **Yamada H, Nakashima Y, Okazaki K, Mawatari T, Fukushi JI, Kaibara N, Hori A, Iwamoto Y, and Yoshikai Y**. Th1 but not Th17 cells predominate in the joints of patients with rheumatoid arthritis. *Ann Rheum Dis* 67: 1299-1304, 2008.
292. **Yamaoka K, Kojima S, Takahashi M, Nomura T, and Iriyama K**. Change of glutathione peroxidase synthesis along with that of superoxide dismutase synthesis in mice spleens after low-dose X-ray irradiation. *Biochim Biophys Acta* 1381: 265-270, 1998.
293. **Yang H, Ding Y, Hutchins LN, Szatkiewicz J, Bell TA, Paigen BJ, Graber JH, de Villena FP, and Churchill GA**. A customized and versatile high-density genotyping array for the mouse. *Nat Methods* 6: 663-666, 2009.

294. **Yang Y, Gil MC, Choi EY, Park SH, Pyun KH, and Ha H**. Molecular cloning and chromosomal localization of a human gene homologous to the murine R-PTP-kappa, a receptor-type protein tyrosine phosphatase. *Gene* 186: 77-82, 1997.
295. **Yasukawa K, Oshiumi H, Takeda M, Ishihara N, Yanagi Y, Seya T, Kawabata S, and Koshiba T**. Mitofusin 2 inhibits mitochondrial antiviral signaling. *Sci Signal* 2: ra47, 2009.
296. **Ye Q, Shieh JH, Morrone G, and Moore MA**. Expression of constitutively active Notch4 (Int-3) modulates myeloid proliferation and differentiation and promotes expansion of hematopoietic progenitors. *Leukemia* 18: 777-787, 2004.
297. **Yonezawa M, Takeda A, and Misonoh J**. Acquired radioresistance after low dose X-irradiation in mice. *J Radiat Res (Tokyo)* 31: 256-262, 1990.
298. **Yu Y, Okayasu R, Weil MM, Silver A, McCarthy M, Zabriskie R, Long S, Cox R, and Ullrich RL**. Elevated breast cancer risk in irradiated BALB/c mice associates with unique functional polymorphism of the Prkdc (DNA-dependent protein kinase catalytic subunit) gene. *Cancer Res* 61: 1820-1824, 2001.
299. **Zeng G, Day TK, Hooker AM, Blyth BJ, Bhat M, Tilley WD, and Sykes PJ**. Non-linear chromosomal inversion response in prostate after low dose X-radiation exposure. *Mutat Res* 602: 65-73, 2006.
300. **Zhang Y, Chesler EJ, and Langston MA**. On Finding Bicliques in Bipartite Graphs: a Novel Algorithm with Application to the Integration of Diverse Biological Data Types. In: *Proceedings, Hawai'i International Conference on System Sciences*. Big Island, HI: 2008.
301. **Zhang Y, Siebert R, Matthiesen P, Yang Y, Ha H, and Schlegelberger B**. Cytogenetical assignment and physical mapping of the human R-PTP-kappa gene (PTPRK) to the putative tumor suppressor gene region 6q22.2-q22.3. *Genomics* 51: 309-311, 1998.
302. **Zhang ZL, Constantinou D, Mandel TE, and Georgiou HM**. Lymphocyte subsets in thymus and peripheral lymphoid tissues of aging and diabetic NOD mice. *Autoimmunity* 17: 41-48, 1994.
303. **Zhou H, Randers-Pehrson G, Geard CR, Brenner DJ, Hall EJ, and Hei TK**. Interaction between radiation-induced adaptive response and bystander mutagenesis in mammalian cells. *Radiat Res* 160: 512-516, 2003.
304. **Zielinski JM, Garner MJ, Band PR, Krewski D, Shilnikova NS, Jiang H, Ashmore PJ, Sont WN, Fair ME, Letourneau EG, and Semenciw R**. Health outcomes of low-dose ionizing radiation exposure among medical workers: a cohort study of the Canadian national dose registry of radiation workers. *Int J Occup Med Environ Health* 22: 149-156, 2009.

APPENDIX

ASSESSING THE PULMONARY TOXICITY OF SINGLE-WALLED CARBON NANOHORNS

This data was published in the journal *Nanotoxicology* in 2007. This research does not directly relate to low dose radiation biology, therefore it is presented in its entirety here instead of in the body of the dissertation. This study is the first study published, to our knowledge, assessing the potential toxicology of single-walled carbon nanohorns, and one of the first in vivo toxicology studies of carbon nanoparticles.

This data is adapted from the following publication:

Lynch R, Voy B, Glass D, Mahurin S, Zhao B, Hu H, Saxton A, Donnell R, Cheng M. *Nanotoxicology*. 1: 157-166, 2007.

Abstract

Previous studies have suggested that single-walled carbon nanotubes (SWCNTs) may pose a pulmonary hazard. We investigated the pulmonary toxicity of single-walled carbon nanohorns (SWCNHs), a relatively new carbon-based nanomaterial that is structurally similar to SWCNTs. Mice were exposed to 30 µg of surfactant-suspended SWCNHs or an equal volume of vehicle control by pharyngeal aspiration and sacrificed 24 hours or 7 days post-exposure. Total and differential cell counts and cytokine analysis of bronchoalveolar lavage fluid demonstrated a mild inflammatory response which was mitigated by day 7 post-exposure. Whole lung microarray analysis demonstrated that SWCNH-exposure did not lead to robust changes in gene expression. Finally, histological analysis showed no evidence of granuloma formation or fibrosis following SWCNH aspiration. These combined results suggest that

SWCNH is a relatively innocuous nanomaterial when delivered to mice in vivo using aspiration as a delivery mechanism.

Introduction

Burgeoning use of engineered nanoparticles and nanomaterials in commercial applications has raised concern about the potential health effects of both intentional and accidental exposures. Although exposure can occur by a variety of mechanisms, the inhalation route is of primary interest because of the ease with which particles of nanoscale dimensions become aerosolized (5). The lung is particularly susceptible to respirable toxicants because it has a large surface area which is in constant contact with the external environment (11). Unlike larger particles which are mainly deposited in the nasopharyngeal compartment, nano-sized particles can be deposited in the alveolar region of the lung with high efficiency (1). Once resident in the alveoli, nanoparticles may promote oxidative stress and trigger inflammation through proinflammatory cytokines released from epithelial cells and macrophages (12). If unchecked, persistent pulmonary inflammation may trigger fibrotic changes and loss of pulmonary function (23).

While nanoparticles have been developed from an array of materials, carbon-based particles are at the center of the nanotechnology revolution (15). Most in vivo toxicity data for engineered carbon-based nanoparticles are from studies using single-walled carbon nanotubes (SWCNTs). Carbon nanotubes have unique physico-chemical, electrical, thermal, and mechanical properties which make them attractive for a variety of applications (3). Animal studies conducted with SWCNTs suggest that exposure to aggregates of SWCNTs induces pulmonary toxicity (16, 17, 21, 24). In each of these studies, rodents were exposed to a large bolus of nanotubes to mimic chronic inhalation exposure.

Although all of the studies reported that SWCNT-exposure induced the formation of granulomas and/or fibrosis, they disagreed on the presence or degree of pulmonary inflammation. These differences in these studies could be due to the preparation of the nanotubes (e.g., degree of purity or method of dispersion), the animal studied (e.g., mice or rats), the exposure method (e.g., intratracheal instillation or aspiration), dose, or even the agglomeration state of the SWCNTs. It is important to note that the results from previous SWCNT toxicity studies do not immediately imply the toxicity of other carbon-based nanoparticles. Indeed, it has been demonstrated that carbon-based nanoparticles exhibited differential cytotoxic effects to alveolar macrophages depending on the geometric arrangement of the carbon atoms (14). Surprisingly, SWCNTs were more cytotoxic than multi-walled carbon nanotubes (MWCNTs) and fullerene (C_{60}). In addition, SWCNTs and MWCNTs were more cytotoxic than quartz (SiO_2), a well-documented pulmonary hazard. Therefore, the potential toxicity of a nanomaterial cannot be inferred from its elemental composition alone.

Here we investigated the pulmonary toxicity of single-walled carbon nanohorns (SWCNHs), a relatively new engineered carbon-based nanomaterial. Carbon nanohorns are of particular interest to hydrogen storage in energy (10) and fuel cell applications. In addition, SWCNH aggregates were studied as a carrier for the chemotherapy drug cisplatin (2).

Individual carbon nanohorns are engineered as short (in length) horn-shaped tube structures, the tips of which are capped with five-membered carbon rings. Individual SWCNHs tend to self-aggregate into a larger structure approximately 80-100nm in diameter during formation, with the tips of individual nanohorns projecting outward from the center in all directions. Although individual SWCNH structure is similar to individual carbon nanotubes, the former may find interesting and large-scale applications earlier than SWCNTs. For example, SWCNHs can be produced through laser ablation of a pure carbon target without the use of transition metal catalysts. This is of particular relevance for toxicity studies because metal

contaminants themselves could provoke inflammatory responses and oxidative stress. Although SWCNTs can be acid-washed to remove the majority of the catalysts, the residual metals can still contribute to the inflammatory response (17) making it difficult to assess the toxicity of SWCNTs. In a recent in vitro cell line based study, amino-modified SWCNH aggregates were shown be taken up by mammalian cells but caused little cytotoxicity (13). At the time of this writing, however, we are not aware of any published studies documenting the in vivo toxicity of SWCNHs.

Our primary objective in this study was to characterize the pulmonary response of SWCNHs and compare the results to published SWCNT data. Keep in mind SWCNTs can be completely different from SWCNHs in eliciting biological responses and the comparison was made with care. We were not intending to establish a dose-response relationship of SWCNHs nor were we interested in dose rate of this new nanomaterial in this research. Thus, a single dose was chosen for this exploratory toxicity study. Each mouse in this study was exposed to 30 µg of surfactant-suspended SWCNHs or to an equal volume of vehicle control by pharyngeal aspiration. To assess the pulmonary inflammatory response, the accumulation of cytokines and chemokines, total cell counts, and differential cell counts in bronchoalveolar lavage (BAL) fluid were measured. Oxidative stress was estimated by the reduction of glutathione (GSH) in lung tissue. Gene expression profiling by microarray analysis was used as an unbiased estimator of overall changes within the whole lung in response to SWCNH exposure. The ability of SWCNHs to induce granuloma formation and/or fibrosis was evaluated by histological examination of lung tissue following the exposure.

Methods

SWCNH preparation and exposure

Single-walled carbon nanohorns (SWCNHs) were synthesized using laser ablation of a pure carbon source as previously described (8). The detailed characterization of SWCNHs and their formation could also be found in Cheng et al. (2007). In order to expose the mice to a homogenous suspension of nanoparticles, SWCNHs were solubilized in phosphate buffered saline (PBS) using the nonionic surfactant Pluronic F-127 (Molecular Probes), which is biocompatible. A 1 mg mL^{-1} solution of SWCNHs suspended in PBS with 1% Pluronic was used for nanoparticle aspiration; 1% Pluronic in PBS was used for vehicle exposure. The SWCNH suspension was sonicated for 5 minutes just prior to aspiration.

Male C57BL6/J mice were obtained from The Jackson Laboratory (Bar Harbor, ME). The mice were housed in a specific pathogen-free vivarium maintained at Oak Ridge National Laboratory (ORNL) and were acclimated to this facility for at least two weeks before use. All experiments were performed under an approved ORNL Animal Care and Use Committee protocol. Mice were exposed to 30 µg of SWCNHs or an equal volume of vehicle control (surfactant/PBS only) via pharyngeal aspiration. Aspriation is a minimally invasive technique that effectively delivers particles to the alveolar region of the lung with even distribution (20) and has been used in previous nanotoxicology studies to assess the pulmonary response to SWCNTs (17, 21). The mouse was anesthetized using isoflurane in a bell jar and once it reached the appropriate anesthetic plane, it was suspended by its front incisors on a thin wire attached to an inclined board. The tongue was extended with blunt forceps and the fluid was placed on the back of the tongue and aspirated into the lungs upon inspiration. When there was no more fluid within the mouth cavity, the tongue was released.

Bronchoalveolar Lavage

Mice were sacrificed 24 hours or 7 days after aspiration by an overdose of isoflurane followed by exsanguination. Bronchoalveolar lavage (BAL) was performed as previously described (21) with minor modifications. A blunt 22-gauge needle was inserted into the trachea and secured with suture material. BAL was performed three times with cold, sterile Ca^{+2} and Mg^{+2} – free PBS. For the first lavage, 0.6 mL of PBS was used, and the recovered fluid was kept separate from subsequent lavages for cytokine analysis. Two additional lavages were performed with1.0 mL of PBS each and pooled together. After centrifugation at 4°C, the BAL cellular pellet was resuspended in cold PBS for total and differential cell counts. A hemocytometer was used to determine the total number of cells in the BAL fluid. Differential cell counts were performed on cytospin slides stained with a Hema-3 kit (Fisher Scientific). A minimum of 200 cells per slide were counted. The supernatant from the first lavage was stored at -80°C until analyzed. Cytokine and chemokine analysis of BAL samples was performed by Linco Diagnostics. The full panel of mouse cytokines and chemokines, a total of 22 analytes, were measured.

Oxidative Stress

As a biomarker of oxidative stress, lung glutathione (GSH) levels were quantified on samples obtained from mice 24 hours after aspiration using a Glutathione Assay Kit (Cayman Chemical). Post-lavaged lungs were homogenized, deproteinated, stored at -20°C, and assayed according to the manufacturer's instructions. This assay utilizes an enzymatic recycling method for the quantification of total glutathione or oxidized glutathione (GSSG) levels. The production of the product was monitored using the absorbance at 405 nm. The total glutathione and GSSG levels were determined in separate assays. Each sample was performed in duplicate. The

concentrations of GSSG and total GSH were calculated based on appropriate standard curves of known concentrations.

Histology

For histological analysis, vehicle and SWCNH-exposed mice were sacrificed 7 days after exposure by isoflurane overdose in a bell jar followed by exsanguination, and lung fixation was performed using standard protocols. The trachea was cannulated as described above, and the lungs were fixed with 10% neutral buffered formalin suspended 20 cm above the work surface to allow the lungs to fill through the cannulated trachea. The flow of formalin was stopped when the lungs were fully inflated with fixative. The trachea was sealed off with sutures, and the trachea, lungs, and heart were removed and submerged in additional formalin. After 24 hours, the tissues were switched to 70% ethanol for gross trimming and sectioning. Thin sections were stained with haematoxylin and eosin.

Gene Expression Profiling

For analysis of lung RNA expression, 3 vehicle and 3 SWCNH-exposed mice were euthanized by cervical dislocation 24 hours after aspiration. The lungs were immediately extracted and submerged in RNAlater (Ambion) and stored at 4°C until processed. Total RNA was isolated from homogenized lungs using an RNeasy kit (QIAGEN) according to the manufacturer's protocols. RNA samples were shipped to the Microarray Core Facility at Washington University for analysis. RNA quality and concentration was analyzed using the Agilent Bioanalyzer. Gene expression profiling was performed using the Mouse-6 Expression BeadChip (Illumina). Differentially expressed genes were identified using mixed model analysis of variance (ANOVA) implemented in Statistical Analysis Software (SAS Institute, Inc.) (25), and controlling the false discovery rate at 5% using QVALUE software (22) implemented in the statistical language R (bioconductor.org).

Electron microscopy

A high resolution transmission electron microscope (HR-TEM; Hitachi HF-2000) was used to confirm the morphology and size of the SWCNHs as previously described by Cheng et al. (2007). Scanning electron microscopy (SEM) analysis was performed to assess the morphology of BAL macrophages after SWCNH exposure. SEM analysis was performed on BAL cells harvested from SWCNH and vehicle-exposed mice 24 hours after aspiration. Lavage cells were isolated using the BAL procedure described above, except all lavages from each animal were pooled together and a total of 4.6 mL of PBS was used in order to maximize the total cell yield. The BAL cells were centrifuged at 4°C and resuspended in warmed Dulbecco's Modified Eagle's Medium supplemented with 10% fetal bovine serum (Invitrogen™). Cells were seeded on 12 mm glass coverslips in 12-well tissue culture plates and incubated at 37°C and 5% CO_2 for one hour to adhere. The media and non-adherent cells were aspirated off, and the cells were fixed in 3% gluteraldehyde (Sigma ®) in 0.1M phosphate buffer (pH 7.4) for 1 hour at room temperature. Samples were rinsed in phosphate buffer 3 times for 10 minutes each and then post-fixed in 2% osmium tetraoxide in 0.1M phosphate buffer for 1 hour at room temperature. The samples were dehydrated in a graded ethanol series and critical-point dried with CO_2. Samples were sputter-coated with a thin layer of gold for imaging.

Results

As shown in Fig. A-1A, individual SWCNH aggregate structures were approximately 80-100nm in diameter with horn-like projections, consistent with that reported earlier (8). To facilitate a homogenous particle suspension for exposures, SWCNHs were suspended in PBS with 1% Pluronic and sonicated prior to aspiration.

SWCNH-exposed mice exhibited no overt clinical symptoms of distress from the time of anesthesia recovery until the time of sacrifice 24 hours or 7 days post-exposure. Lungs of

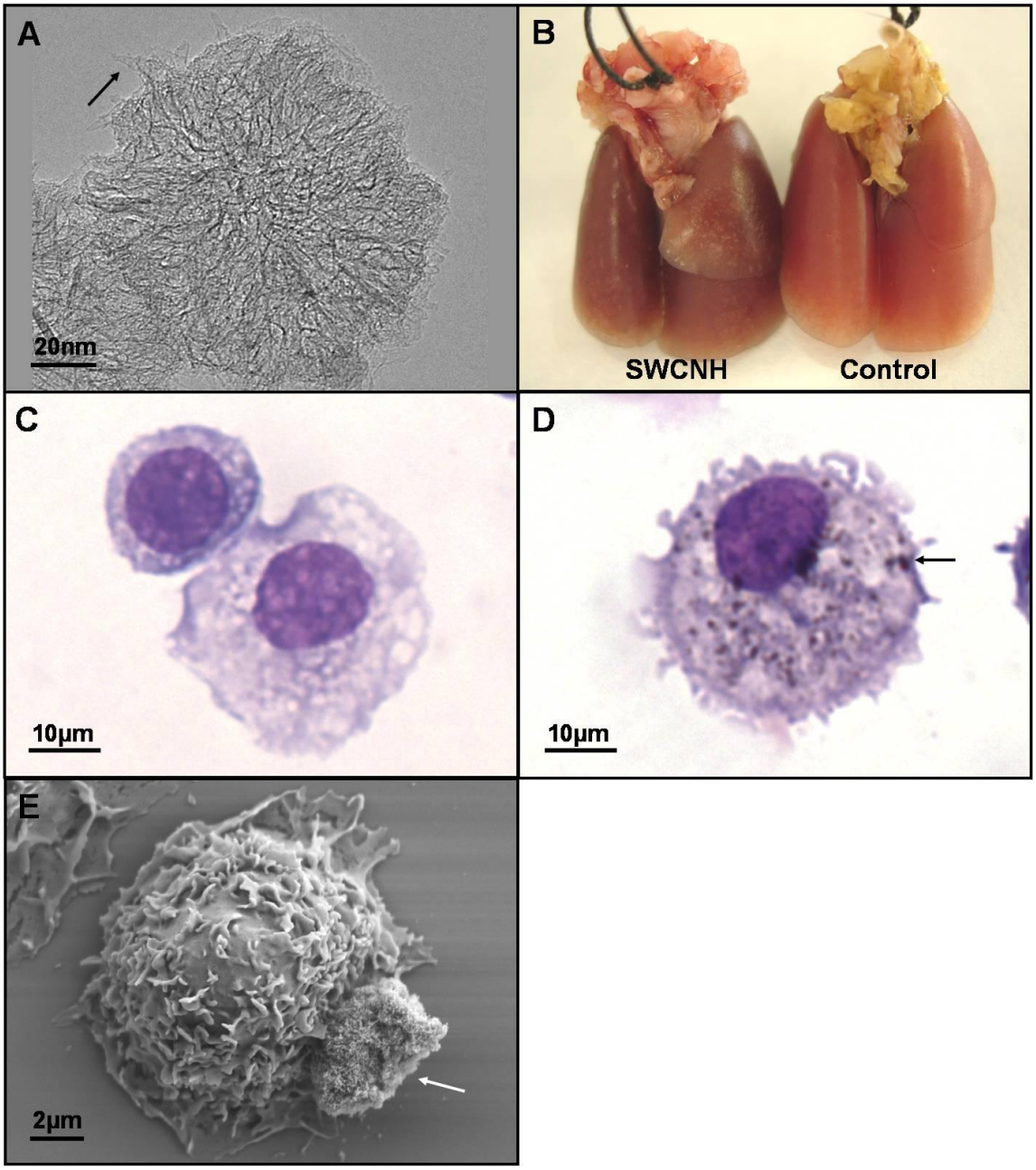

Figure A-1. Single-walled carbon nanohorn (SWCNH) exposures. (A) TEM image of an aggregate of SWCNHs containing individual cone-shaped SWCNHs in a spherical orientation. The arrow indicates a single SWCNH projecting from the aggregate. Image reproduced with permission of Nanotechnology (IOP Publishing Limited, Cheng et al. 2007). (B) Dorsal view of formalin-filled lungs from SWCNH (left) and sham-exposed (right) mice 7d after aspiration. Cytospin preparations of BAL cells from sham (C) and SWCNH-exposed (D) mice 24h after aspiration. The arrow points to one of the multiple aggregates of SWCNHs. (E) SEM image of a BAL cell from a SWCNH-exposed mouse 24h after exposure. Note the large aggregate of SWNCH adjacent to the cell indicated by the arrow.

SWCNH-exposed mice were slightly darker in color than were those from vehicle-exposed controls 7 days post-exposure (Fig. A-1B), indicating that the nanoparticles were well distributed through the lung and that complete clearance of SWCNHs had not occurred. BAL fluid was examined for increases in total cell count as a general assessment of neutrophil and macrophage recruitment in an inflammatory response to SWCNHs. Total number of cells in BAL fluid did not differ between SWCNH and vehicle-exposed mice 24 hours or 7 days post-exposure. Consistent with these results, neutrophils were rarely observed in BAL fluid from SWCNH-exposed mice, and macrophage numbers did not significantly differ between the two exposure groups. Visible differences in macrophages were, however, observed. Carbonaceous material was clearly visible as dark aggregates within the cytoplasm of alveolar macrophages in SWCNH-exposed mice (Fig. A-1D) but was not present in samples obtained from vehicle-exposed mice (Fig. A-1C). Although the SWCNHs were coated with surfactant and delivered as a suspension of particles in the 100 nm size range, their visibility with light microscopy in macrophage cytoplasm suggests the presence of larger aggregates within the cell. Whether formation of larger aggregates occurred before or after phagocytosis by macrophages cannot be determined from these samples. As shown in Fig. A-1E, large aggregates of SWCNHs near or on the surface of lavage cells were detected in samples obtained from mice 24 hours post-exposure.

To investigate the pulmonary cellular response to SWCNH exposure, the concentration of 22 cytokines and chemokines in the acellular BAL fluid was measured to assess early (24 hours post-exposure) and sustained (7 days) inflammatory responses. Seventeen of the 22 analytes were not significantly different between control and nanoparticle-exposed mice at either time point: IFN-γ, IL-10, IL-12, IL-13, IL-15, IL-17, IL-1α, IL-1β, IL-2, IL-4, IL-6, IL-7, IL-9, MCP-1, MIP-1α, RANTES, and TNF-α. Five analytes were statistically different between exposure groups ($\alpha = .05$) (see Fig. A-2). Granulocyte macrophage colony-stimulating factor

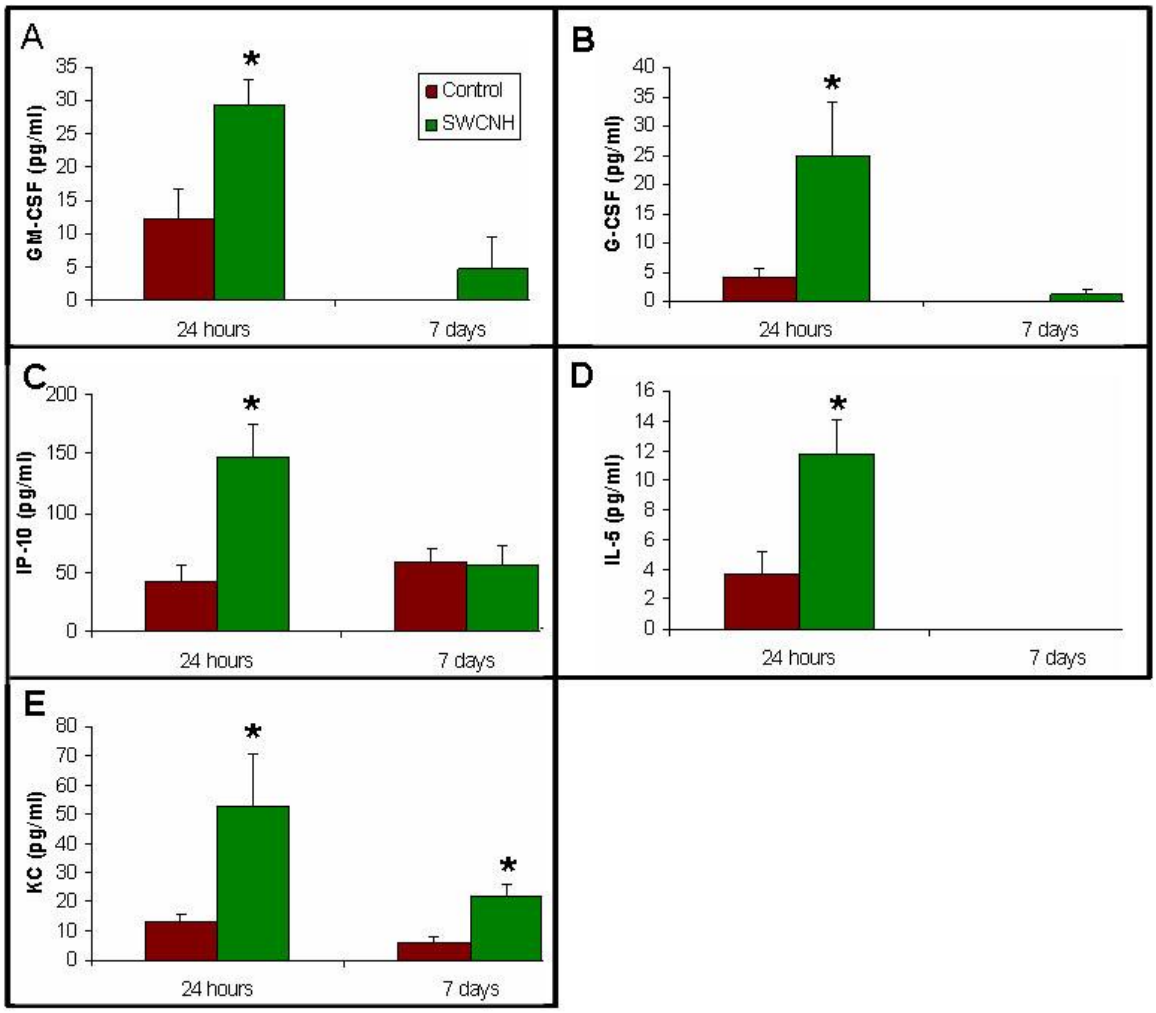

Figure A-2. Cytokine accumulation in BAL fluid 24h and 7d after aspiration of SWNCH solution or vehicle. (A) GM-CSF, (B) G-CSF, (C) IP-10, (D) IL-5, (E) KC. Results are the mean ± SE of duplicate measurement (n = 4 mice / group). Compared with sham-exposed mice, * P<.05.

(GM-CSF), granulocyte colony-stimulating factor (G-CSF), interferon-inducible protein-10 (IP-10), and interleukin-5 (IL-5) were significantly elevated in BAL fluid from SWCNH-exposed mice compared to the vehicle-exposed mice 24 hours after aspiration (Fig. A-2A-D). These differences did not persist at 7 days, at which time there were no significant differences in GM-CSF, G-CSF, IL-5 and IP-10 concentrations between SWCNH and vehicle-exposed mice. Only one cytokine, the neutrophil chemoattractant KC, was significantly higher in SWCNH-exposed mice at both 24 hours and 7 days after aspiration (Fig. A-2E). These results suggest an early but mild inflammatory response which is primarily resolved by 7 days post-exposure. The responses might be different (e.g., enhanced), if the mice were predisposed with allergic genes.

In addition to inducing inflammation, various nanoparticles can trigger oxidative stress after uptake into cells (6, 19). The ratio of oxidized to total glutathione (GSSG:GSH) in lung homogenates was used to assess the overall pulmonary anti-oxidative balance after SWCNH exposure. The GSSG:GSH ratio was not different between the two experimental groups (vehicle-exposed ratio = 0.298 $\pm$ 0.043; SWCNH-exposed ratio = 0.292 $\pm$ 0.034), indicating that the presence of SWCNH particles within pulmonary macrophages did not promote a generalized oxidative stress within the lung.

While BAL fluid data presented in Fig. A-2 indicate a mild but significant acute increase in inflammation, the response of the lung itself determines the long-term effect on pulmonary function. Global gene expression profiling was used to detect potential SWCNH-induced changes in the lung in an unbiased and comprehensive manner, and to identify molecular events that could signal activation of response pathways not captured by cytokine/chemokine assays or by assay of oxidative stress.

Total RNA extracted from both lungs of the vehicle and SWCNH-exposed mice was used to profile relative expression levels of approximately 46,000 mRNAs (n = 3 / group). While some transcripts showed a treatment-related trend for altered expression levels, no statistically

significant differences in expression were identified when using statistical procedures to control for multiple testing. These results are consistent with the mild inflammatory changes in BAL fluid and with the lack of indication of oxidative stress in lung.

Histological analysis was used to determine if SWCNHs resulted in pulmonary structural changes that could be suggestive of inflammation or early fibrosis development, as has been reported for SWCNT exposure in rodents (16, 21, 24). Lung sections from four SWCNH and four vehicle-exposed mice were analyzed by microscopic examination. There were no signs of granulomas or early fibrosis in either group. No other indicators of inflammation (increased neutrophils, lymphocytes, plasma cells, vascular dilation, or fibrin accumulation) were observed. The only discernible difference between the two groups was the presence of carbonaceous material within the cytoplasm of intra-alveolar and septal macrophages in the SWCNH-exposed lungs (Fig. 3), consistent with the presence of carbon in BAL macrophages (Fig. 1D).

Discussion

As research and development of engineered carbon-based nanomaterials races forward, it is expected that the risk of intentional and unintentional pulmonary exposure will increase. Recent animal studies have shown that carbon nanotubes, a cousin of carbon nanohorns, can cause pulmonary inflammation and/or lung tissue damage with granuloma formation and fibrosis (16, 17, 21, 24). Because engineered carbon nanoparticles of different geometries have shown differential toxicity in vitro (14), we investigated whether exposure to SWCNHs could lead to similar lung inflammation as SWCNTs did in rodents. Mice were exposed to SWCNHs in suspension using pharyngeal aspiration. Using the same technique, Shvedova et al. (2005) exposed mice to 0, 10, 20, or 40 µg of SWCNTs. This range was chosen to be comparable to occupationally relevant exposures. They had determined that a 20 µg dose of SWCNTs per mouse was equivalent to 20 8-hour workdays of exposure to graphite particles at the USA

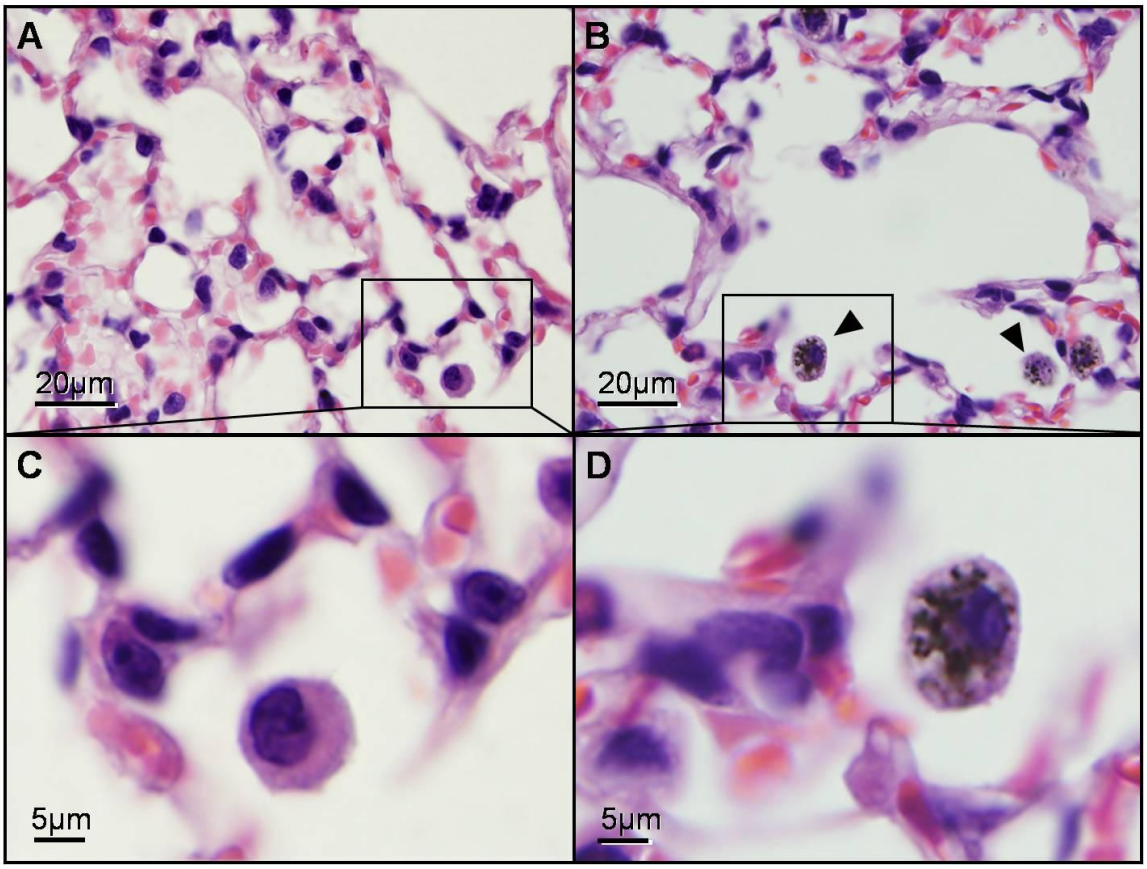

Figure A-3 SWCNH in lungs of exposed mice. Thin lung sections from a sham (A) and SWCNH-exposed (B) mice 7d after aspiration. Carbonaceous material is visible within alveolar macrophages (arrow heads in B). (C) and (D) higher resolution images of images A and B, respectively. Carbonaceous material is clearly visible within the alveolar macrophages of SWCNH-exposed mice (D).

Occupational Safety and Health Administration (OSHA) permissible exposure limit. In our study, mice were exposed to a comparable amount (30 μg) of SWCNHs.

We found evidence of mild but significant acute pulmonary inflammation in response to SWCNH exposure, indicated by increased levels of GM-CSF, G-CSF, IP-10, IL-5 and KC in BAL fluid 24 hours post-exposure. Levels of all but one chemokine (KC) were no longer statistically different from vehicle-exposed controls at 7 days post-exposure, suggesting a transient response. Both KC and IP-10 act as neutrophil chemoattractants by recruiting neutrophils to sites of inflammation and tissue damage. However, despite these increases, no evidence was found of neutrophil recruitment into the lung following exposure. This could be due to the relatively modest induction of KC and IP-10 levels. Of the cytokines that were increased at 24 hours post-exposure, only GM-CSF has been implicated in the formation of fibrosis (26). Other cytokines known to pro-fibrotic, such as interleukin-1β (IL-1β), tumor necrosis factor-α (TNF-α), and transforming growth factor-β1 (TGF-β1) were not significantly elevated in SWCNH-exposed mice over vehicle-exposed controls (data not shown). These results are consistent with lack of pre-fibrotic lesions in the lung 7 days after SWCNH exposure. No evidence for granuloma formation was observed, which is consistent with the mild and transient inflammatory response measured by cytokines and differential cell counts. In addition, there was no evidence of alveolar wall thickening or hypertrophied epithelial cells. The only apparent difference between SWCNH and vehicle-exposed controls was the presence of carbonaceous material within the cytoplasm of alveolar macrophages. Although it is possible that fibrosis could develop at a later point after exposure, the previous studies with SWCNTs reported obvious granuloma formation within 7 days post-exposure (16, 21, 24).

Collectively, the BAL cytokine profiles and histological analysis of lung after SWCNH aspiration differ significantly from what has been reported for in vivo exposure to SWCNTs. Both Warheit et al. (2004) and Lam et al. (2004) described the presence of granulomas and

inflammation following intratracheal delivery of SWCNTs to rodents. In a more comprehensive study, Shvedova et al. (2005) performed a dose-response and time course study of SWCNT toxicity in mice, using particles that had been purified to remove the majority of contaminating iron particles. Granulomas were only found in association with dense SWCNT aggregates, but alveolar wall thickening was described at sites distal to aggregates, leading to the conclusion that even dispersed SWCNTs promoted fibrosis. In parallel, levels of TNF-α and IL-1β were markedly increased (up to 16-fold over vehicle-exposed levels) 24 hours post-exposure in BAL fluid, as were neutrophil and macrophage recruitment, followed by increased levels of the pro-fibrotic cytokine TGF-β1 7 days post-exposure. The amounts of nanoparticles (i.e., SWCNTs) used in that study were comparable to those used herein, indicating that the differences in outcomes were not due to large differences in particle load. We also did not find evidence for increased oxidative stress based on the general marker of glutathione levels. A variety of nanoparticles have been shown to create reactive oxygen species in vitro and in vivo (4, 7). Specifically, SWCNTs have been shown to deplete the antioxidant glutathione (GSH) store in the lung with the most severe decrease occurring about 24 hours post-exposure (21). In contrast, we found no effects of SWCNH exposure on either total or oxidized GSH levels 24 hours post-exposure.

The basis for what appear to be marked differences in the potential pulmonary toxicity of SWCNTs and SWCNHs after in vivo exposure remains to be determined. As a relatively new nanomaterial, little is known about the interaction of SWCNHs with cells and with intracellular biochemistry. To our knowledge, only a single study has explored the response to SWCNHs, and it used an in vitro system (13). The authors found minimal cytoxicity associated with amino-modified SWCNHs. There are several possible explanations for the difference in pulmonary toxicity of SWCNHs compared to previous studies with SWCNTs. First, although nanotubes and nanohorns are structurally similar, their inherent physiochemical differences could affect their

biological impact. These apparent toxicity differences within the general class of engineered carbon-based nanoparticles are not unprecedented. For example, SWCNTs show significantly increased cytotoxicity compared to similar amounts of multi-walled carbon nanotubes, quartz, and fullerene (14).

Another contributing factor could be that the agglomeration state of the engineered nanoparticles affects their toxicity (18). The agglomeration in our studies was minimized by using a non-ionic surfactant (Pluronic) and vigorously sonicating the material prior to aspiration. It is possible that coating the particles with surfactant not only facilitates material dispersion, but also affects their bioavailability and cellular uptake. Prior in vivo studies have relied on aggressive mechanical dispersion methods to maintain particle suspensions prior to delivery, which we combined with surfactant coating.

A recent in vitro study reported that SWCNTs solubilized in Pluronic were readily phagocytosed by macrophages in a time- and temperature-dependent manner, but that uptake did not lead to cellular toxicity (9). On this note, we were able to easily identify particle aggregates within the cytoplasm of macrophages from BAL samples of mice exposed to Pluronic-suspended SWCNHs. In contrast, Shvedova et al. (2005) noted that RAW 264.7 macrophages did not actively engulf SWCNTs in vitro. Further studies may be necessary to determine exact immunological pathways and the extent to which macrophage clearance of engineered carbon-based nanoparticles contributes to the net effect on pulmonary inflammation and pathological changes.

Another important distinction between SWCNTs and SWCNHs is the lack (in SWCNHs) of metal contaminants. SWCNT production typically relies on metal catalysts that remain in final particle preparations, and trace amounts persist even after purification steps. In contrast, the SWCNHs used in this study were produced using laser ablation of pure carbon containing no metals. This difference in SWCNTs and SWCNHs could be an important factor in their relative

utility for in vivo applications, if future studies do reveal that trace metals promote secondary, detrimental responses to particles in vivo.

Although we found that SWCNH-exposure resulted in an increase in the levels of several cytokines and chemokines in BAL fluid within 24 hours of exposure, we did not find parallel changes in gene expression in lung. In fact, we did not identify any genes with changes in expression between SWCNH and vehicle-exposed mice that were robust to statistical methods that controlled for multiple testing. In part this may be due to the low statistical power from a relatively small sample size (n=3) that is typical of microarray experiments due to their cost. In addition, we noted significant inter-individual variation in the expression of numerous genes, which would further reduce overall statistical power. The goal of the array hybridizations was to identify genes and pathways that were activated or repressed in the lung as part of the mitigation of SWCNH exposure.

In light of the relatively modest increase in inflammatory cytokines, the lack of histopathological lesions, and the fact that gene expression was profiled in the whole lung (rather than in BAL fluid), it is perhaps not surprising that we did not observe marked alteration in gene expression. To our knowledge, this is the first attempt to profile the global transcriptomic response to engineered carbon nanoparticle exposure in vivo. The lack of detectable differences with SWCNH exposure will serve as a reference point for future studies of gene expression changes in response to other types of nanoparticles and with other experimental manipulations.

In conclusion, we report that SWCNHs are a relatively innocuous agent when delivered to mice in vivo using aspiration as a delivery mechanism. As described above, these results are in contrast to those with other types of engineered carbon-based nanoparticles, raising the potential value of SWCNHs for in vivo applications such as drug delivery. Further study will be

necessary to more precisely characterize the physiochemical properties of SWCNHs and to define their interactions within the physiological milieu.

Appendix References

1. Human respiratory tract model for radiological protection. A report of a Task Group of the International Commission on Radiological Protection. *Ann ICRP* 24: 1-482, 1994.
2. **Ajima K, Yudasaka M, Murakami T, Maigne A, Shiba K, and Iijima S**. Carbon nanohorns as anticancer drug carriers. *Mol Pharm* 2: 475-480, 2005.
3. **Baughman RH, Zakhidov AA, and de Heer WA**. Carbon nanotubes--the route toward applications. *Science* 297: 787-792, 2002.
4. **Beck-Speier I, Dayal N, Karg E, Maier KL, Schumann G, Schulz H, Semmler M, Takenaka S, Stettmaier K, Bors W, Ghio A, Samet JM, and Heyder J**. Oxidative stress and lipid mediators induced in alveolar macrophages by ultrafine particles. *Free radical biology & medicine* 38: 1080-1092, 2005.
5. **Borm PJ, Robbins D, Haubold S, Kuhlbusch T, Fissan H, Donaldson K, Schins R, Stone V, Kreyling W, Lademann J, Krutmann J, Warheit D, and Oberdorster E**. The potential risks of nanomaterials: a review carried out for ECETOC. *Part Fibre Toxicol* 3: 11, 2006.
6. **Brown DM, Donaldson K, Borm PJ, Schins RP, Dehnhardt M, Gilmour P, Jimenez LA, and Stone V**. Calcium and ROS-mediated activation of transcription factors and TNF-alpha cytokine gene expression in macrophages exposed to ultrafine particles. *Am J Physiol Lung Cell Mol Physiol* 286: L344-353, 2004.
7. **Brown DM, Wilson MR, MacNee W, Stone V, and Donaldson K**. Size-dependent proinflammatory effects of ultrafine polystyrene particles: a role for surface area and oxidative stress in the enhanced activity of ultrafines. *Toxicology and applied pharmacology* 175: 191-199, 2001.
8. **Cheng MD, Lee DW, Zhao B, Hu H, Styers-Barnett DJ, Puretzky AA, DePaoli DW, Geohegan DB, Ford EA, and Angelini P**. Formation studies and controlled production of carbon nanohorns using continuous in-situ characterization techniques. *Nanotechnology* In press, 2007.
9. **Cherukuri P, Bachilo SM, Litovsky SH, and Weisman RB**. Near-infrared fluorescence microscopy of single-walled carbon nanotubes in phagocytic cells. *J Am Chem Soc* 126: 15638-15639, 2004.
10. **Geohegan DB, Hu H, Puretzky AA, Zhao B, Styers-Barnett DJ, and Ivanov I**. Synthesis and Processing of Single-Walled Carbon Nanohorns for Hydrogen Storage and Catalyst Supports. *FY 2006 Annual Progress Report for DOE Hydrogen Program* 473-475, 2006.
11. **Harvey BG, and Crystal RG**. Pulmonary response to chronic inorganic dust exposure. In: *The lung*, edited by Crystal RG. Philadelphia: Lippincott-Raven, 1997, p. 2339–2352.
12. **Hoet PH, Bruske-Hohlfeld I, and Salata OV**. Nanoparticles - known and unknown health risks. *J Nanobiotechnology* 2: 12, 2004.
13. **Isobe H, Tanaka T, Maeda R, Noiri E, Solin N, Yudasaka M, Iijima S, and Nakamura E**. Preparation, purification, characterization, and cytotoxicity assessment of water-soluble, transition-metal-free carbon nanotube aggregates. *Angew Chem Int Ed* 45: 6676-6680, 2006.
14. **Jia G, Wang H, Yan L, Wang X, Pei R, Yan T, Zhao Y, and Guo X**. Cytotoxicity of carbon nanomaterials: single-wall nanotube, multi-wall nanotube, and fullerene. *Environ Sci Technol* 39: 1378-1383, 2005.
15. **Lam CW, James JT, McCluskey R, Arepalli S, and Hunter RL**. A review of carbon nanotube toxicity and assessment of potential occupational and environmental health risks. *Crit Rev Toxicol* 36: 189-217, 2006.

16. **Lam CW, James JT, McCluskey R, and Hunter RL**. Pulmonary toxicity of single-wall carbon nanotubes in mice 7 and 90 days after intratracheal instillation. *Toxicol Sci* 77: 126-134, 2004.
17. **Mangum JB, Turpin EA, Antao-Menezes A, Cesta MF, Bermudez E, and Bonner JC**. Single-Walled Carbon Nanotube (SWCNT)-induced interstitial fibrosis in the lungs of rats is associated with increased levels of PDGF mRNA and the formation of unique intercellular carbon structures that bridge alveolar macrophages In Situ. *Part Fibre Toxicol* 3: 15, 2006.
18. **Oberdorster G, Maynard A, Donaldson K, Castranova V, Fitzpatrick J, Ausman K, Carter J, Karn B, Kreyling W, Lai D, Olin S, Monteiro-Riviere N, Warheit D, and Yang H**. Principles for characterizing the potential human health effects from exposure to nanomaterials: elements of a screening strategy. *Part Fibre Toxicol* 2: 8, 2005.
19. **Pulskamp K, Diabate S, and Krug HF**. Carbon nanotubes show no sign of acute toxicity but induce intracellular reactive oxygen species in dependence on contaminants. *Toxicol Lett* 168: 58-74, 2007.
20. **Rao GV, Tinkle S, Weissman DN, Antonini JM, Kashon ML, Salmen R, Battelli LA, Willard PA, Hoover MD, and Hubbs AF**. Efficacy of a technique for exposing the mouse lung to particles aspirated from the pharynx. *J Toxicol Environ Health A* 66: 1441-1452, 2003.
21. **Shvedova AA, Kisin ER, Mercer R, Murray AR, Johnson VJ, Potapovich AI, Tyurina YY, Gorelik O, Arepalli S, Schwegler-Berry D, Hubbs AF, Antonini J, Evans DE, Ku BK, Ramsey D, Maynard A, Kagan VE, Castranova V, and Baron P**. Unusual inflammatory and fibrogenic pulmonary responses to single-walled carbon nanotubes in mice. *Am J Physiol Lung Cell Mol Physiol* 289: L698-708, 2005.
22. **Storey JD, and Tibshirani R**. Statistical significance for genomewide studies. *Proc Natl Acad Sci U S A* 100: 9440-9445, 2003.
23. **Thannickal VJ, Toews GB, White ES, Lynch JP, 3rd, and Martinez FJ**. Mechanisms of pulmonary fibrosis. *Annu Rev Med* 55: 395-417, 2004.
24. **Warheit DB, Laurence BR, Reed KL, Roach DH, Reynolds GA, and Webb TR**. Comparative pulmonary toxicity assessment of single-wall carbon nanotubes in rats. *Toxicol Sci* 77: 117-125, 2004.
25. **Wolfinger RD, Gibson G, Wolfinger ED, Bennett L, Hamadeh H, Bushel P, Afshari C, and Paules RS**. Assessing gene significance from cDNA microarray expression data via mixed models. *J Comput Biol* 8: 625-637, 2001.
26. **Xing Z, Ohkawara Y, Jordana M, Graham F, and Gauldie J**. Transfer of granulocyte-macrophage colony-stimulating factor gene to rat lung induces eosinophilia, monocytosis, and fibrotic reactions. *The Journal of clinical investigation* 97: 1102-1110, 1996.

VITA

Rachel Lynch received her Bachelor of Science degree in Biology at Cedarville University in Ohio in 2003. Upon graduation, Rachel married Ben Lynch and they both started their graduate studies at the University of Tennessee. Rachel and Ben have a wonderful son, James, who brings endless amounts of joy to their lives. Upon graduation, the family is moving to Raleigh, NC where Rachel is starting a post-doctoral position at North Carolina State University.